Spring 4-5-2012

I. Synthesis of β-Sitosterol and Phytosterol Esters; II. New Methodology for Singlet Oxygen Generation from 1,1-Dihydroperoxides

Jiliang Hang
University of Nebraska-Lincoln, hangjiliang@gmail.com

I. Synthesis of β-Sitosterol and Phytosterol Esters;

II. New Methodology for Singlet Oxygen Generation from 1,1-Dihydroperoxides Derivatives

By

Jiliang Hang

A DISSERTATION

Presented to the Faculty of

The Graduate College at the University of Nebraska

In Partial Fulfillment of Requirements

For the Degree of Doctor of Philosophy

Major: Chemistry

Under the Supervision of Professor Patrick H. Dussault

Lincoln, Nebraska

April, 2012

I. Synthesis of β-Sitosterol and Phytosterol Esters;

II. New Methodology for Singlet Oxygen Generation from 1,1-Dihydroperoxides Derivatives

Jiliang Hang

University of Nebraska, 2012

Advisor: Patrick H. Dussault

Phytosterols are steroid compounds structurally similar with cholesterol and vary in the nature of carbon side chain. β-Sitosterol is commercially available in preparative amount only as mixtures with other phytosterols. New semipreparative synthesis of pure β-sitosterol and sidechain-modified phytosterols is discussed in this dissertation. This new synthesis is achieved via a temporary masking of the stigmasterol 5,6-alkene as an epoxide. Following performance of the desired modification, the alkene is regenerated through a mild deoxygenation. Preparation of phytosterol esters for cholesterol metabolism study is also discussed in this dissertation.

Singlet oxygen ($^1O_2$) is the lowest excited state of oxygen molecule. Due to its special properties, $^1O_2$ has been widely used as the oxidant in chemistry, biology, and medicine. In the past decades, two major generation methods have been developed, photosensitization and chemical generation. However, most of the reported chemical generations require the water-rich media, which is associated with short $^1O_2$ lifetime as a

major drawback. Therefore, there is a need for $^1O_2$ generation from organic solvents. The investigation of fragmentation of monoactivated derivatives of 1,1-dihydroperoxides is discussed in this dissertation. This previously unobserved fragmentation can be conducted in various organic solvents and generate high yield of $^1O_2$. This reaction is general for a range of skeletal frameworks and activating groups, and can be applied directly to 1,1-dihydroperoxides via in situ activation. Kinetic and mechanistic investigation suggests it involving rate-limiting formation of a peroxyanion, which decompose to generate $^1O_2$ via Grob-like process.

Acknowledgements

Foremost, I would like to thank my advisor, Professor Patrick Dussault, for his continuous support of my Ph.D study and research. His guidance helped me in all the time of research and writing of this thesis. I am very lucky to have such a great advisor.

Besides my advisor, I would like to thank my committee members: Professor Stephen G. DiMagno, Professor Liangcheng Du, Professor Wonyoung Choe, Professor Timothy Carr for their encouragement and advice. I would like to thank Dr. Joe Dumais and Sara Basiaga for their help with NMR.

I would also like to thank my fellow labmates: Dr. Prasanta Ghorai, Dr. Charles Schiaffo, Dr. Chris Schwartz, Thomas J. Fisher, Wantanee Sittiwong, Shiva Kumar Kyasa, Benjamin W. Puffer, Michael W. Richardson and Rachel Alexandria Willand-Charnley for the help and useful discussions in my research projects.

Finally, I would like to thank my parents, Zhengqing Hang and Aiqin Yu, and my wife, Lili Lou for their love and understanding. They always supported me in all my pursuits. Without their encouragement it would be impossible for me to finish my study. I would also like to thank my son Kevin for bringing me so much fun.

Table of Contents

Chapter 1

Synthesis of pure β-sitosterol and other phytosterols

(A portion of the results from this chapter have been published: Hang J, Dussault PH, A concise synthesis of β-sitosterol and other phytosterols, *Steroids*, **2010**, 75, 879-883)

1. Introduction

The term phytosterols refers to sterols and stanols synthesized in plants. The phytosterols have the same tetracyclic core structure as mammalian sterols such as cholesterol but differ in the presence or absence of a double bond at C22 and the nature of the substitution at C24.. Some examples are shown in Figure 1. Stigmasterol **1** is an unsaturated sterol, having one double bond in the sterol ring structure and one double bond in the side chain. β-sitosterol **2** is an unsaturated sterol with one double bond in sterol ring structure. Campesterol **4** is structurally similar to β-sitosterol but has a methyl substituent at C24 position instead of an ethyl group. Stigmastanol **3** is a saturated sterol both in sterol ring structure and side chain. So far, more than 200 sterols and related compounds have been identified.[1] However, β-sitosterol **2** and campesterol **4** are predominant, comprising 95% of isolated phytosterols.[2]

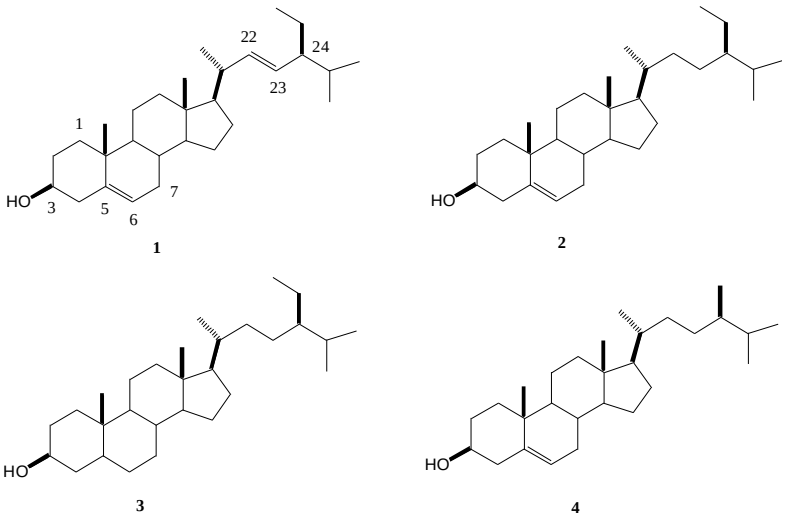

Figure 1. Structures of stigmasterol (**1**), β-sitosterol (**2**), stigmastanol (**3**), campesterol (**4**).

In the past decades, phytosterols and their derivatives have been widely applied in different areas such as the food and cosmetic industries, and have recently received a lot of attention as nutraceutical additives.[3] Because of their ability to lower the level of cholesterol in the human body, phytosterols have drawn greater interest and have been widely used as food additives.[4] Dietary intake of phytosterols is projected to increase in western countries as consumers respond to health messages to increase vegetable oil consumption at the expense of animal fats.[5] Besides the nutraceutical application, phytosterols have also attracted attention as inhibitors of sarcoplasmic reticulum calcium ATPase and transportation through potassium ion channels.[6]

As part of a collaboration investigating the structural influences of sterol ester structure on uptake and processing, I needed preparative amounts of pure β-sitosterol However, β-sitosterol is commercially available in preparative amounts only as mixtures with other phytosterols, typically stigmasterol and campesterol. The few reported separations are

relatively laborious.[7] We therefore became interested in the synthesis of sitosterol from stigmasterol, which is available in pure form. Two routes have been reported for this conversion.

The first route is illustrated in Scheme 1,[8] and is based upon selective saturation of the sidechain ($\Delta_{22\text{-}23}$) alkene. Selective hydrogenation of the side chain $\Delta_{22\text{-}23}$ alkene with Raney Nickel was found to produce β-sitosterol contaminated with the fully saturated stigmastanol. Since β-sitosterol and stigmastanol are very similar in size, shape, and polarity, it is very difficult if not impossible to isolate pure β-sitosterol from crude hydrogenation products. However, treatment of the crude mixture of products with Br_2 resulted in conversion of the the $\Delta_{5\text{-}6}$ alkene in β-sitosterol to a dibromide **5**, which can be separated from stigmastanol via column chromatography. Finally, the alkene group could be regenerated via Zn/AcOH reduction of the dibromide, producing β-sitosterol as a pure compound.

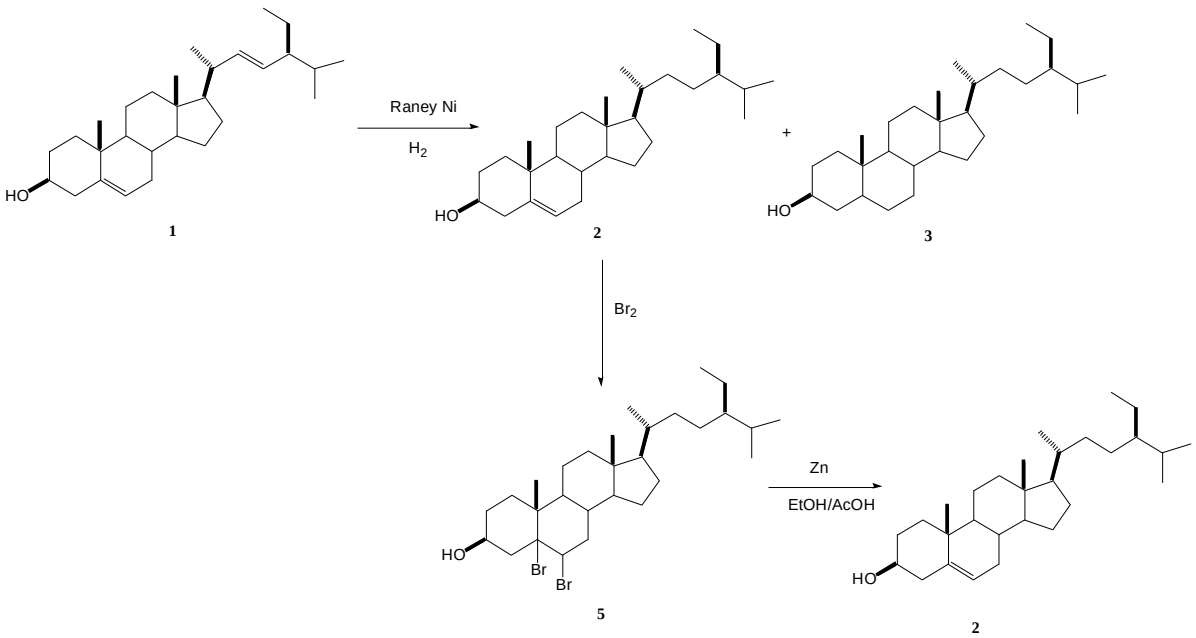

Scheme 1. Synthetic route to pure beta-sitosterol via dibromide

The second route is illustrated in Scheme 2.[9] This approach, which has been applied to the synthesis of β-sitosterol and related sterols, circumvents the need for selective hydrogenation by protecting the $\Delta_{5\text{-}6}$ alkene as a cyclopropyl carbinyl ether **7**. Following hydrogenation of the $\Delta_{22\text{-}23}$ side chain double bond with Pd/C as catalyst, solvolysis of the cyclopropane reintroduces both the C3-alcohol and the $\Delta_{5\text{-}6}$ alkene. Although this approach is very useful as a means of obtaining very pure samples of β-sitosterol, semipreparative applications were challenging in terms of removal of sterol methyl ether byproducts **8**.

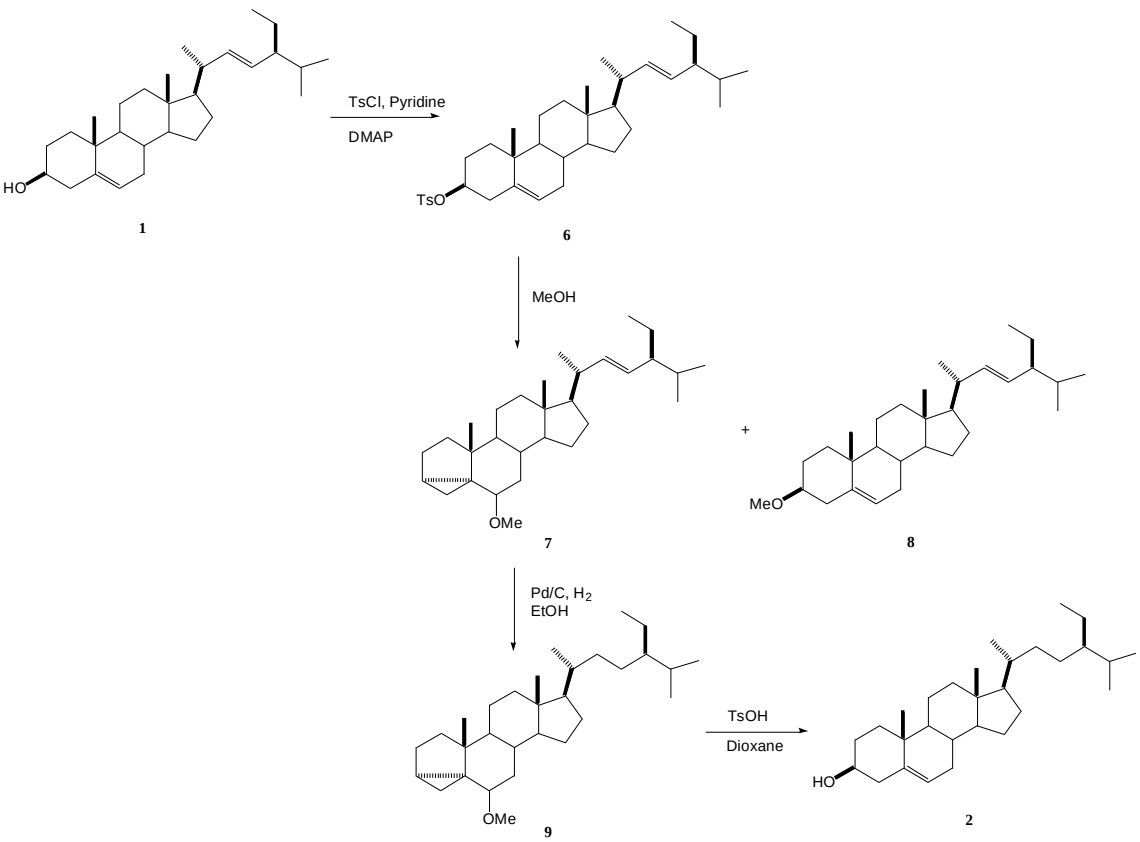

Scheme 2. Synthetic route to pure β-sitosterol via cyclopropyl carbinyl ether

As discussed in more detail below, we reinvestigated the hydrogenation of stigmasterol and developed an improved approach to sitosterol and sidechain-modified sitosterols based upon temporary protection of the A-ring alkene as an epoxide.

2. Result and discussion

2.1 Stigmasterol hydrogenation with Raney Nickel

Raney nickel is a finely-divided gray powder which is composed of fine grains of a nickel-aluminum alloy. It was developed in 1926 by Murray Raney,[10] and the original purpose is to catalyze the hydrogenation of vegetable oils in industrial processes. However, because of the special properties of massive irregular size pores in its three dimension structure and large Brunauer-emmett-Teller surface area, [11] Raney nickel exhibit high catalytic activity, and has been widely used as a heterogeneous catalyst in organic synthesis.[12]

Raney nickel is prepared when a block of nickel-aluminum alloy is treated with concentrated sodium hydroxide.[13] The resulting reaction is shown in Equation 1.

Equation 1. Preparation of Raney Nickel

Fresh Raney Nickel was prepared according to standard procedure.[10] Commercially available pure stigmasterol was used to test the selective hydrogenation efficiency with stoichiometric amount Raney Nickel (3 equiv.). Results were shown in Table 1. Hydrogenation of stigmasterol with Raney nickel could give a mixture of β-sitosterol and over reduced saturated stigmastanol. The ratio of these two compounds depends on the reaction times. However, as shown in Table 1, we found that reduction with Raney Nickel is not useful as a method to provide pure β-sitosterol (>95%).

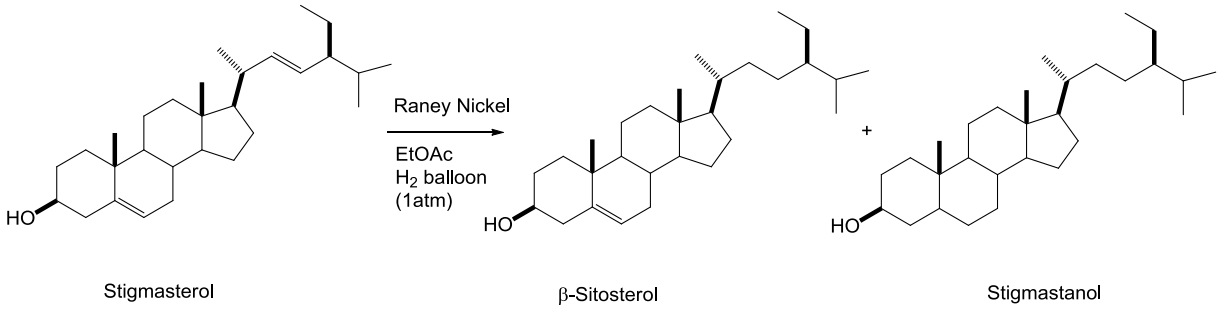

Stigmasterol β-Sitosterol Stigmastanol

Reaction scale	Time	Products (Stigmasterol : β-sitosterol : stigmastanol)
1mmol	4h	4: 88: 8
1mmol	6h	0 : 89 : 11
1mmol	8h	0 : 85 : 15
1mmol	24h	0 : 61 : 39

Table 1. Hydrogenation of stigmasterol with Raney Nickel

2.2 Stigmasterol hydrogenation with Rieke Nickel

Rieke metals are a type of highly reactive metal powders, which are prepared by the methods developed by Reuben D. Rieke.[14] The reactivity of Rieke metals results from a very high surface area and the lack of surface oxides which retard reaction. Highly reactive Rieke metals are generally prepared by reducing metal salts in ethereal or hydrocarbon solvent, using alkali metals as reducing agents[15] (Equation 2). Typical alkali metals used in this method are potassium, sodium, and lithium. Among the many metals that have been generated by this method are Mg, Ca, Ti, Fe, Co, Ni, Cu, Zn, and In.

Equation 2. Typical method of preparing Rieke Metal

In some cases the reaction is carried out with a catalytic amount (5-10% mole percent) of an electron carrier such as biphenyl or naphthalene.[16] During the reaction performance, the coprecipitated alkali metal salt is usually not separated from the highly reactive metal, which is generally used in situ.

A recent study indicates that the selective hydrogenation of multiple carbon-carbon bonds could be promoted by Rieke Nickel particles.[17] Selective hydrogenations of dienes are shown in Table 2. In the entry 4, the less hindered alkene in the side chain of (*R*)-limonene was reduced while the trisubstituted alkene in the ring was not affected at all.

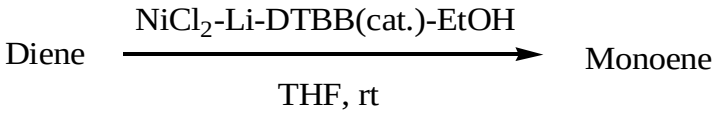

Entry	Starting diene	T(h)	Product	Yield(%)
1	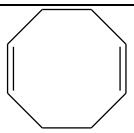	24	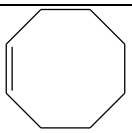	95
2	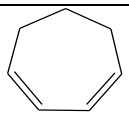	21	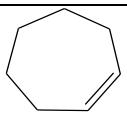	99
3	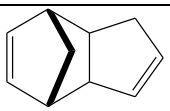	22	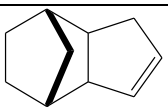	88
4	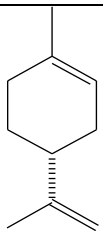	22	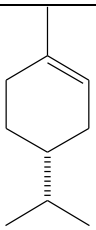	99

Table 2. Selective hydrogenation of diene with Rieke Nickel.[17]

We investigated the reduction of stigmasterol by Rieke Ni under conditions which could either allow direct reduction of the alkene by the Rieke Ni or could allow Ni-catalyzed hydrogenation (Table 3). Superstoichiometric Rieke nickel (3 equiv.) reacted with pure stigmasterol under an atmosphere of hydrogen at room temperature. However, no β-sitosterol was obtained after the attempted reduction. Instead, only the starting material was recovered.

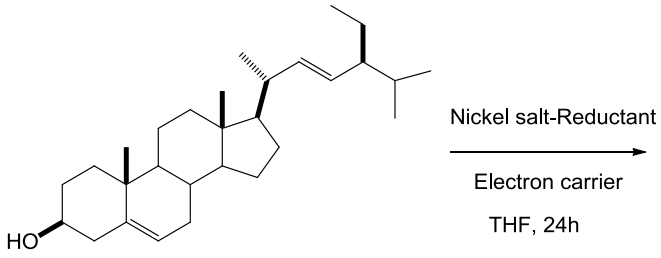

Stigmasterol

Nickel salt	Reductant	Electron carrier	Result
$NiCl_2$	Li	DTBB (cat.)	No reduction
$NiBr_2$	Li	Naphthalene (cat.)	No reduction
$NiBr_2$	Mg	-	No reduction
$NiCl_2$	Mg	-	No reduction

Table 3. Attempt of Rieke Nickel reduction

2.3 Stigmasterol hydrogenation with platinum dioxide

Platinum dioxide (PtO_2), also known as Adams' catalyst, is a commercially available dark brown powder usually represented as platinum(IV) oxide hydrate, $PtO_2 \cdot H_2O$. It is widely used as a precursor to a useful catalyst for hydrogenation and hydrogenolysis in organic synthesis.[18] In the reaction, the platinum dioxide itself is not an active catalyst. But as soon as this black powder is exposed in hydrogen gas, it will be converted to active black platinum metal, which is the real reductant and is responsible for reactions.

PtO_2 has been widely applied to the selective hydrogenation of dienes in many organic molecules. It was reported that PtO_2 can catalyze the hydrogenation of (-)-perillyl alcohol

with high selectivity and high yield[19] (Scheme 3). The less hindered terminal alkene can be reduced while the more hindered alkene remains unaffected.

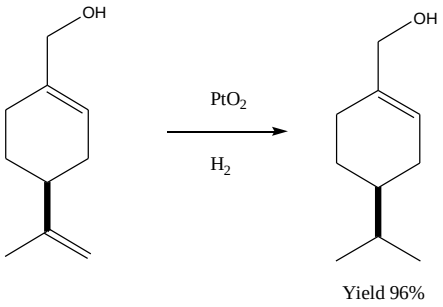

Scheme 3. Selective hydrogenation of (-)-perillyl alcohol with PtO_2.[21]

A suspension containing a mixture of a catalytic amount of PtO_2 and pure stigmasterol was reacted under an atmosphere of hydrogen (balloon) at room temperature to test the selectivity of hydrogenation. Results are shown in Table 4. We found that hydrogenation in the presence of PtO_2 provides inseparable mixtures of unreacted stigmasterol, β-sitosterol, and the saturated stigmastanol. The exception is for prolonged reaction, where the undesired stigmastanol becomes the only product.

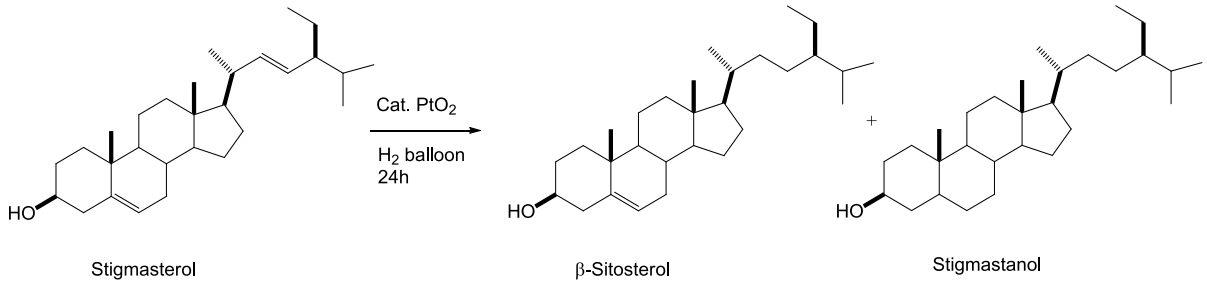

PtO_2 %	Solvent	Result (Stigmasterol: β-sitosterol: stigmastanol)
1	MeOH	85:15:0

1	EtOH	12:68:20
5	EtOH	0:0:100 (48h)
1	EtOAc	38:38:24

Table 4. Hydrogenation of stigmasterol with PtO_2

2.4 Attempts to separate phytosterols by recrystallization.

Recrystallization is a widely used procedure for purifying compounds and removing impurities, and it has been reported that β-sitosterol can be purified from a mixture of different sterols via recrystallization procedure[20] (Table 5). Our initial investigations employed a mixture of phytosterols obtained from our collaborator, Prof. Tim Carr (UNL Nutrition Sciences) and including mainly β-sitosterol (65%) and α-sitosterol (19%). Recrystallization of 5g of this mixture in a solvent mixture of 20ml toluene, 15ml acetone and 2ml water increased the amount of β-sitosterol to approximately 93%, and other phytosterols were mainly removed.

Before crystallization		After crystallization	
β-sitosterol	64.8%	β-sitosterol	93.3%
α-sitosterol	19.0%	α-sitosterol	1.5%
Campesterol	5.5%	Campesterol	4.9%
others	10.7%	others	0.3%

Table 5. Recrystallization of sterols mixture. [22]

However, application of the same recrystallization conditions to 5 g of a sterol mixture derived from a Raney Nickel hydrogenation (70% β-sitosterol, 8% stigmasterol, and 22% stigmastanol) provided a mixture of β-sitosterol (71%), stigmasterol (5%), and stigmastanol (24%). Similarly, recrystallization of a commercial β-sitosterol sample from Acros (β-sitosterol 75%, campesterol 10%, and other undefined phytosterols 15%) provided a mixture of β-sitosterol (87%), campesterol (13%). Overall, our results demonstrate that it is not practical to obtain pure β-sitosterol from a sterols mixture by recrystallization.

2.5 Synthetic route to pure β-sitosterol

After experiencing disappointing results with both selective hydrogenation and recrystallization, I started to research new synthetic routes that could provide pure β-sitosterol in amounts sufficient for use in animal feeding studies.

2.5.1 Synthetic route involving McMurry reaction

A retrosynthesis of a new route to sitosterol is shown in Figure 2. It starts with the reduction of commercially available stigmasterol by Raney Nickel to give a mixture with β-sitosterol and stigmastanol. Then the $\Delta_{5\text{-}6}$ alkene of the β-sitosterol was cleaved via ozonolysis to the dicarbonyl compound, which would presumably be easily separated from unreacted stigmastanol by chromatography. Finally, the alkene would be reformed via the intramolecular McMurry reaction.

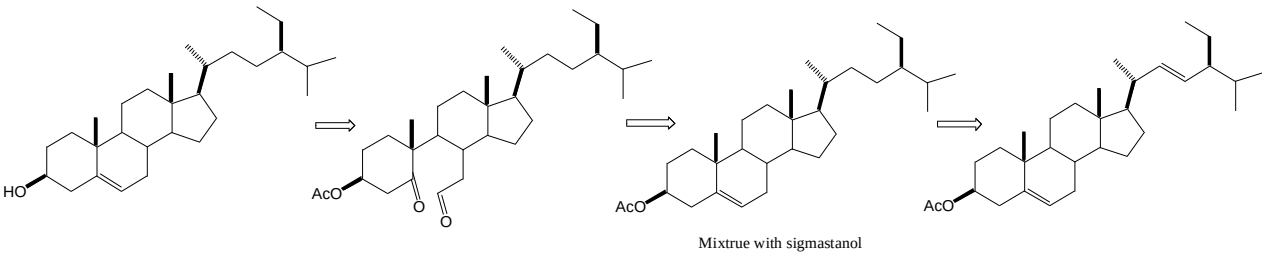

Figure 2. Retrosynthesis analysis

The McMurry reaction is an organic reaction in which two ketone or aldehyde groups are reductively dimerized to form an alkene. The reaction uses a reduced titanium reagent most often prepared from reaction of titanium(III) chloride and a reducing agent, often an alkali metal.[21] This reductive coupling involves two steps. A radical coupling induced by single electron transfer to the carbonyl groups from alkali metal generates a 1,2-diol as a titanium alkoxide; a subsequent deoxygenation of the 1,2-diol with low-valent titanium yields the alkene (Figure 3).

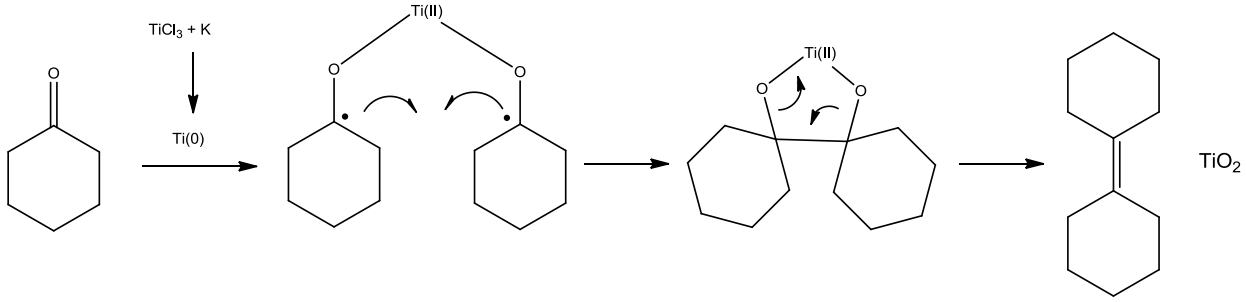

Figure 3. McMurry reaction

Our approach began with commercially available stigmasterol (Scheme 3). Raney nickel reduction produces an inseparable mixture of β-sitosterol (75%) and stigmastanol (25%) which was converted to the acetates. The mixture of acetates **10** and **11** was reacted with

ozone, followed by Zn/AcOH reduction. The dicarbonyl **12** derived from oxidative cleavage of β-sitosterol acetate was easily separated from the unreacted stigmastanol acetate. McMurry reaction was applied to the intermediate **12** under the condition of $TiCl_3$ and K in THF refluxing. However, none of the desired β-sitosterol acetate **10** was obtained.

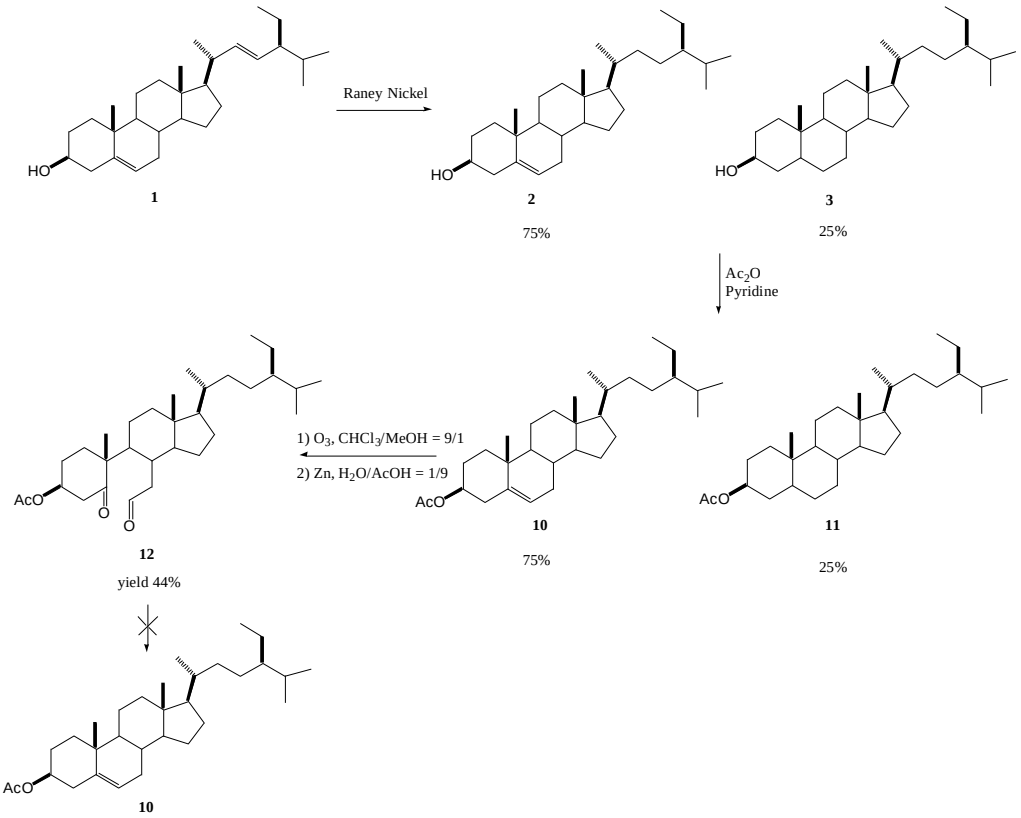

Scheme 3. Synthesis of β-sitosterol

It is possible that the failure resulted from the incompatibility of the acetate groups with the McMurry reagent. We therefore investigated the application of the McMurry reaction on substrates containing triethylsilyl ethers. As shown in Scheme 4, this approach was initially modeled on the mixture of triethylsilyl ethers derived from the mixture of sitosterol and stigmastanol. The mixture was treated with ozone, and the crude products

were reduced with PPh_3 reduction to generate an easily separated mixture of dicarbonyl compound **14** and the unreacted stigmastanol ether. It should be noted that a phosphine reduction was employed because the Zn/AcOH reduction employed in the previous example was anticipated to be incompatible with the triethylsilyl ether. A pure sample of **14** was treated with typical McMurry reaction condition ($TiCl_3$ and K). However, once again, the reaction failed to generate the desired sitosterol skeleton (**13**).

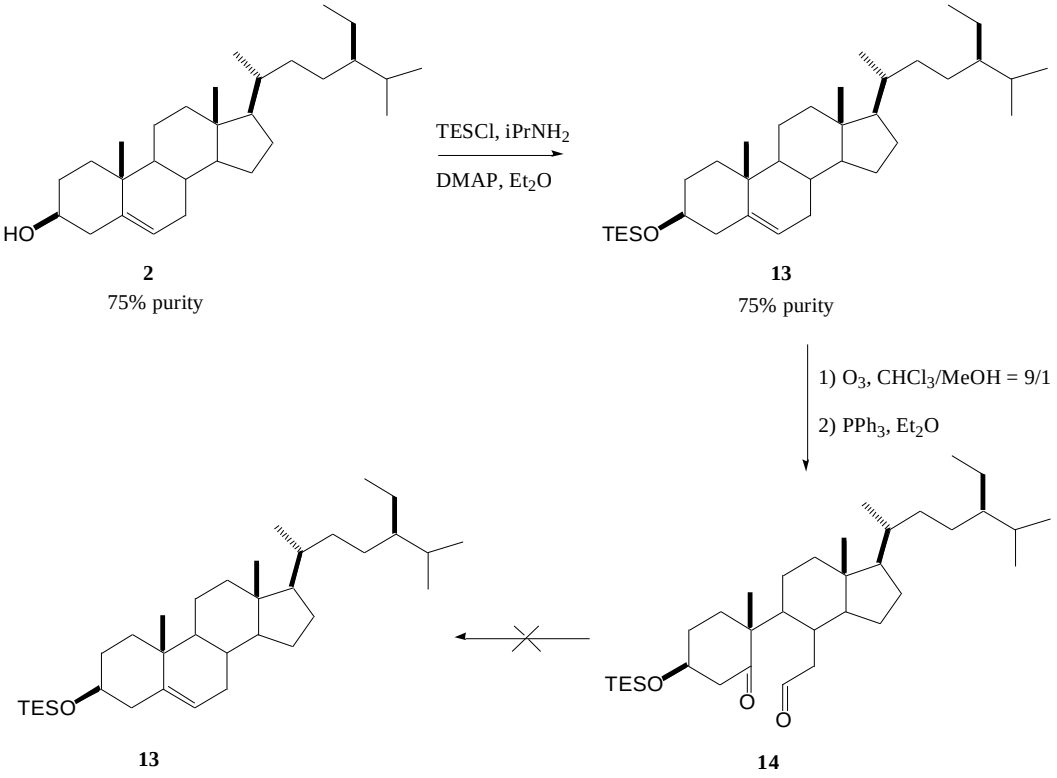

2
75% purity

13
75% purity

13

14

Scheme 4. Reaction attempts with TES protecting group

2.5.2 Synthetic route involving epoxide intermediate

We ultimately developed a successful synthetic route to pure β-sitosterol based on a sequence involving selective epoxidation of $\Delta_{5\text{-}6}$ alkene, hydrogenation of the sidechain alkene, and deoxygenation of the epoxide (Figure 4).

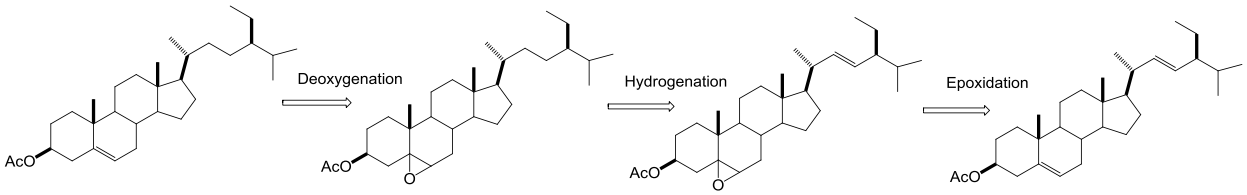

Figure 4. Retrosynthesis analysis

Our approach was inspired by a recent study[22] of epoxidation of cycloolefins by the t-BuOH copper-permanganate system. This study included an example of the selective oxidation of stigmasteryl acetate at $\Delta_{5\text{-}6}$ alkene, producing a mixture of 5α,6α-epoxide and 5β,6β-epoxide with the ratio β/α= 6/1 (Figure 5).

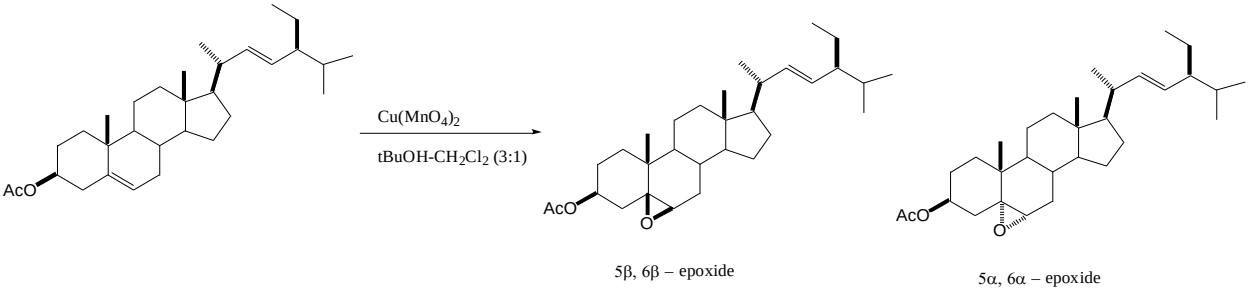

Figure 5. Selective oxidation of stigmasterol acetate via $Cu(MnO_4)_2$

However, if we were going to use an epoxide as an alkene protecting group, we would also require a mild method of regenerating the alkene. Although a number of reagents have been reported for reductive deoxygenation of epoxides,[23] most are relatively harsh. We became interested in a report describing the deoxygenation of epoxides at room temperature using aluminium triiodide.[24] The deoxygenation is thought to involve an iodoalcohol intermediate (Figure 6).

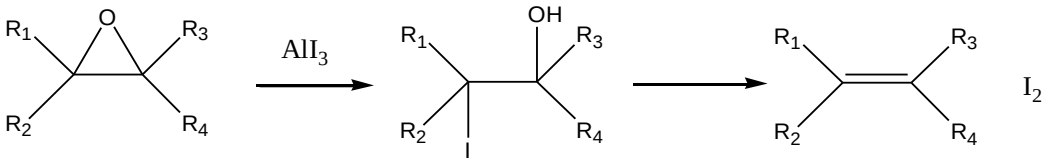

Figure 6. Reduction of epoxide with AlI_3

Based on the above reports, we developed a new synthesis of β-sitosterol as illustrated in Scheme 5. $Cu(MnO_4)_2$ was prepared in situ by reaction of $KMnO_4$ and $CuSO_4$. Selective epoxidation of the $\Delta_{5\text{-}6}$ alkene of stigmasterol acetate **15** with $Cu(MnO_4)_2$ formed a 6:1 mixture of the 5β,6β-epoxide **16a** and 5α,6α-epoxides **16b**. The ratio of two isomers was determined by NMR (Figure 7). Hydrogenation of the mixture of **16a** and **16b** over Pd/C cleanly furnished a 1:6 mixture of stigmastanol epoxides **17a** and **17b**. Then deoxygenation of the saturated epoxides with AlI_3 proceeded rapidly to furnish a good yield of β-sitosteryl acetate **10**. Saponification afforded pure β-sitosterol **2**, with mp 134-135 ℃ and $[\alpha]_D$ = - 37, which matched very closely with literature values.[26]

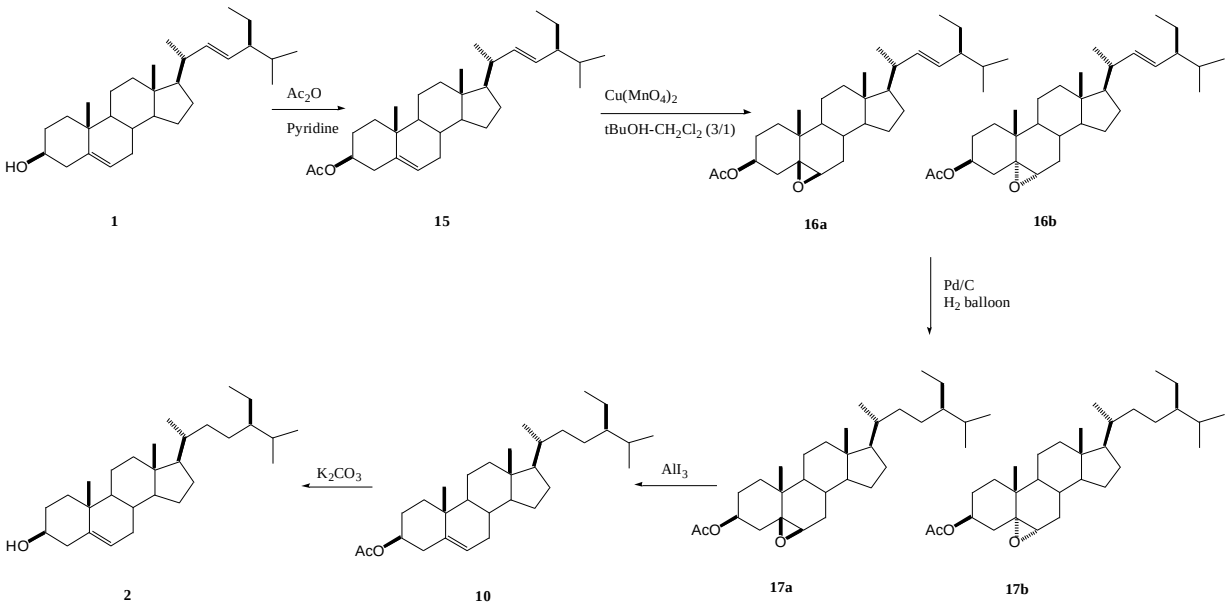

Scheme 5. Synthesis of β-sitosterol

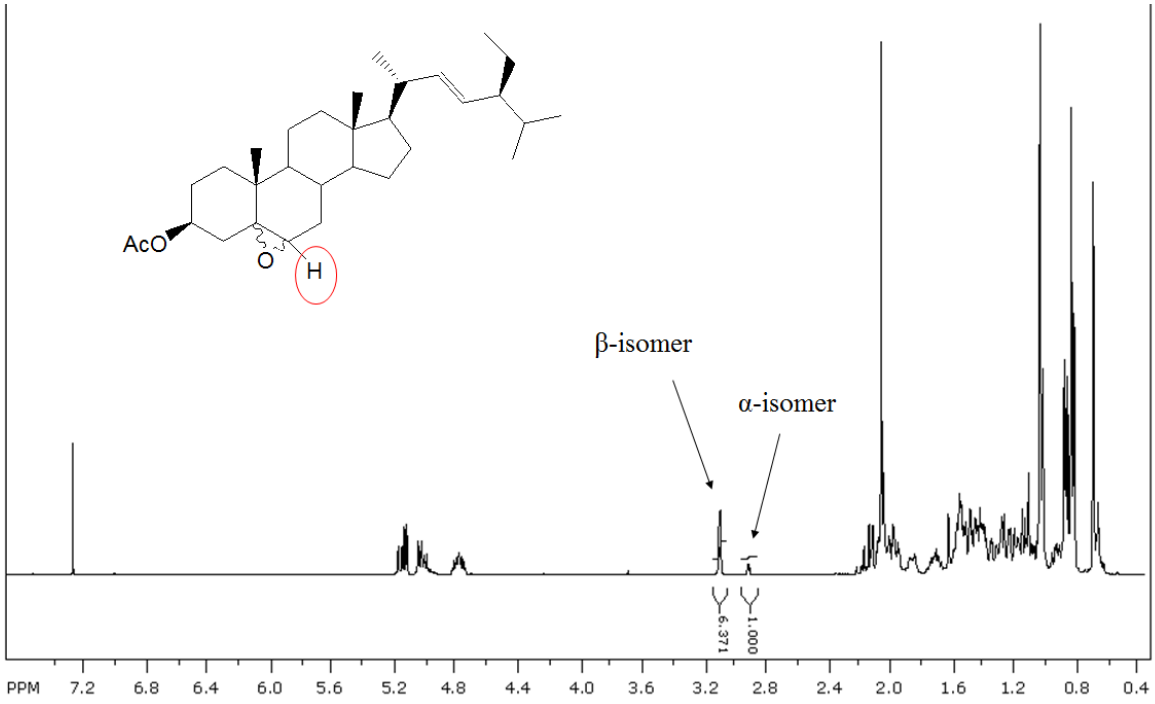

Figure 7. ^{1}H NMR spectra of 5α,6α and 5β,6β-epoxide of stigmasteryl acetate

I also investigated a variant of this route based upon epoxidation with the commercially available peracid *m*-chloroperbenzoic acid (mCPBA). The use of this oxidant also resulted in regioselective oxidation of the $\Delta_{5\text{-}6}$ alkene, but now produced a 2.6:1 mixture of stigmasterol oxides favoring the α-isomer **16a**. Hydrogenation proceeded uneventfully to furnish the corresponding mixture of sitosterol oxides **17a** and **17b**. However, attempted deoxygenation under the same conditions as employed earlier (AlI_3, 10 min, CH_3CN/CH_2Cl_2) now furnished only 33% of β-sitosterol acetate **10**, accompanied by a significant amount (estimated > 60% by mass) of a more polar product which yellowed immediately upon exposure to room light. The formation of the byproduct could be

avoided almost completely by allowing the deoxygenation to proceed for 40 min. Alternatively, the byproduct could be converted to β-sitosterol acetate **10** by treatment with additional AlI_3. The results suggest that the deoxygenation of the α- and β-epoxides proceeds at very different rates, with the 5α, 6α-diastereomer **16a** reacting via the intermediacy of a semistable iodohydrin. I therefore focused on the use of the $CuMnO_4$ system for my studies.

The ability to protect the $\Delta_{5,6}$-alkene of stigmasterol also suggested a facile means of preparing other sidechain-modified phytosterols. Phytosterols with sidechain-modification have been important in studying phytosterol metabolism in human body.[25] Although methods have been reported for preparation of sidechain-modified phytosterol, [26] these synthetic routes are not efficient. Since the epoxide intermediates **16a** and **16b** are quite stable, we reasoned that they would be easily converted to the corresponding aldehydes via ozonolysis, allowing introduction of new side chains via Wittig or Julia chemistry (Figure 8).

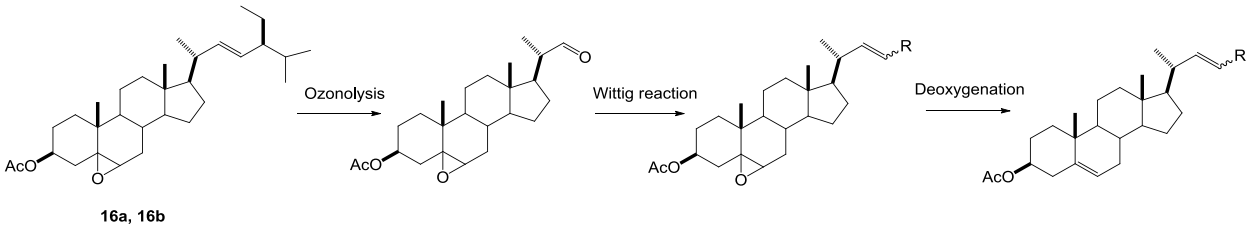

Figure 8. Strategy to prepare sidechain-modified phytosterols

As an example of this methodology, we chose to convert stigmasterol to campesterol, using a Julia olefination for introduction of the campesterol sidechain. The necessary

sulfone (**22**) was prepared as a single enantiomer as illustrated in scheme 6.[27] Alkylation of (*S, S*)-pseudoephedrine isovalerylamide with 3-methylbut-3-enyl triflate led to the formation of hydroxyamide **19**. Reduction of **19** with lithium aminotrihydroborate (LAB) gave the (*S*)-2,3-dimethylbutanol **20** with 90% ee. Then the alcohol **20** could be converted to sulfide **21** through Mitsunobu reaction. Oxidation of **21** with molybdenum salt afforded sulfone **22**.

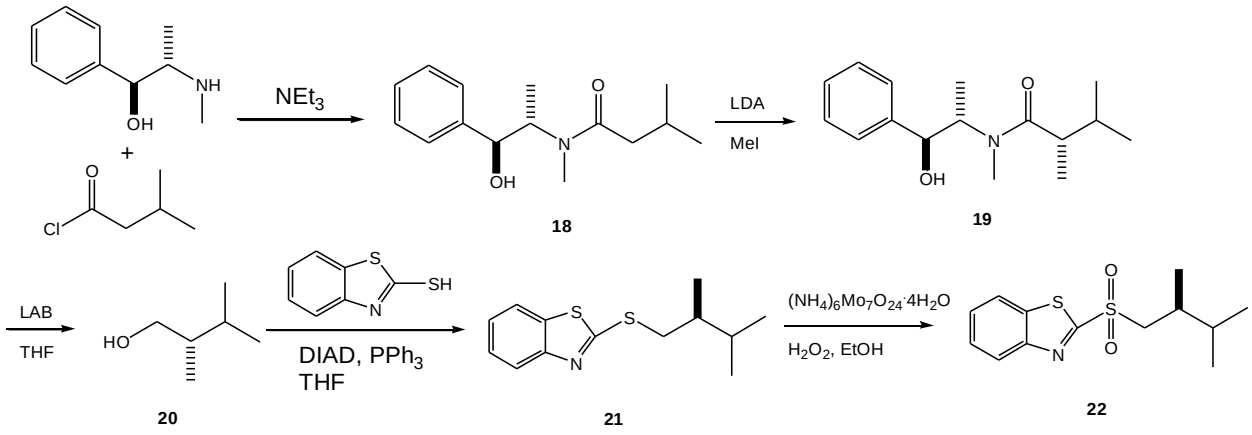

Scheme 6. Preparation of enantiomerically pure sulfone intermediate.

Ozonolysis of the mixture of **16a**/**16b** furnished an approximately 1:6 mixture of aldehydes **23a** and **23b**. Julia-Kocienski olefination, using the sulfone **22**, furnished exclusively the alkene corresponding to the monoepoxide of the Z-isomer of crinosterol.[28] The Z-stereochemistry was assigned from the 10.6 Hz coupling constant for H22-H23. Finally, hydrogenation, followed by deoxygenation of the epoxide as before, furnished campesterol acetate **26** (Scheme 7).

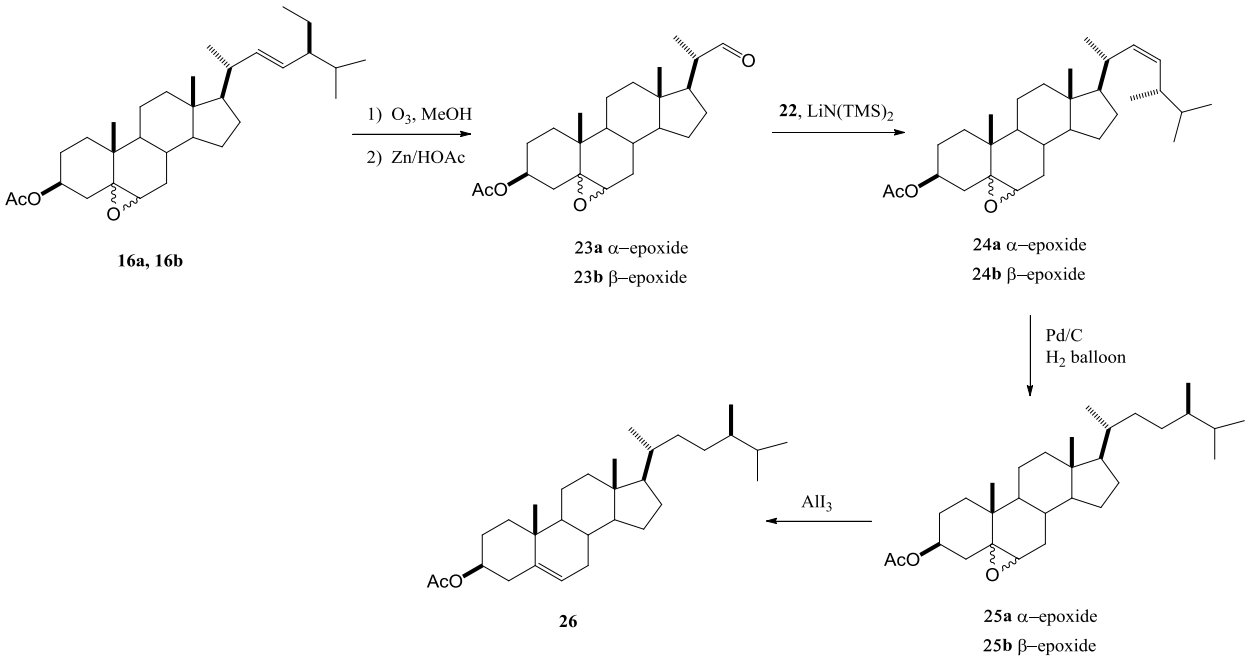

Scheme 7. Synthesis of campesterol acetate

The selective formation of Z-alkenes is unusual in Julia-Kocienski couplings, since most of time this reaction produces E-alkenes as the final product. I therefore investigated the olefination of **16a**,**b** with a model isobutyl sulfone **27** derived from isobutyl alcohol (Figure 8). This reaction also selectively furnished the Z-alkene; the lower selectivity (2:1) compared with that observed for the synthesis of **24a**,**b** may reflect the reduced degree of steric encumbrance in this model system. The ability to readily prepare Z-isomers of phytosterols opens the door to a number of steroid analogs not available from synthetic routes based upon Claisen rearrangements of C22 allylic alcohols.[29]

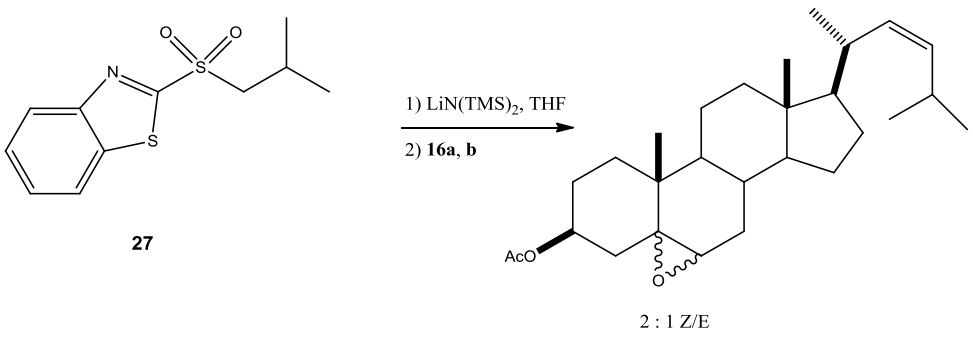

Figure 8. Generality of Z-selective olefination

Overall, the formation of beta-sitosterol has been achieved in 52% overall yield from commercially available stigmasterol using relatively simple chemistry and via easily purified intermediates. The core strategy, protection of the $\Delta_{5\text{-}6}$ alkene as an epoxide, holds potential for synthesis of other phytosterols, including Z-isomers of existing phytosterols.

3. Experimental

General Experimental Conditions

All reagents and solvents were used as supplied commercially, except CH_2Cl_2 and THF, which were distilled from CaH_2, and Na/benzophenone, respectively. All reactions were conducted under an atmosphere of N_2 except where noted; "RBF" indicates round-bottom flask. Thin layer chromatography (TLC) was performed on 0.25 mm hard-layer silica G plates. Developed TLC plates were visualized with a hand-held UV lamp or by staining: 1% ceric sulfate and 10% ammonium molybdate in 10% H_2SO_4 (general stain, after

charring); 1% N,N'-dimethyl-p-phenylenediamine solution in 1:20:100 acetic acid/water/methanol (specific for peroxides); Melting points are uncorrected. Unless noted, NMR spectra were acquired at 400 MHz (^{1}H) or 100 MHz (^{13}C) in $CDCl_3$. IR spectra were recorded as neat films on a ZrSe crystal with selected absorbances reported in cm^{-1}. Mass spectroscopy was conducted at the Nebraska Center for Mass Spectrometry.

Raney Nickel preparation

A solution of NaOH (12.6 g, 0.315 mol) in distilled water (50 ml) is cooled in an ice bath to 10℃. Nickel-Aluminum alloy (10 g) was added to the stirred solution in small portion and at a rate to prevent the temperature from rising above 25℃.When the entire alloy has been added, the reaction mixture is allowed to heat until there is no gas from the solution. Stirring was stopped and the reaction mixture was allowed to settle. After the aqueous supernatant was decanted. The residue was washed with distilled water for 20 times until it is neutral, and then the solid was washed with EtOH for 3 times and stored in EtOH for future use.

Raney Nickel reduction

To the stigmasterol (4.2g, 10mmol) in EtOAc 400 ml, Raney Nickel (5g) was added. Then the reaction mixture was stirred in room temperature under the H_2 balloon at 1 atm overnight. The Raney Nickel was filtered through Celite, and the organic solvent was removed under vacuo to afford the crude product, which was analyzed by GC-MS.

GC-MS conditions: injector 270℃, FID detector 300℃, oven 270℃ for 1min, ramp at 15℃ /min to 300℃ as final temperature.

Stigmasterol acetate (**15**)

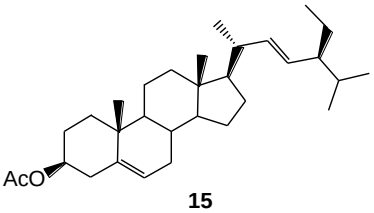

15

Stigmasterol acetate was prepared as a white solid (97%, mp 138-140℃) by a variant of the procedure of Wang.[30] Other physical data were identical to the literature.[31]

5α,6α- and 5β,6β-epoxides of stigmasterol acetate (**16a**, **16b**)

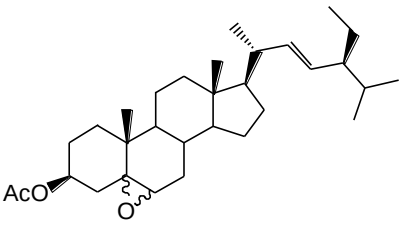

16a α-isomer
16b β-isomer

A mixture of $KMnO_4$ (10 g, 60 mmol) and $CuSO_4 \cdot 5H_2O$ (5 g, 20 mmol) was ground to a fine powder in a mortar and pestle. Water 0.5 mL was added, and the slightly wet mixture was transferred to the reaction flask. To the stirred suspension of this mixture in 25 mL CH_2Cl_2, compound 2 (2.12 g, 5 mmol) was added, followed by t-BuOH 2.5 mL. Reaction mixture reflux for 1 hour and then cool down. The reaction mixture was filtered through a silica pad, washed with ether. After evaporation the solvent, crude solid was recrystallized from methanol to give a white solid 1.59 g, overall yield 75%. NMR data indicates the product was a 1:6 mixture of epoxides **16a** and **16b**.[26]

5α,6α- and 5β,6β-epoxy sitosterol acetate (**17a**, **17b**)

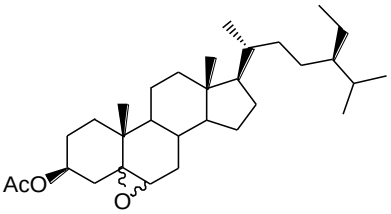

17a α-isomer
17b β-isomer

A 1:6 mixture of 17a and 17b (1.35 g, 3.0 mmol) was dissolved in EtOAc 150 mL. 10% Pd/C (0.32 g) was added, and reaction mixture stirred at room temperature under an atmosphere of H_2 balloon for 12 hours. The reaction mixture was filtered through a Celite pad, and evaporated to a white solid (1.28 g, 96%) as a 1:6 mixture of epoxides **17a** and **17b**.[32]

Sitosterol acetate (**10**)

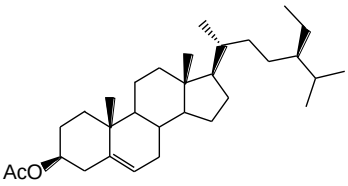

10

The mixture of epoxides **17a** and **17b** (470 mg, 1.0 mmol) was dissolved in 2:1 CH_3CN/CH_2Cl_2 30 mL. Aluminum triiodide was added (610 mg, 1.5 mmol) and the resulting mixture was stirred at room temperature for 10 minutes. The reaction was quenched with aq. 10% $Na_2S_2O_3$ 100 mL and the resulting mixture was extracted with CH_2Cl_2 (3 x 100 mL). The combined organic layers were dried over Na_2SO_4, and the residue from the concentrated filtrate was purified by flash chromatography (hexane/EtOAc, 95:5) to give 360 mg (80%) of sitosterol acetate **10** as a white solid. Mp 111-112℃, $[\alpha]_D$ = -34.5 ($CHCl_3$). Other physical data were identical to the literature.[26]

β-Sitosterol (**2**)

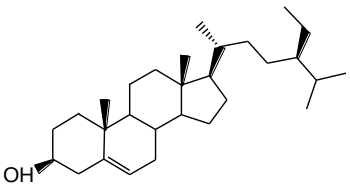

2

Sitolsterol acetate **10** (240 mg, 0.47 mmol) was dissolved in a mixture of 15 mL CH_3OH and 15 mL CH_2Cl_2, K_2CO_3 (140 mg, 1 mmol) was added. Reaction mixture stirred at room temperature for 12 hours. Remove solvent under vacuum. The residue was extracted with 30 mL CH_2Cl_2 and 30 mL water. Combined organic layer dried over Na_2SO_4, filtered and evaporated. Crude solid was purified through flash chromatography (hexane/EtOAc, 80:20) to to give white solid 220 mg, yield 93%. Mp 134-135℃, $[\alpha]_D$ = -37 ($CHCl_3$). Physical data was identical to the literature.[26]

(S)-2,3-Dimethylbutan-1-ol (**20**)

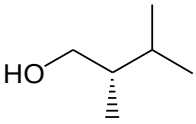

20

(S)-2,3-Dimethylbutan-1-ol **20** was prepared as a colorless liquid, overall yield 60%, $[\alpha]_D$ = 4.4 ($CHCl_3$), by the procedure of Tietze from (+)-(1S,2S)-Pseudoephedrine. Other physical data were identical to literature values.[29]

(S)-2-(2,3-dimethylbutylthio)benzothiazole (**21**)

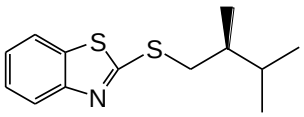

21

To a mixture of **20** (102 mg, 1 mmol), 2-mercaptobenzothiazole (183 mg, 1.1 mmol) and PPh_3 (288 mg, 1.1 mmol) in freshly distilled THF (4 mL) was added DIAD (0.21 mL, 1.1 mmol) dropwise at 0℃ under argon. After being stirred for 3 hours at the same temperature, the reaction was quenched by water. The aqueous layer was extracted with EtOAc (10mL x 3). The combined organic layer was dried over anhydrous Na_2SO_4, filtered and concentrated in vacuo. Flash chromatography (hexane/EtOAc, 99:1) afforded thioether **21** (228 mg, 91%) as a light yellow oil. $[\alpha]_D$ = 42.3 ($CHCl_3$); IR 2957, 1455, 1426, 1057, 991, 752 cm^{-1}; ^1H NMR (400 MHz, $CDCl_3$): δ 7.89 (d, J= 8.06 Hz, 1H), 7.75 (d, J= 8.06 Hz , 1H), 7.42 (t, J= 7.19 Hz, 1H), 7.29 (t, J= 7.19, 1H Hz), 3.50 (dd, J=12.66 Hz, 4.84 Hz, 1H), 3.18 (dd, J= 12.65Hz, 8.18 Hz, 1H), 1.88-1.77 (m, 2H), 1.04 (d, J=6.67 Hz, 3H), 0.99 (d, J= 6.56 Hz, 3H), 0.94 (d, J= 6.56 Hz, 3H); ^{13}C NMR (100Hz, $CDCl_3$): δ 167.75, 153.38, 135.15, 125.99, 124.08, 121.44, 120.91, 38.87, 38.78, 31.62, 20.37, 17.96, 15.29; HRMS (m/z) $[M-H]^+$ calcd for $C_{13}H_{18}NS_2^+$: 252.0881, found: 252.0875

(S)-2-(2,3-dimethylbutylsulfonyl)benzothiazole (**22**)

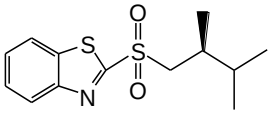

22

A solution of **21** (183 mg, 0.73 mmol) in EtOH (10 mL) was oxidized with ammonium heptamolybdate tetrahydrate (1.8 g, 1.46 mmol) and 30% H_2O_2 (2.5 mL, 21.9 mmol) at 0℃

for 2 hours. The mixture was extracted with EtOAc (10 mL x 3). The combined organic extracts were washed with brine (10 mL x 3), dried over anhydrous Na_2SO_4, filtered and concentrated in vacuo. Flash chromatography (hexane/ EtOAc, 90:10) afforded sulfone **22** (177mg, 86%) as a pale yellow oil. $[\alpha]_D$ = 15.5 ($CHCl_3$); IR 2961, 1470, 1324, 1140, 1085, 758 cm^{-1}; ^1H NMR (400 MHz, $CDCl_3$): δ 8.23 (d, J= 7.92, 1H), 8.03 (d, J= 7.92, 1H), 7.68-7.59 (m, 2H), 3.59(dd, J= 14.36, 3.54Hz, 1H), 3.31(dd, J= 14.11, 8.95Hz, 1H), 2.29-2.19(m, 1H), 1.82-1.73(m, 1H), 1.10(d, J= 6.89Hz, 3H), 0.89(d, J= 6.80Hz, 3H), 0.85(d, J= 6.89Hz, 3H); ^{13}C NMR (100Hz, $CDCl_3$): δ 166.66, 152.70, 136.74, 128.00, 127.67, 125.43, 122.38, 58.83, 38.68, 32.47, 19.23, 17.89, 15.93; HRMS (m/z) $[M-H]^+$ calcd for $C_{13}H_{18}NO_2S_2^+$: 284.0779, found: 284.0778

5α,6α-and 5β,6β-epoxides of (3β,20R)-3-acetyloxy-pregnane-20-carboxaldehyde (**23a**, **23b**)

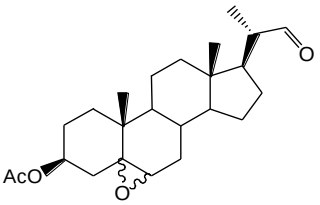

23a α-isomer
23b β-isomer

A solution of **16a**, **16b** (100 mg, 0.21 mmol) in 10 mL of 50/50 CH_2Cl_2/MeOH was ozonolyzed at -78℃ for 5 minutes, then solvent was removed under vacuum. Residue was dissolved in 10 mL of 10/90 H_2O/AcOH, Zinc powder (55 mg, 0.84 mmol) was added, and reaction mixture stirred for 2 hours at room temperature. 50 mL CH_2Cl_2 was added. Organic layer was washed with water (25 mL x 3), then dried over anhydrous Na_2SO_4, filtered and concentrated in vacuo. Flash chromatography (hexane/ EtOAc,

90:10) afforded white solid (81mg, 99%) as 1:6 mixture of epoxides **23a** and **23b**. IR: 2950, 1727, 1367, 1262, 1238, 1042, 783cm^{-1}; ^{1}H NMR (400 MHz, $CDCl_3$): δ 9.57 (d, J= 3.29 Hz, 0.76H, b), 9.55 (d, J= 3.3 Hz, 0.16H, a), 4.99-4.91 (m, 0.14H, a), 4.81-4.73(m, 0.87H, b), 3.09(d, J= 2.23Hz, 0.88H, b), 2.90 (d, J= 4.18Hz, 0.13H, a), 2.38-2.31(m, 1H), 2.13-1.82(m, 9H), 1.54-0.89(m, 20H), 0.7(s, 3H); ^{13}C NMR (100Hz, $CDCl_3$): δ 204.95, 170.52, 71.25, 63.41, 62.48, 55.39, 51.05, 50.93, 49.42, 42.89, 39.43, 37.95, 36.67, 35.06, 32.41, 29.74, 27.17, 26.97, 24.54, 21.84, 21.30, 17.03, 13.40, 12.11; HRMS (m/z) $[M-Li]^+$ calcd for $C_{24}H_{36}LiO_4^+$: 395.2774, found: 395.2778

5α,6α- and 5β,6β-epoxides of (3S,10S,13R,17R)-17-((2R,5S,Z)-5,6-dimethylhept-3-en-2-yl)-10,13-dimethylhexadecahydro-1H-cyclopenta[a]phenanthren-3-yl acetate (**24a**, **24b**)

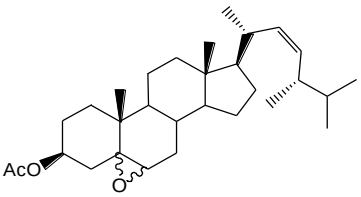

24a α-isomer
24b β-isomer

To sulfone **22** (62 mg, 0.22 mmol) in 5 mL THF was added LiHMDS (0.22mL, 1M in THF, 0.22 mmol) dropwise at -78℃ and stirred for 1 hour. Aldehyde **23a** and **23b** (85 mg, 0.22 mmol) was added in 5 mL THF. Stirring was continued for 1 hour, and reaction was gradually warmed to room temperature. The reaction was quenched by 15 mL water. The aqueous layer was extracted with EtOAc (10 mL x 3), then dried over anhydrous Na_2SO_4, filtered and concentrated in vacuo. Flash chromatography (hexane/ EtOAc, 95:5) afforded white solid (90 mg, 90%) as 1:16 mixture of epoxides **24a** and **24b**. IR: 2950, 2867, 1743, 1368, 1037, 764cm^{-1}; ^{1}H NMR (400 MHz, $CDCl_3$): δ 5.02(dd, J= 10.96,

9.88 Hz, 2H), 4.83-4.73(m, 1H), 3.09(d, J=2 Hz, 0.95H, b), 2.91(d, J=4.4 Hz, 0.06, a), 2.43-2.33(m, 1H), 2.21-1.80(m, 9H), 1.68-0.83(m, 31H), 0.69(s, 3H); ^{13}C NMR (100Hz, $CDCl_3$): δ 170.56, 135.13, 131.22, 71.34, 63.58, 62.52, 56.27, 56.02, 51.02, 42.18, 39.72, 38.32, 38.01, 36.68, 35.04, 34.48, 33.35, 32.43, 29.74, 28.32, 27.20, 24.15, 21.92, 21.34, 20.55, 20.36, 19.94, 18.63, 17.06, 12.06; HRMS (m/z) $[M-H]^+$ calcd for $C_{30}H_{49}O_3^+$: 457.3682, found: 457.3668

5α,6α-and 5β,6β-epoxides of campesterol acetate (**25a**, **25b**)

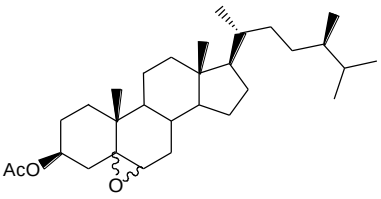

25a α-isomer
25b β-isomer

The mixture of epoxides **24a** and **24b** (30mg, 0.07 mmol) was dissolved in 5mL EtOAc. 10% Pd/C (7 mg) was added, and reaction mixture stirred at room temperature under an atomphere of H_2 balloon for 12 hours. The reaction mixture was filtered through a Celite pad, and evaporated to a white solid (28mg, 94%) as 1:9 mixture of epoxides **25a** and **25b**. IR: 2953, 2867, 1729, 1367, 1263, 1043, 784cm^{-1}; ^{1}H NMR (300 MHz, $CDCl_3$): δ 5.01-4.93(m, 0.15H, a), 4.83-4.73(m, 0.96H, b), 3.09(d, J=2.07 Hz, 0.9H, b), 2.90(d, J= 4.35 Hz, 0.1H, a), 2.12-1.8(m, 8H), 1.58-0.77(m, 37H), 0.65(s, 3H); ^{13}C NMR (75Hz, $CDCl_3$): δ 170.54, 71.34, 63.58, 62.51, 56.19, 56.14, 50.97, 42.28, 39.78, 38.81, 38.01, 36.66, 35.82, 35.03, 33.65, 32.47, 32.41, 30.26, 29.73, 28.14, 27.21, 24.18, 21.92, 21.31, 20.19, 18.66, 18.24, 17.03, 15.37, 11.76; HRMS (m/z) $[M-H]^+$ calcd for $C_{30}H_{51}O_3^+$: 459.3838, found: 459.3820

Campesterol acetate (**26**)

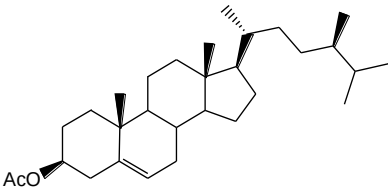

26

The mixture of epoxides **25a** and **25b** (28 mg, 0.06 mmol) was dissolved in 2:1 CH_3CN/CH_2Cl_2 (3 mL). Aluminum triiodide was added (37 mg, 0.09 mmol) and the resulting mixture was stirred at room temperature for 30 minutes. The reaction was quenched with aq. 10% $Na_2S_2O_3$ (10 ml) and the resulting mixture was extracted with CH_2Cl_2 (3 x 10 mL). The combined organic layers were dried over Na_2SO_4, and the residue from the concentrated filtrate was purified by flash chromatography (hexane/EtOAc, 95:5) to give 24mg (91%) of campesterol acetate **26** as a white solid. Mp 130-131℃, $[\alpha]_D$ = -32 ($CHCl_3$); IR 2954, 1730, 1367, 1247, 1037, 735cm^{-1}; ^1H NMR (400 MHz, $CDCl_3$): δ 5.39(d, J=4.77Hz, 1H), 4.66-4.58(m, 1H), 2.33(d, J=7.87Hz, 2H), 2.05(s, 3H), 1.90-1.84(m, 2H), 1.59-0.78(m, 38H), 0.68(s, 3H); ^{13}C NMR (100Hz, $CDCl_3$): δ 170.56, 139.66, 122.66, 73.99, 56.69, 56.08, 50.02, 42.31, 39.73, 38.84, 38.12, 36.99, 36.59, 35.90, 33.70, 32.43, 31.90, 31.86, 30.27, 28.24, 27.78, 24.29, 21.46, 21.03, 20.22, 19.32, 18.70, 18.26; HRMS (m/z) $[M-Na]^+$ calcd for $C_{30}H_{51}O_2Na^+$: 465.3709, found: 465.3703

2-[(2-Methylpropyl)sulfonyl] benzothiazole (**27)**

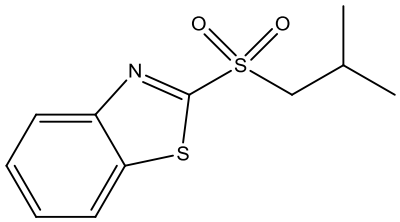

27

Compound **27** was prepared using the same procedure with benzothiazole **22**. Mp 44-45℃. Other physical data were identical to the literature.[33]

Model reaction of **27** with **16a**,**b**

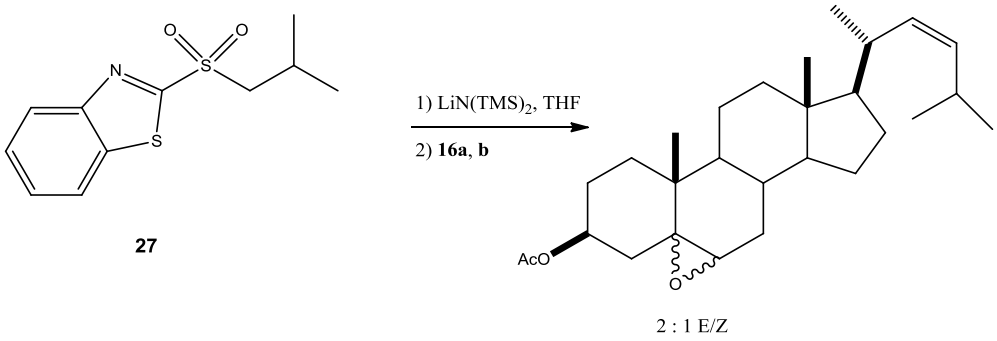

27

2 : 1 E/Z

The reaction procedure was the same with the formation of **24a**,**b**. Yield (88%). IR: 2953, 2869, 1740, 1355, 1053cm^{-1}; ^{1}H NMR (400 MHz, $CDCl_3$): δ 5.28(dd, J=15.3, 6.4 Hz, 0.35H, trans-alkene), 5.16 (dd, J=15.3, 8.1Hz, 0.36H, trans-alkene), 5.02(dd, J=8.15, 2.61, 0.63H, cis-alkene), 4.98(dd, J=8.14, 2.94Hz, 0.62H, cis-alkene), 4.81-4.72(m, 1H), 3.09(d, J=2 Hz, 0.95H, β-isomer), 2.91(d, J=4.4 Hz, 0.06, α-isomer), 2.66-2.54(m, 1H), 2.48-2.37(m, 1H), 2.23-1.67(m, 9H), 1.58-0.89(m, 29H), 0.69(s, 2H), 0.66(s, 1H); ^{13}C NMR (100Hz, $CDCl_3$): δ 170.55, 134.91, 134.24, 133.97, 133.49, 71.33, 63.66, 62.52, 58.26, 56.04, 51.01, 42.19, 39.82, 39.71, 38.00, 36.67, 36.05, 34.52, 32.44, 30.92, 29.73,

28.34, 28.27, 27.20, 26.80, 24.16, 23.58, 23.14, 22.75, 21.91, 21.32, 21.10, 17.05, 12.07, 11.97; HRMS (m/z) $[M\text{-}Na]^+$ calcd for $C_{28}H_{44}O_3Na^+$: 451.3188, found: 451.3194

Chapter 2. Study of phytosterol ester and phytosterol ether metabolism mechanism

(Portions of the material included in this chapter have been published. Brown, A. W., Hang, J. Dussault, P. H., Carr, T. P. Phytosterol ester constituents affect micellar cholesterol solubility in model bile, *Lipids* **2010**, 45, 855; Brown, A. W., Hang, J., Dussault, P. H., Carr, T. Sterol and stanol substrate specificity of pancreatic cholesterol ester lipase, *J. Nutr. Biochem*. **2010**, 21, 736)

2.1 Introduction

In the United States, cardiovascular disease is the leading cause of death over the last two decades, and now accounts for over 25% of all deaths each year.[34] These cardiovascular diseases are often linked with chronic kidney disease and hypercholesterolaemia, especially the high concentration of cholesterol in low-density lipoprotein (LDL).[35] A lipoprotein is a protein that exists as an aggregate or complex including a substantial number of fats and lipids. Lipoproteins transport fats and lipids in the bloodstream, providing a means for fats to move through a water-rich environment. The five major classes of proteins are classified according to their density (Table 1). Low-density lipoprotein (LDL) has the highest concentration of cholesterol (50%) of any lipoprotein and increased levels of LDL have been associated with increased risk of cardiovascular disease. Therefore, the goal in many pharmaceutical and nutraceutical therapies is to decrease LDL concentration in the human body. One of the most successful nutraceutical approaches to reducing LDL levels is through consumption of free plant sterol or sterol esters.[36]

Density(g/ml)	Class	%protein	%cholesterol	%phospholipid	%triacylglycerol
>1.063	HDL	33	30	29	4
1.019-1.063	LDL	25	50	21	8
1.006-1.019	IDL	18	29	22	31
0.95-1.006	VLDL	10	22	18	50
<0.95	Chylomicrons	<2	8	7	84

Table 1. Classification of lipoprotein.[37]

The mechanism by which phytosterol consumption decreases LDL has not been clarified yet. A recent study suggested that phytosterols could decrease the incorporation of cholesterol into intestinal micelles, thus reducing cholesterol absorption and increasing excretion of cholesterol.[38] Besides free phytosterols, phytosterol esters are found to show similar ability to decrease the concentration of cholesterol. As dietary additives, both free phytosterols and phytosterol esters are shown to be effective in displacing cholesterol. However, using in-vitro models, only free phytosterols have the same ability.[39] This observation suggests that the phytosterol esters must be hydrolyzed in the digestive tract to generate phytosterols which can be subsequently micellarized and absorbed. The enzyme pancreatic cholesterol esterase (PCE) is the likely agent responsible for the

hydrolysis of phytosterol esters.[40] PCE, an ester hydrolase with broad substrate specificity,[41] has showed important functions in the intestine, including controlling the bioavailability of cholesterol from dietary cholesterol esters and contributing to incorporation of cholesterol into mixed micelles.[42]

Collaborating with Dr. Carr research group (UNL Department of Nutrition and Health Sciences), we studied the mechanisms why consumption of phytosterols and phytosterol esters could decrease the LDL concentration, and examined the effect of simulated phytosterol esters hydrolysis products concentration on micellar cholesterol solubility in a model bile system. Our role in this collaboration was the preparation of phytosterol esters and ethers.

2.2 Results and discussion

Preparation of phytosterol esters

As illustrated in scheme 1, phytosterol esters were prepared via the reaction between free sterol and acid chloride, respectively. Each phytosterol ester was prepared on a 120 gram scale.

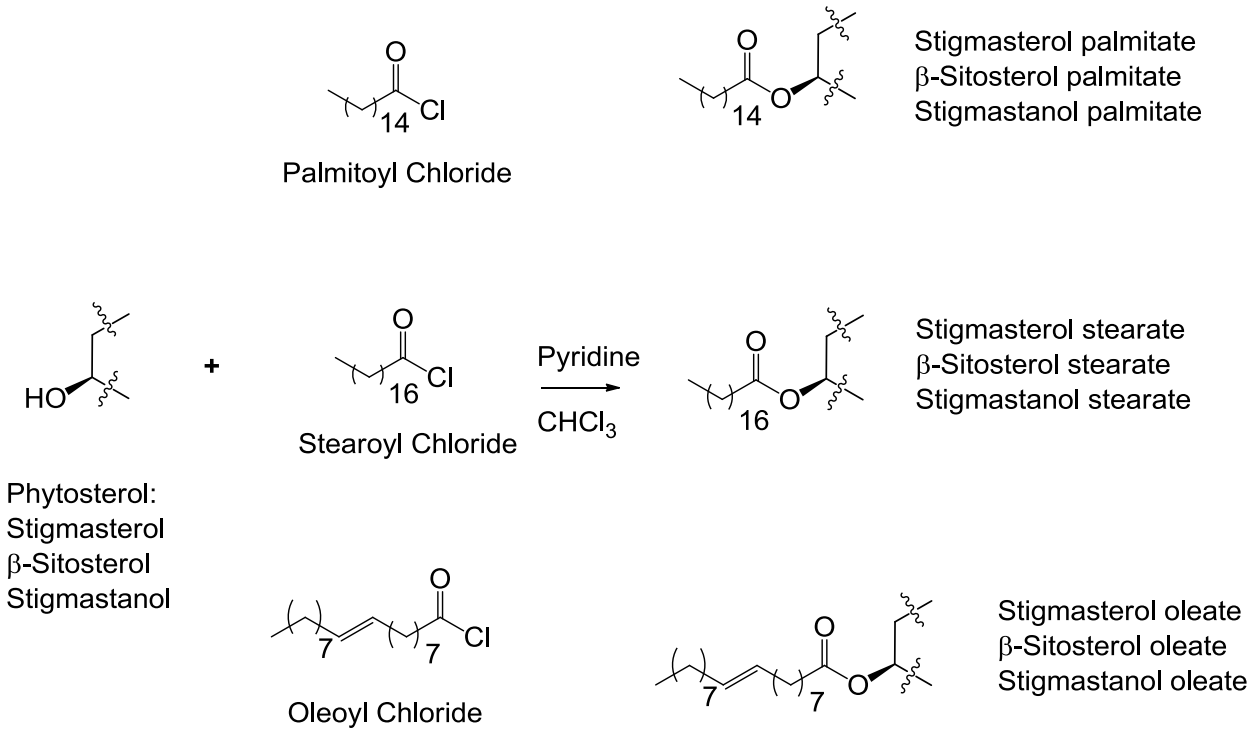

Scheme 1. Synthesis of phytosterol esters

Preparation of phytosterol octadecyl ether

The Carr group had formulated a hypothesis that the free phyotosterol, generated upon hydrolysis of phytosterol esters within the intestine, is able to displace cholesterol from micelles. In order to demonstrate that the micellar effect results from the free sterols and not the esters, we were interested in molecules that were structural analogs of the phytosterol esters but would not undergo hydrolysis by PCE or similar enzymes. We therefore prepared octadecyl ethers of the phytosterol on 120 gram scale (scheme 2).

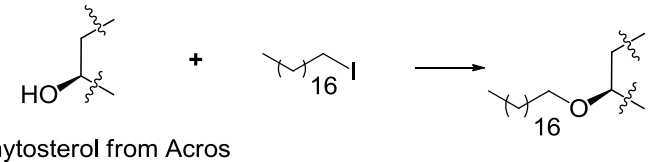

Phytosterol from Acros
β-sitosterol : 75%,
campesterol : 10%

Scheme 2. Synthesis of phytosterol octadecyl ether.

While there are numerous methods for making short-chain ethers of sterols, particularly cholesterol,[43,44] there are few reports describing synthesis of long-chain ethers. Zhang reported the alkylation of cholesterol in the condition of dodecyl bromide, sodium hydride and THF solvent afforded the cholesteryl dodecyl ether with 29% yield in the 5 gram scale.[45] However, it is difficulty to apply this method to 120 gram scale preparation, which could not use column chromatography as the purification tool. In order to overcome this problem, I screened different reaction conditions for phytosterol octadecyl ether synthesis in preparative reaction (Table 1). In the solo THF solvent, this reaction requires as much as 8 eq. alkyl iodide to complete starting sterol, with an isolation yield about 56% (Entry 1 and 2). If 18-crown-6 was added to reaction mixture to help the alkoxy anion more soluble in THF solvent, this reaction will furnish at 50% conversion of sterol (Entry 3). However, if the mixture solvent system THF/DMF(3/1) was used, the conversion and isolation yield will increase significantly (Entry 4, 5, and 6). Considering the atomic efficiency and affordable isolation yield, reaction ratio of 2 eq. alkyl iodide, 2 eq. sodium hydride was used to prepare phytosterol octadecyl ether, which could be purified by recrystallization from hot ethyl acetate.

Entry	phytosterol (eq.)	$C_{18}H_{37}I$ (eq.)	NaH (eq.)	Solvent	Yield
1	1	2	2	THF	<20% form TLC
2	1	8	8	THF	56% (10g scale)
3	1 (with 1eq. 18-crown-6)	2	2	THF	Conversion 50% from TLC
4	1	4	4	THF/DMF(3/1)	60% (10g scale)
5	1	4	8	THF/DMF(3/1)	57% (10g scale)
6	1	2	2	THF/DMF(3/1)	45% (50g scale)

Table 1. Reaction conditions screen for synthesis of phytosterol octadecyl ether.

Summary of investigations of: 1) influence of the phytosterols and phytosterol esters on micellarization of cholesterol; and, 2) the role of phytosterol ester or ether structure on the acctivity of pancreatic cholesterol esterase. This part of research was performed by Andrew Brown (PhD, 2011) in the research group of Dr. Tim Carr in the UNL Department of Nutrition and Health Sciences.

1) The presence of an equal amount of stigmasterol, β-sitosterol or stigmastanol decreases the cholesterol solubility in micelles by approximately 50%. The results indicate stigmasterol is more effective than β-sitosterol and stigmastanol in displacing cholesterol. Andrew Brown also compared different fatty acids to simulate the byproducts of ester hydrolysis of fatty esters. Unsaturated fatty acids increased the

micelle solubility of sterols compared with saturated fatty acids or no fatty acids, and the result does not depend on the size of model micelles. Finally, an in vivo study indicates that the combination of stigmasterol and saturated fatty acids is the most effective for lowing cholesterol micelle solubility. They also demonstrated that in vivo models, both free and esterified esters could lower the cholesterol concentration in micelles, which confirms the sterol esters must be firstly hydrolyzed to impart the cholesterol-lowering properties. The detailed results are reported in Brown, A. W., Hang, J., Dussault, P. H., Carr, T. *J. Nutr. Biochem*. **2010**, 21, 736.

2) Pancreatic cholesterol esterase hydrolyzes palmitate, oleate and stearate esters of cholesterol, stigmasterol, stigmastanol and β-sitosterol. The rate of hydrolysis was dependent on both the sterol and the fatty acid moieties in the following order: cholesterol > β-sitosterol = stigmasterol >stigmastanol; oleate > palmitate = stearate. The addition of free phytosterols to the system did not change hydrolytic activity of pancreatic cholesterol esterase, while addition of palmitate, oleate or stearate increased activity. The detailed results are reported in: Brown, A. W., Hang, J. Dussault, P. H., Carr, T. P. *Lipids* **2010**, 45, 855

2.3 Experimental Section

Stigmasterol (95%) was purchased from TCI America. β-Sitosterol (75%) was purchased from ACROS Organics. Stigmastanol (95%) was prepared via hydrogenation of stigmasterol.[46]

Synthesis of phytosterol esters (illustrated for β-sitosteryl palmitate):

Palmitoyl chloride (30 g, 0.11 mol) were added dropwise to a stirred mixture of β-sitosterol (30 g, 0.072mol) and dimethylaminopyridine (2.4 g, 0.021 mol) in 100 ml of dry pyridine and 400 ml of dry chloroform at room temperature, and stirred overnight. The reaction was diluted with 1L of water. The resulting suspension was acidified to a pH of 3–4 with 3 M HCl and subsequently extracted with three washes of 500 ml of dichloromethane. The combined organic layers were dried over sodium sulfate and solvent was removed under reduced pressure. The residue was recrystallized from hot ethyl acetate to furnish sitosteryl palmitate (44 g, 88% yield) as a white solid (mp 79–80 ℃). Other physical data were identical to literature reports.[47] Analysis by 1H NMR suggested the sitosteryl palmitate was 92% pure and contained approximately 8% of a mixture of stigmasteryl and stigmastanyl palmitates. The experiment was performed in three batches to collect 120 g phytosterol ester.

Other phytosterol esters were prepared with the similar procedure (Table 2).

Phytosterol ester	**Yield %**
Stigmasterol palmitate	92
β-Sitosterol palmitate	89
Stigmastanol palmitate	93
Stigmasterol stearate	94
β-Sitosterol stearate	88

Stigmastanol stearate	90
Stigmasterol oleate	83
β-Sitosterol oleate	85
Stigmastanol oleate	79

Table 2. Preparation of phytosterol esters.

Synthesis of phytosterol octadecyl ether

To a commercial mixture of phytosterol (50 g, 0.10 mol; contains β-sitosterol 75%, campesterol 10%), tetrahydrofuran (500 ml) and dimethylformamide (160 ml), sodium hydride (11 g, 0.25 mol; sodium hydride 60% dispersion in mineral oil was washed with hexane for three times) was added slowly at 0 ℃. After no evolution of gas, the reaction mixture then refluxed for 1 hour. The reaction was allowed to cool to r.t., and octadecyl iodide (91 g, 0.24 mol) was added. Then reaction mixture was refluxed for 12 hours. Tetrahydrofuran was removed under vacuum, and the residue was extracted with ether (200 ml) three times. The combined ether layer was dried over Na_2SO_4, filtered, and concentrated to afford crude product. Recrystallization from hot ethyl acetate furnished phytosterol octadecyl ether, mp 67- 68 ℃ (30 g, 45%). This experiment was performed in four batches to collect 120 g phytosterol octadecyl ether.

Chapter 3

A new peroxide fragment: generation of singlet oxygen from 1,1-dihydroperoxide and its derivatives

(Portions of the material included in this chapter have been published. Jiliang Hang, Prasanta Ghorai, Solaire A. Finkenstaedt-Quinn, Ilhan Findik, Emily Sliz, Keith T.Kuwata, and Patrick H. Dussault; Generation of Singlet Oxygen from Fragmentation of Monoactivated 1,1-Dihydroperoxides; *J. Org. Chem*, **2012**, 77, 1233.)

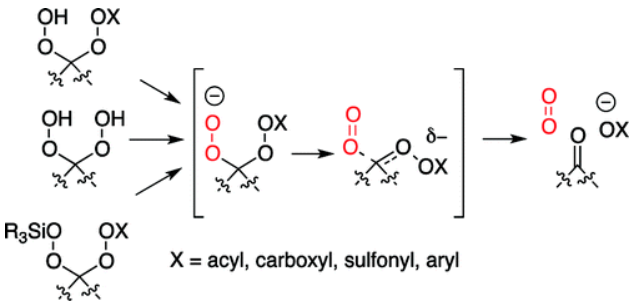

We reported that monoactivated derivatives of 1,1-dihydroperoxides undergo a previously unobserved fragmentation to generate high yields of singlet molecular oxygen ($^1O_2$).

3.1 Introduction

Oxygen, represented by the symbol O, is an element with atomic number 8 and molecular weight 16. It is one of the most abundant elements on the earth and comprises about 21% in the atmosphere, 89% in seawater, 47% in Earth's crust and 60% in the human body. In nature, one simplest but most important substance that contains oxygen element is oxygen gas (O_2), which is composed by two oxygen atoms. This colorless, odorless, and tasteless gas plays an important role for almost all living organisms, it is essential for

energy generation and respiration. Nowadays, oxygen has been widely applied in many different industries, including steel manufacturing, chemical processing, metal fabrication, petroleum refining, and etc.[48, 49]

The electronic configuration for ground state oxygen is $(1\sigma_s)^2(1\sigma_s^*)^2(2\sigma_s)^2(2\sigma_s^*)^2(2\sigma_p)^2(2\pi_x)^2(2\pi_y)^2(2\pi_x^*)^1(2\pi_y^*)^1$. This ground state is triplet ($^3\Sigma_g^-$) and paramagnetic because of two parallel electronic spins. Except for the two electrons at the antibonding $2\pi_x^*$ and $2\pi_y^*$ orbitals, all other molecular orbitals are fully occupied. For the excited state of oxygen, there are two different singlet states, $^1\Delta g$ and $^1\Sigma_g^+$ (Figure 1).

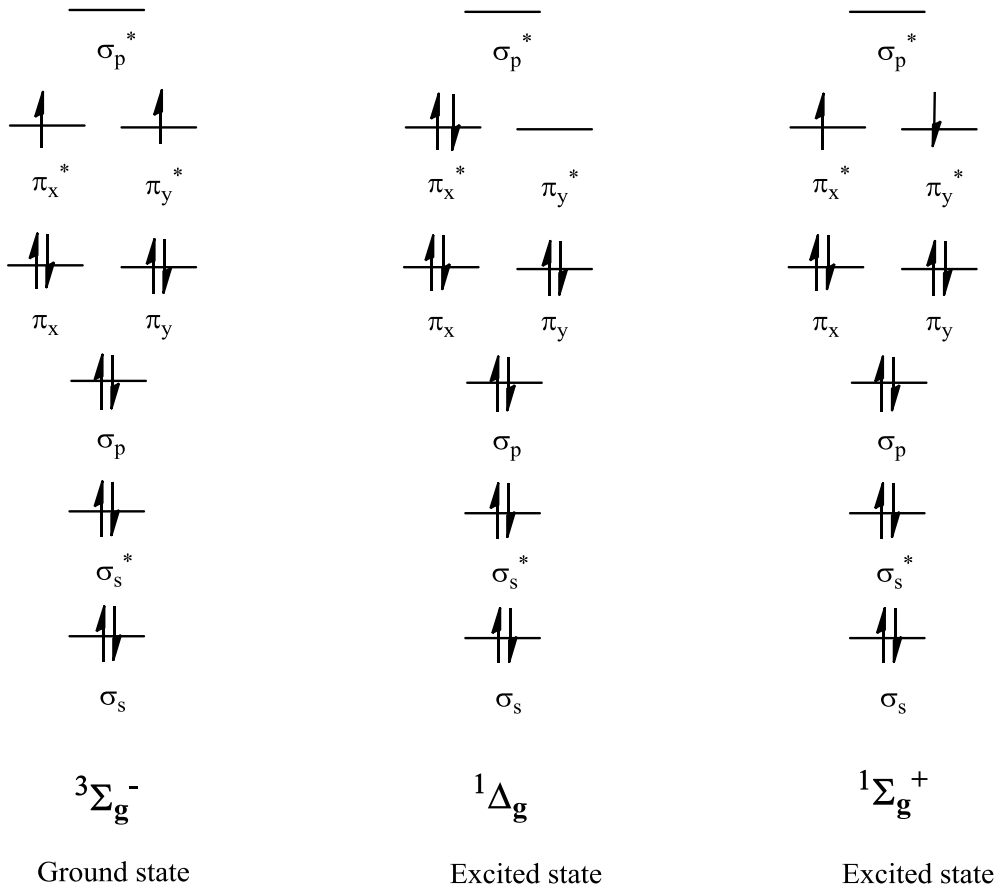

Figure 1. Electronic configurations of oxygen molecular in ground and excited states.

The $^1\Delta_g$ state is 22 kcal/mole higher in energy compared with the ground state. The radiative lifetime is 45 minutes at very low gas pressure and 10^{-6} – 10^{-3} s in solutions. The $^1\Sigma_g^+$ excited state, is 37 kcal/mole above the ground state and the radiative lifetime is 7 seconds and 10^{-11} – 10^{-9} s in solutions.[50,51] The energy diagram is illustrated in Figure 2. In condensed materials, for example reaction solvents, the high energy excited state $O_2(^1\Sigma_g^+)$ rapidly converts to the low energy excited state $O_2(^1\Delta_g)$.[52] Therefore, the "singlet oxygen" or "singlet O_2" is generally referred to the $^1\Delta_g$ state. Only the $^1\Delta_g$ oxygen is believed to be involved in organic transformations.

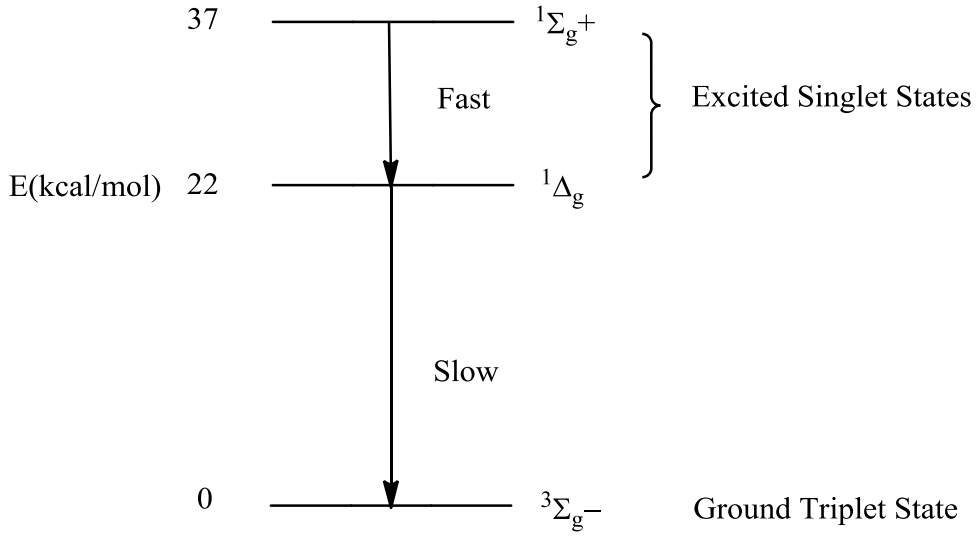

Figure 2. Energy diagram for oxygen molecule

Generation of singlet oxygen ($^1\Delta_g$)

Since high excited state singlet oxygen ($^1\Sigma_g^+$) can be converted to low excited state ($^1\Delta_g$) rapidly in condensed material, most generation methods can be considered to create the $^1\Delta_g$ state of singlet oxygen. In the past decades, researchers have developed two major types of generation methods, photosensitization and chemical generation. Both of these two methods can be used generate $^1O_2$ in preparative amounts.

Photosensitized production of singlet oxygen

Photosensitization is a light-activated process, which requires a light-absorbing photosensitizer, which is often a dye or natural pigment. Photosensitization is the most convenient method for singlet oxygen generation. As shown in Figure 3, a sensitizer absorbs the light in a specific wavelength region and is converted to an electronically excited state (sensitizer*). Then, the energy transfer from the sensitizer* to the oxygen ($^{3}\Sigma_{g}^{-}$), produces singlet oxygen and regenerating the sensitizer. The scheme is oversimplified, as the spin selection rules for the excitation require a triplet state of the sensitizer* in order to achieve excitation of the triplet ground state of oxgen. Depending upon the excited state energy of the sensitizer*, both $O_2(^{1}\Sigma_{g}^{+})$ and $O_2(^{1}\Delta_{g})$ may be formed by the energy transformation. However, the conversion from $O_2(^{1}\Sigma_{g}^{+})$ to $O_2(^{1}\Delta_{g})$ occurs spontaneously with extremely high rate constant in condensed mediums. As a result, only $O_2(^{1}\Delta_{g})$ will be generated from photosensitization.

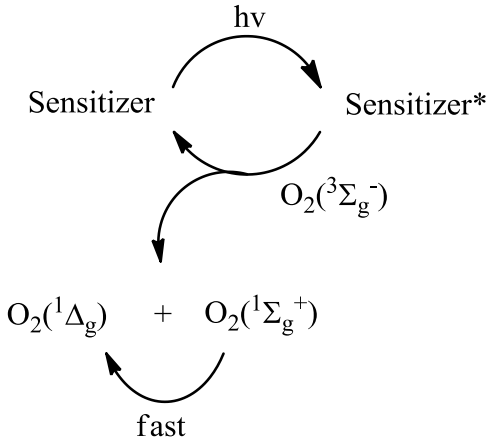

Figure 3. Generation of $^{1}O_2$ by photosensitization

A lot of dyes and pigments have been used as photosensitizers, such as Rose Bengal, methylene blue, porphyrins and phthalocyanines (Figure 4**)**. Different light sources have also been used in this process, including medium-pressure sodium lamp, tungsten lamp, xenon and mercury lamps.[53] Due to side reaction of peroxide decomposition, ultraviolet light is not generally used for photosensitization. Since visible light has more than enough energy to create a sensitizer*, it is the common light source for these photosensitizers.

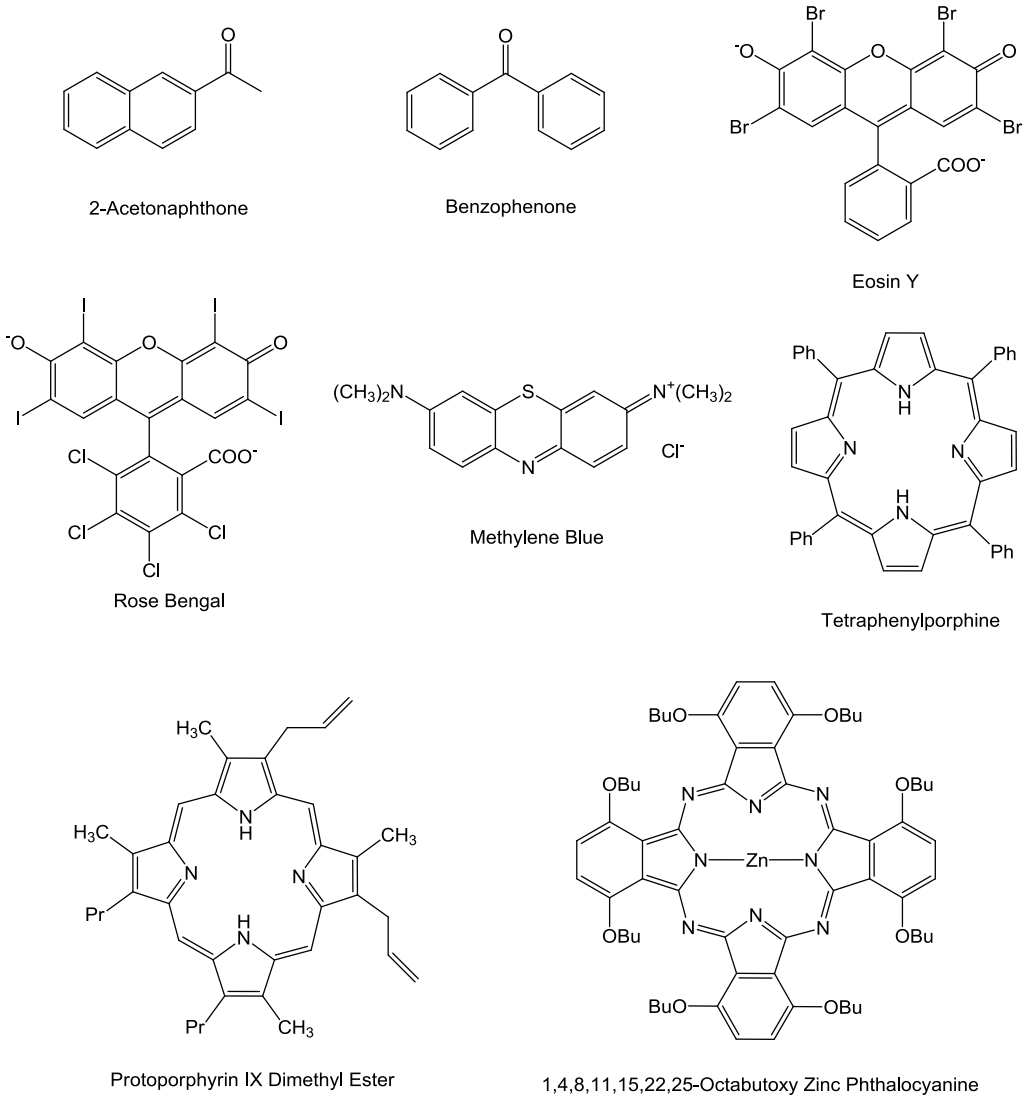

Figure 4. Structure of some photosensitizers

The singlet oxygen quantum yield is a key property for a photosensitizer. It is defined as the number of molecules of $^1O_2$ molecules generated for each photon absorbed by a photosensitizer. The quantum yields of some photosensitizer are listed in Table 1.

Photosensitizer	**Solvent**	**$^1O_2$ quantum yield**
2-Acetonaphthone	C_6H_6	0.71
Benzophenone	C_6H_6	0.36
Acridine	C_6H_6	0.83
Rose Bengal	H_2O	0.76
Methylene Blue	CH_3OH	0.51
Tetraphenylporphine	C_6H_6	0.66
$(BuO)_8ZnPc$	C_6D_6	0.47

Table 1. Singlet oxygen quantum yield of some photosensitizer.[54]

Chemical generation of singlet oxygen

Chemical sources for singlet oxygen generation are quite diverse. Many different chemical reactions have been developed to produce singlet oxygen. Most of these reactions need the water-enriched media. The first developed reaction was based upon the reaction of sodium hypochlorite with H_2O_2, which produces $^1O_2$ in nearly quantitative yield.[55] Phosphite ozonides, which are produced by reaction of ozone with phosphite, can

generate $^1O_2$ by decomposition. [56] Many other methods have also been reported, based upon decomposition of ozone, [57] hydrogen peroxide, [58] hydrotrioxides, [59] and some inorganic peroxides.[60] Generation of $^1O_2$ in organic solvent has been achieved through thermal decomposition of calcium peroxide, [61] arene endoperoxides, [62] phosphite ozonides,[63] silyl hydrotrioxides,[64] and alkyl hydrotrioxides.[65] Major classes of reaction for chemical generation of $^1O_2$ are overviewed in Figure 5.

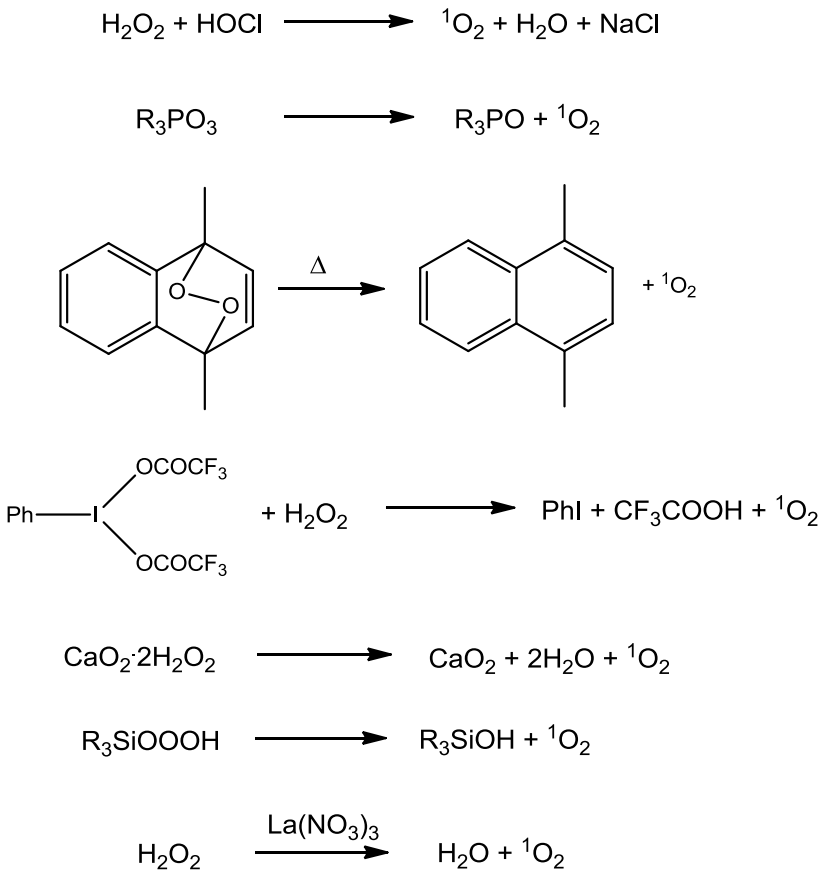

Figure 5. Chemical generation of singlet oxygen

However, the current methods for chemical generation of $^1O_2$ have some drawbacks. The first one is that most reactions require water-enriched media. $^1O_2$ has a very short lifetime in aqueous media. The second one is that when applying these reactions for preparative

purposes, many substrates do not trap $^1O_2$ efficiently, so that a large excess of reagent must be used to obtain appreciable substrate conversion.

In addition to these chemical sources, a number of other reactions have been found to produce singlet oxygen in biological systems.[66] Some enzymatic systems have been suggested to give singlet oxygen. However, most of these sources are still under investigation.

Chemical reaction of singlet oxygen

Singlet oxygen is a very useful reagent, which could allow the stereoselective and regioselective introduction of dioxygen into organic molecules. It can react with many organic compounds, including olefins, dienes, arenes, and sulfide. The reactions with alkenes are most common, and can be divided into three classes: [4+2] cycloadditions with 1,3-dienes, [2+2] cycloadditions and ene reactions with isolated double bonds.

[4+2] Cycloaddition with singlet oxygen

In a reaction that appears similar to a Diels-Alder reaction, singlet oxygen can react with *cis*-1,3-dienes for form the 6-member endoperoxides. It was once suggested that this reaction had the same concerted pathway just like the Diels-Alder reaction. However, recent studies indicates that, the perepoxide intermediate in a stepwise process would have a lower energy compared with the transition state in concerted pathway.[67] Therefore, the stepwise pathway has been suggested, and in this pathway, the formation of perepoxide intermediate would be the rate-determining step (Figure 6).

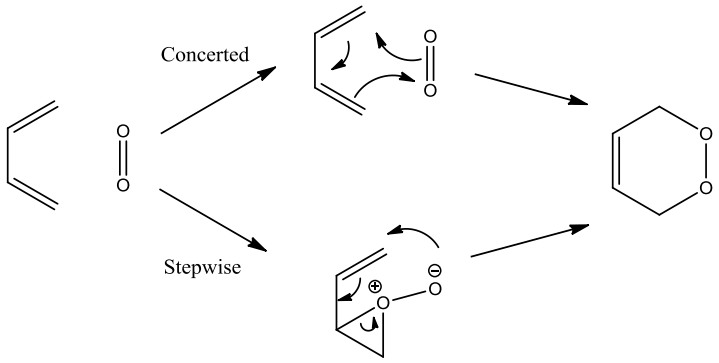

Figure 6. Possible reaction pathway for singlet oxygen [4+2] cycloaddition

1,3-butadienes which undergo [4+2] cycloadditions with $^1O_2$ can be classified into 5 different categories: nonhomoannular 1,3-diene, alkenylarenes, homoannular aliphatic dienes, heterocyclic 1,3-dienes and nonheterocyclic aromatic dienes. These types of substrates and their reaction products are shown in Figure 7. [68]

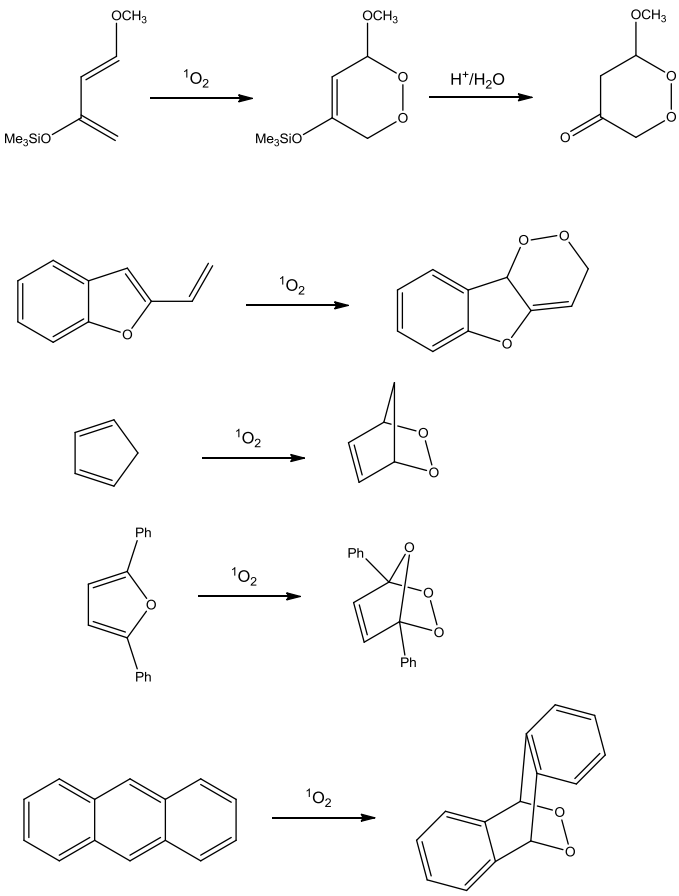

Figure 7. Examples of singlet oxygen reaction with dienes

The $^1O_2$ [4+2] cycloaddition reaction to endoperoxide product has many applications. This reaction has been widely used as key steps in total synthesis of many natural products, such as Ricciocarpin B (Figure 8).[69]

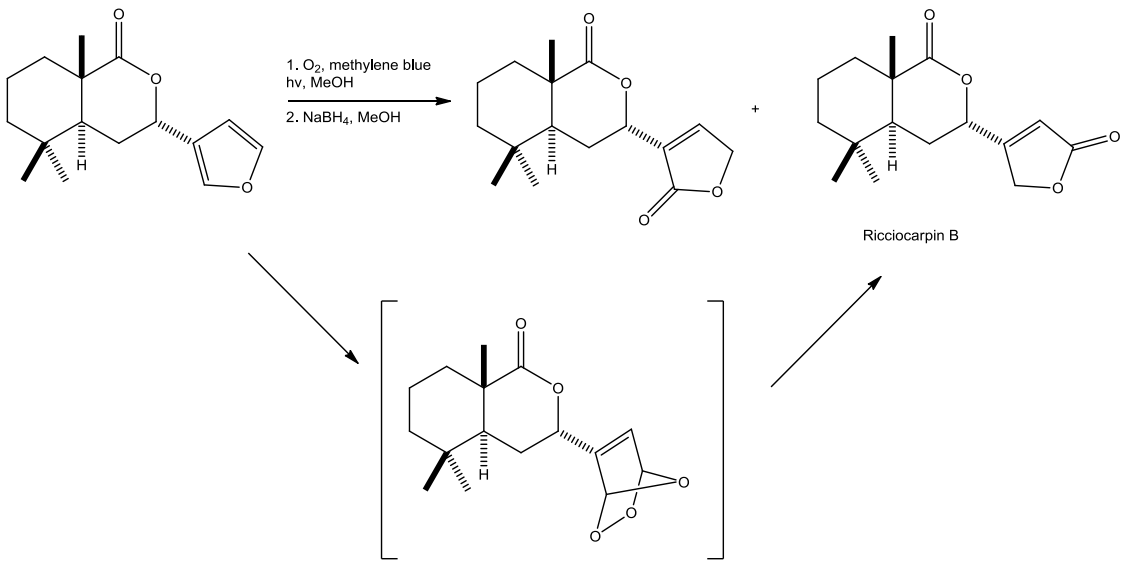

Figure 8. Application of [4+2] cycloaddition in synthesis of Ricciocarpin B

Ene reaction with singlet oxygen

The ene reaction is a type of chemical reaction between an alkene with an allylic hydrogen (the ene) and a compound containing a π-bond (the enophile), in order to form a new σ-bond. The version of this that involves a carbon-carbon bond as an enophile is called an Alder-ene reaction. In the transformation, the double bond of the ene shifts and new Y-H and C-X σ-bonds are formed (Figure 9).

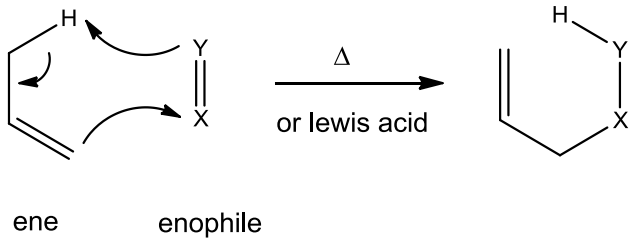

Figure 9. Ene-reaction

The ene reaction with singlet oxygen was firstly discovered by Schenk in 1943.[70] In this reaction, the alkene with allylic hydrogen substrate is oxidized by singlet oxygen to

generate an allylic hydroperoxide, where both double bond and allylic hydrogen have shifted. Study of the mechanism has suggested a stepwise mechanism involving an intermediate perepoxide (Figure 10). [71]

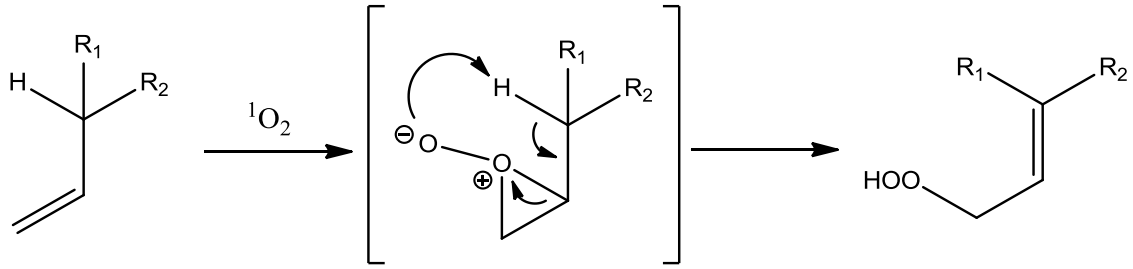

Figure 10. Mechanism of singlet oxygen ene reaction

In the ene reaction, the double bond always shifts to the allylic position, and formation of the new C-O bond and removal of the hydrogen occurs on the same face of the π system (suprafacial), and leads to formation of the *trans* olefin as a major product (Figure 11). [72]

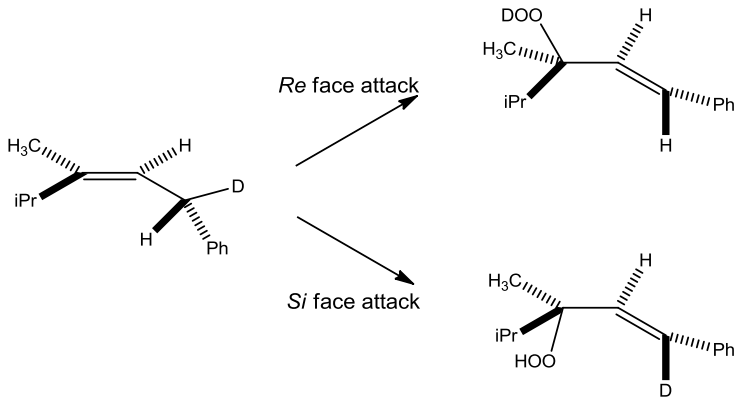

Figure 11. Suprafacial selectivity of singlet oxygen ene reaction

The allylic hydroperoxides products of the ene-reaction are important intermediates, and can undergo a number of different organic transformations (Figure 12). [73]

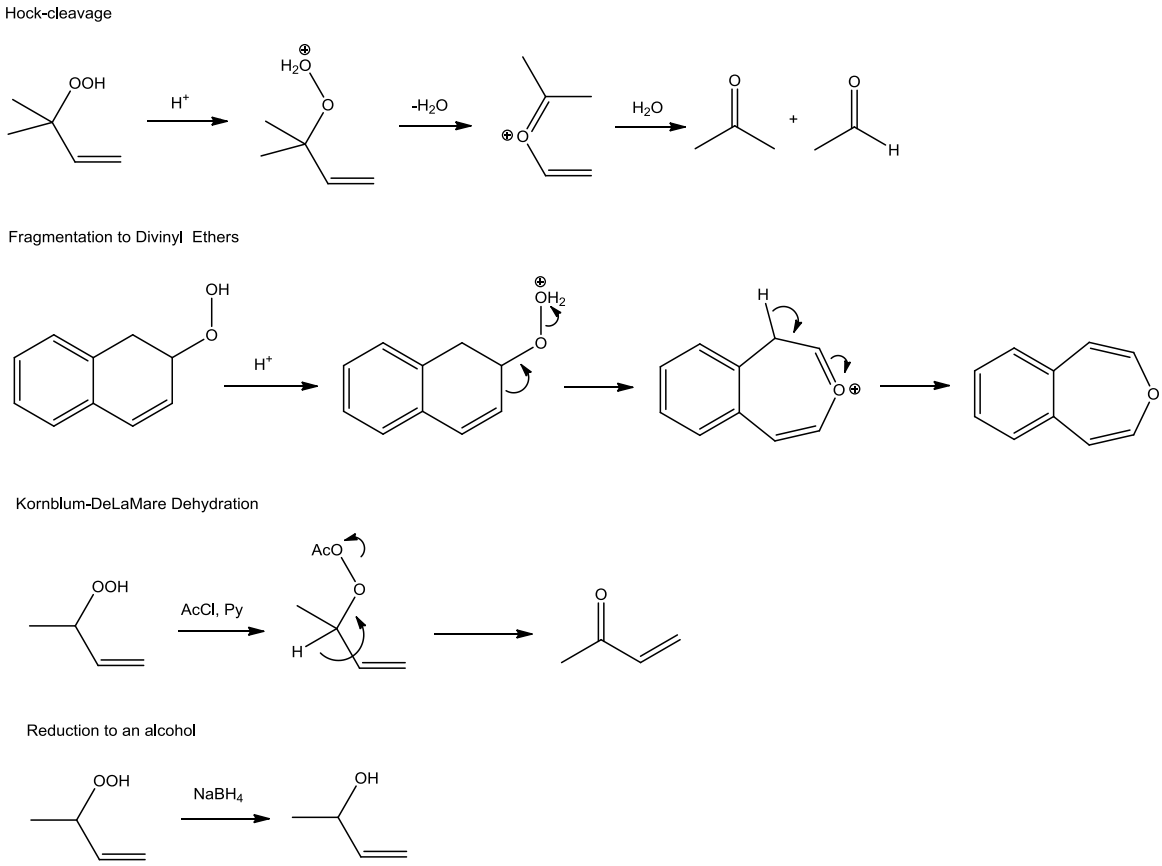

Figure 12. Examples of transformation from allylic hydroperoxides

[2+2] Cycloaddition with singlet oxygen

Beside the ene reaction, singlet oxygen can also react with olefins to form products derived from a [2+2] cycloaddition process. The [2+2] cycloaddition with singlet oxygen is usuallly disfavored compared with the ene reaction.[74] However, the [2+2] cycloaddition will be the dominant if the olefin substrates are extremely electron-rich or if the substrates lack accessible allylic hydrogens. (Figure 13).

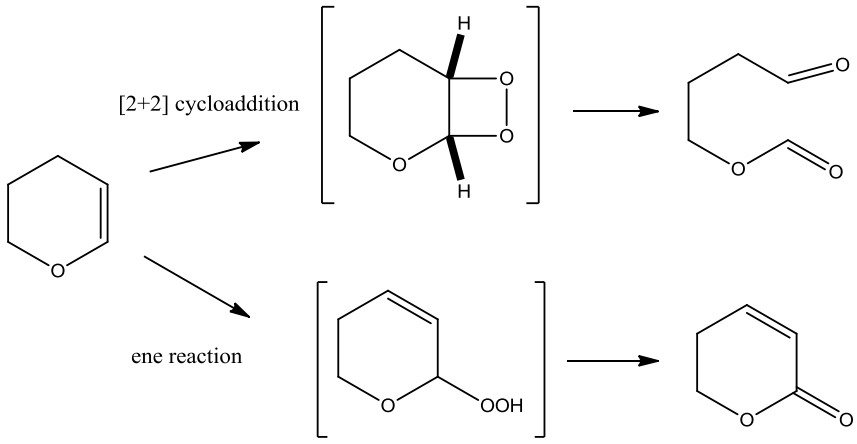

Figure 13. Competence between [2+2] cycloaddition and ene reaction

Similar with ene reaction, the [2+2] cycloaddition of alkenes with singlet oxygen is a stepwise process involving a perepoxide intermediate. Rearrangement of the perepoxide intermediate generates 1,2-dioxetane product (Figure 14).

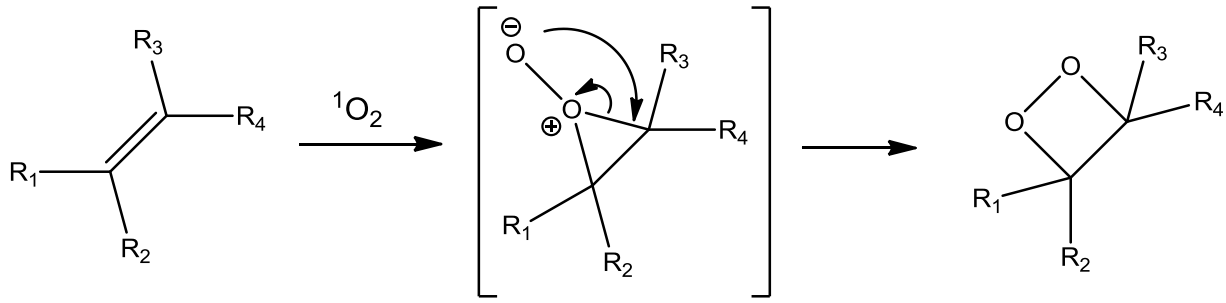

Figure 14. Mechanism of [2+2] cycloaddition with singlet oxygen

Detection of singlet oxygen

Detection of singlet oxygen can be achieved by luminescence (Figure 15). There are two types of luminescence from singlet oxygen, the direct "monomol" phosphorescence at 1270 nm,[75] and the "dimol" emission at 630 and 701 nm.[76]

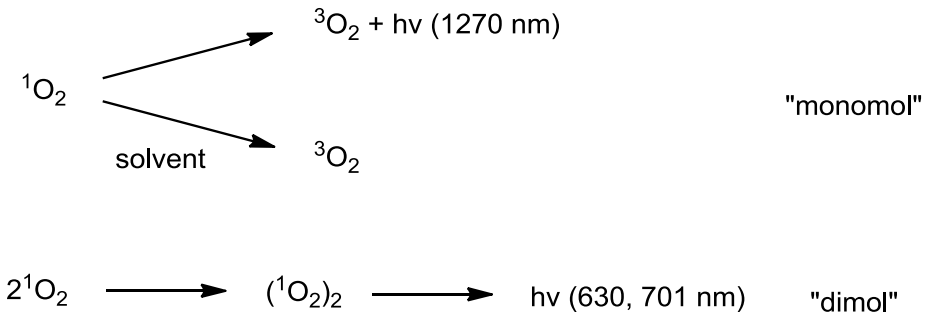

Figure 15. Luminescence from singlet oxygen

The detection at 1270 nm luminescence has become the standard technique for investigation of singlet oxygen photochemistry. The lifetime of singlet oxygen in most solvent systems is ranges from a few microseconds to milliseconds, this luminescence therefore is very weak, and results a low quantum yield from roughly 10^{-6} to 10^{-3}. To observe the luminescence at 1270 nm, specialized detectors has been developed. In the past decades, the germanium diode detector has been developed as a routine measurement of this luminescence. [77]

The singlet oxygen "dimol" luminescence arises from collision between two molecules of singlet oxygen and gives rise to a quantum of twice the energy of the monomol, with emission at 630 and 710 nm. Since this emission requires two molecules, its intensity is related to singlet oxygen concentration.

Chemical trapping of singlet oxygen

A lot of organic compounds can react with singlet oxygen to give the "fingerprint" products. Therefore, these chemicals could be used as the chemical trapping reagents in situ for singlet oxygen in the biological or other systems. Most trapping reagents react

with singlet oxygen through [4+2] reaction or ene reaction. . Some common trapping agents are shown in figure 16. α-terpinene, diphenyl isobenzofuran and 9,10-diphenylanthracene.

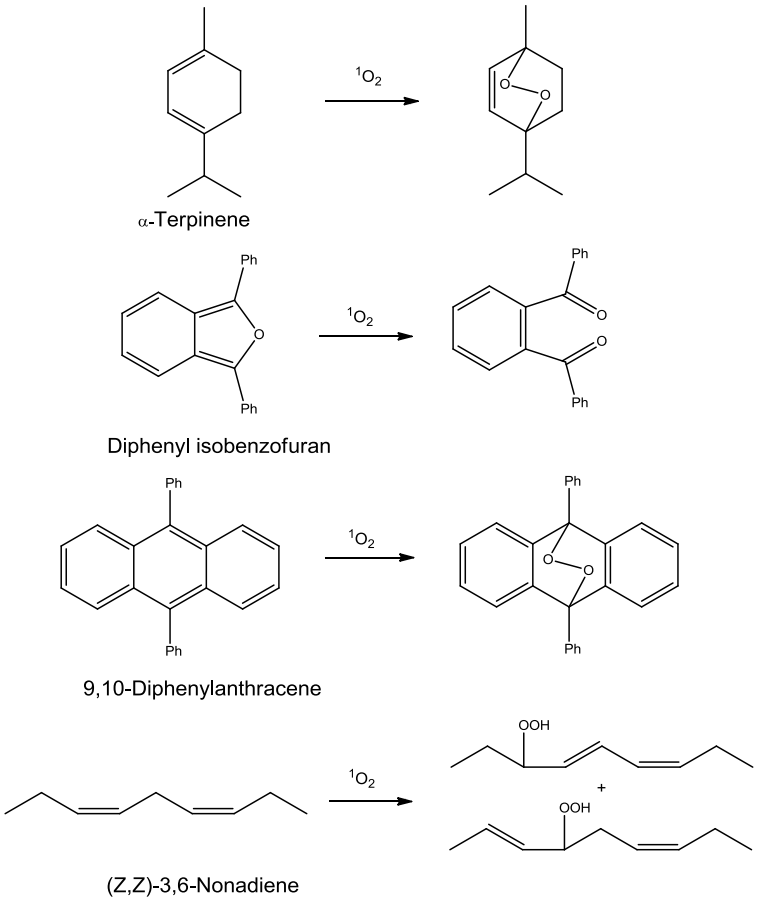

Figure 16. Examples of trapping reagents for singlet oxygen

In addition to these traditional trapping reagents, some new reagents have been developed. A recent study reported a new anthracene derivative which could be used as a singlet oxygen trapping reagent via the fluorescent probe (Figure 17).[78]

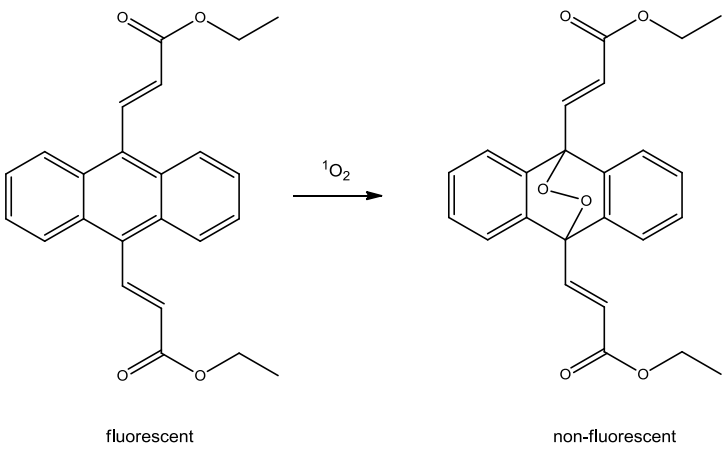

Figure 17. anthracene derivative trapping reagent.

Application of singlet oxygen

Because of its special activity, singlet oxygen has been widely used in many areas. One major application is the photodynamic therapy, which is used clinically to treat a wide range of medical conditions.[79] In photodynamic therapy, a photosensitizer is used and absorbs energy from a light source. Then the energy will transfer to the molecular oxygen in human tissue and create an excited state oxygen molecule, singlet oxygen. Ultimately, singlet oxygen will react rapidly with nearby biomolecules, which could kill cancer cells. Another important application of singlet oxygen is to be the source of chemical oxygen iodine laser.[80] The excited singlet oxygen transfers energy to iodine molecule, then the excited iodine undergoes simulated emission and radiates as laser.

3.2 Result and discussion

In the previous investigation of a "reductive ozonolysis" of alkene, singlet oxygen could be generated during rearrangement of the intermediate. [81] This transformation was hypothesized to involve nucleophilic addition of amine N-oxides to short-lived carbonyl

oxides to generate peroxyanion/oxyammonium acetals. These previously unknown intermediates were surmised to undergo fragmentation to generate the observed "reduction" products, along with a molecule of singlet oxygen, and a molecule of amine (Eq. 1). A similar fragmentation should be possible for any species featuring a geminal relationship between a peroxyanion and a heterolytically activated O-X bond. Previous study revealed the reactivity of monoperesters of readily available 1,1-dihydroperoxides. Deprotonation of these species resulted in rapid fragmentation accompanied by highly efficient liberation singlet oxygen (Eq. 2). [82]

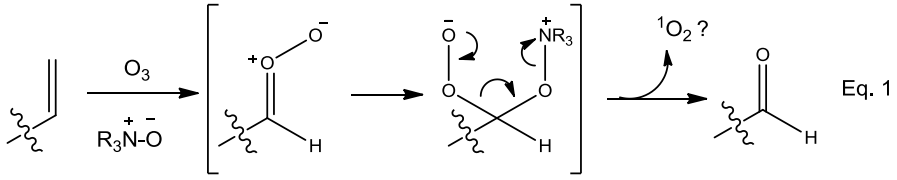

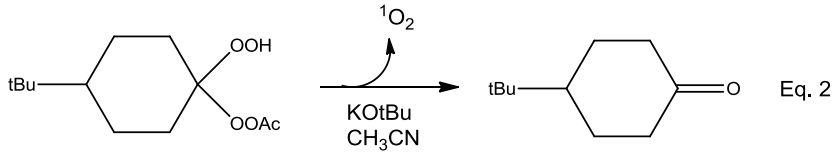

The next section will discuss our investigations of generations of singlet oxygen through decomposition of derivatives of 1,1-dihydroperoxides.

Range of acetal/ketal scaffolds

I firstly investigated the scaffolds of 1,1-dihydroperoxide substrates. A series of 1,1-dihydroperoxides (**1a**-**8a**) were prepared through Re(VII)-promoted peroxyacetalization of the corresponding ketones (Scheme 1).[83] Monoacetylation with acetic anhydride and pyridine furnished isolable monoperesters (**1b**-**4b**, **6b**, and **7b**). The exception was adamantanone dihydroperoxide (**5a**), which underwent ring expansion to a lactone upon

attempted acylation. 1,1-Dihydroperoxides derived from aldehydes reacted to form highly polar byproducts products, presumably resulting from E1cb fragmentation of peresters bearing an adjacent C-H.

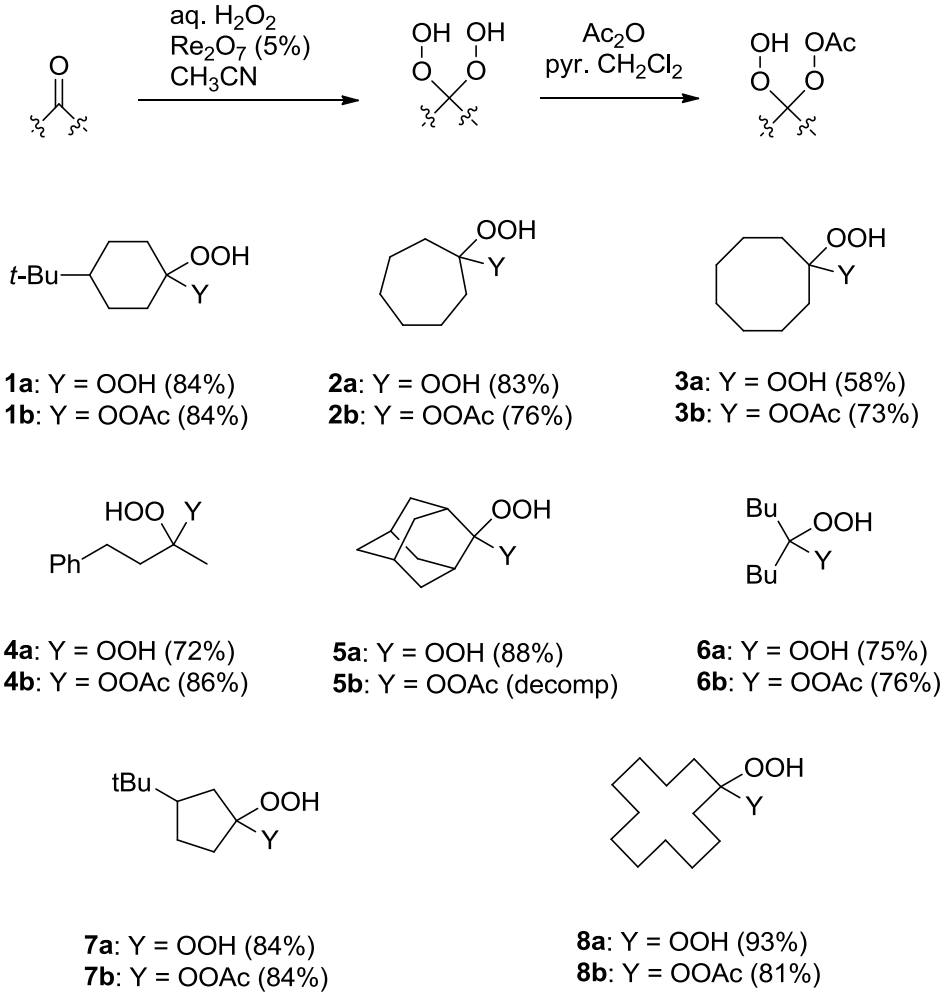

Scheme 1. Synthesis of 1,1-dihydroperoxides and derived monoperesters

Thermal stability

Dihydroperoxide **1a**, which melts without decomposition at 78-80 ℃ and is not detonated by a sharp hammer blow, undergoes a highly exothermic decomposition when heated beyond 100 ℃. Monoacetate **1b**, is stable for prolonged periods at freezer

temperature and for days at room temperature, but the onset of an exothermic decomposition is observed at approximately 76 ℃. Monocarbonate **1d** undergoes partial decomposition within days at room temperature to form a substituted caprolactone and undergoes exothermic decomposition when heated above 70 ℃ (Figure 18).

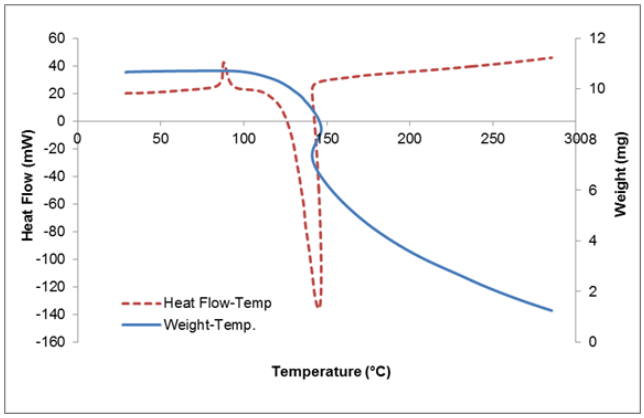

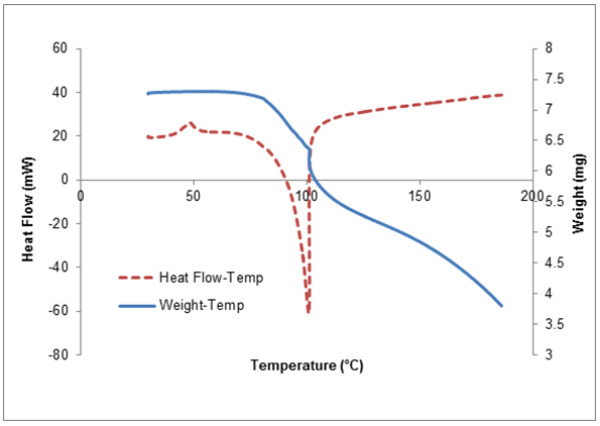

1a **1b**

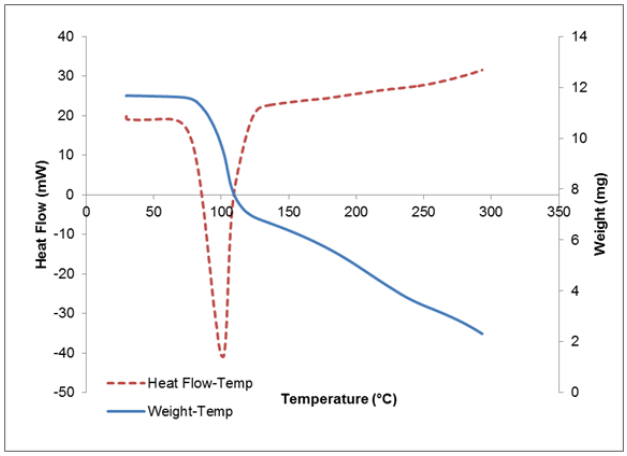

1d

Figure 18. Thermal stability of **1a**, **1b**, **1d**

Assay for $^1O_2$

Based on the synthesized substrates, the assay for $^1O_2$ was tested. The release of $^1O_2$ was quantified by chemical reaction with terpinene (**T**) or diphenylisobenzofuran (**DPBF**, **D**). Terpinene undergoes addition of $^1O_2$ to form the stable endoperoxide ascaridole (**T-O$_2$** Eq. 3). **DPBF** undergoes an even more rapid addition to generate diketone **D-O$_2$** via an unstable endoperoxide (Eq. 4). **T-O$_2$** and **D-O$_2$** are easily quantified through isolation or by NMR or GC/MS analysis in the presence of an internal standard.

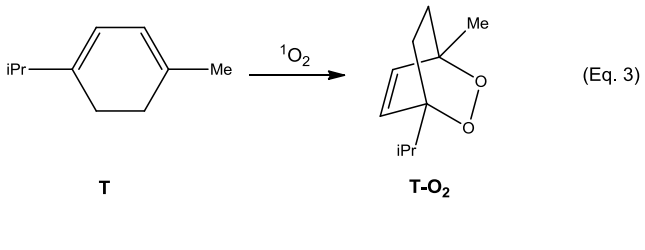

T **T-O$_2$** (Eq. 3)

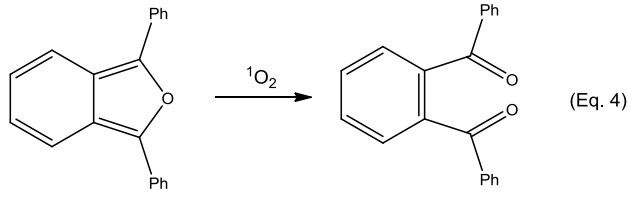

D **D-O$_2$** (Eq. 4)

Variation of the bisperoxyacetal skeleton:

I next investigated the generality of the fragmentation across a range of peroxyacetal skeletons. Solutions of monoesters **1b**-**4b**, and **6b**-**8b** were decomposed with TBAF in the presence of 0.5 equiv of terpinene (Table 2); the relative stoichiometry was chosen to facilitate product separation. Addition of base was accompanied by the disappearance (TLC) of the monoesters and the appearance of the corresponding ketone and ascaridole ($T\text{-}O_2$). The yield of trapped $^1O_2$ varied little with structural variations in the peroxyacetal. By comparison, a 1,1-dihydroperoxide (**1a**) did not react under the reaction conditions.

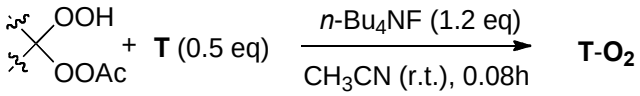

monoperester or diOOH	yield $T\text{-}O_2$ [a]
1b	26%
2b	26%
3b	23%
4b	31%
5b	27%
7b	24%
8b	23%
1a	NR

[a]Yield of $T\text{-}O_2$ relative to monoperester

Table 2. Influence of scaffold on reactivity

Influence of peroxyacetal backbone on relative reactivity

Curious as to the influence of peroxyacetal structure on the relative rate of the reaction, I investigated the decomposition of mixtures of dihydroperoxide monoesters in the presence of a limiting amount of TBAF. The results, illustrated in Scheme 3, demonstrate very little difference in reactivity between acyclic and cyclic substrates (**1b** and **4b**) or between cyclic substrates possessing different amounts of ring strain (**7b** and **1b**).

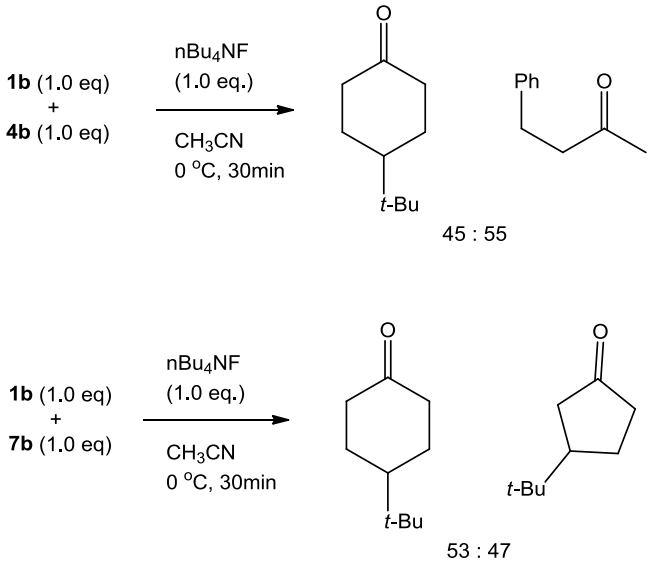

Scheme 3. Influence of peroxyacetal backbone

Influence of Solvent

Singlet oxygen has different lifetime in various solvents (Table 3). The lifetimes are typically 30-100 μs in organic solvents, and could increase to several hundred microseconds in deuterated organic solvents. In perfluorinated solvent, singlet oxygen has longest lifetime.

Solvent	**Lifetimes (μs)**	**Slovent**	**Lifetime (μs)**

H_2O	3.8	Acetone	50
D_2O	62	d_6-Acetone	723
CH_3OH	10	CH_3CN	62
Hexane	31	CD_3CN	554
CH_2Cl_2	86	C_5H_5N	16
$CHCl_3$	264	$C_6H_5CH_3$	27
$CDCl_3$	740	$C_6D_5CD_3$	320
C_6H_6	30	Freon-113	15800
C_6D_6	630	C_6F_6	3900

Table 3. Lifetime of singlet oxygen in various solvents.[84]

Decomposition of monoester **1b** in a number of solvent systems (Table 4) revealed the yield of dioxygen transfer (**T-O_2**) to be increased in solvents associated with greater $^1O_2$ lifetime as evidenced by a comparison reaction in $CDCl_3$ vs. $CHCl_3$. The exception was for perfluorinated media, in which reaction appeared limited by reagent solubility. However, improved yields were possible in fluorocarbon/CH_3CN mixtures.

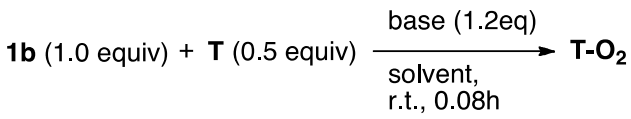

Solvent	**Base**	**Yield T-O_2** [a]
CH_3CN	*n*-Bu_4NF	26%
$CHCl_3$	*n*-Bu_4NF	17%
$CDCl_3$	*n*-Bu_4NF	35%
Acetone-d_6	*n*-Bu_4NF	33%

C_6D_6	*n*-Bu_4NF	30%
C_6F_6	*n*-Bu_4NF	7 %[b]
C_6F_6	KOtBu	1 %[b]
C_6F_6/ CH_3CN (9:1)	*n*-Bu_4NF	24 %
C_6F_6/ CH_3CN (1:1)	*n*-Bu_4NF	36 %
C_6F_{14}/ CH_3CN (1:1)[c]	*n*-Bu_4NF	28 %
Freon-113/CH_3CN (1:1)	*n*-Bu_4NF	39 %

[a]Yield of **T-O_2** based upon **1b**; [b]Limited reagent solubility; [c]biphasic

Table 4. Influence of different solvents

Order of addition

In early experiments involving decomposition of monoperester **1b**,[36] the yield of $^1O_2$ was observed to sometimes depend upon the order of addition of KOtBu and perester, suggesting the possibility of disproportionation to form poorly reactive bisperesters (vida infra). However, I reinvestigated this phenomenon using peracetate **1b** and TBAF and found an insignificant difference (Table 5).

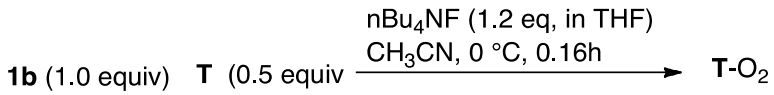

Conditions	Yield T-O_2
Add nBu_4NF to solution of **1b** and **T**	35%
Add **1b** to solution of nBu_4NF to and **T**	38%

Table 5. Influence of order of addition of reagents

Range of activating groups

Base-promoted decomposition of a perbenzoate (**1c**) and a percarbonate (**1d**) proceeded rapidly to furnish yields of trapped $^1O_2$ similar to those observed for the peracetate (**1b**) (Table 6). Attempts to prepare the analogous percarbamate or persulfonate led only to ring-expansion.

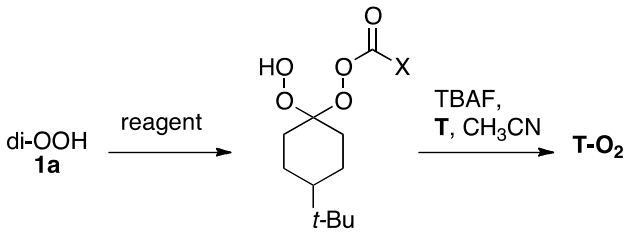

Reagent	Yield of 1c or 1d	Yield T-O_2 [a]
PhCOCl	**1c** (37%)	24%
EtOC(O)Cl	**1d** (76%)	20%
PhNCO	decomp	-
TsCl	decomp	-

[a]Based upon **T-O_2** vs. stoichometry of **1c or 1d**

Talbe 6. Investigation of other peracyl activating groups

Influence of Base/Counterion

The preliminary work had observed rapid decomposition of the dihydroperoxide monoesters in the presence of KOtBu, TBAF, or Cs_2CO_3, but not K_2CO_3 or $KHCO_3$ and we decided to further investigate the importance of the counterion. As shown in **Table 7**, comparing the decomposition of **1b** in the presence of $LiN(TMS)_2$ resulted in much lower

yields of $^1O_2$ trapping compared to reactions involving the comparably basic KOtBu or TBAF.

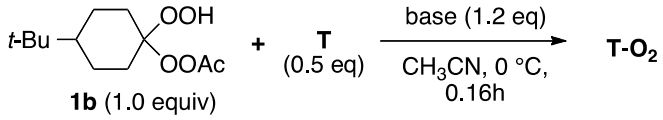

Base	Yield T-O_2 [a]
KOtBu	30%
$LiN(SiMe_3)_2$ (in THF)	4.1%
nBu_4NF (in THF)	35%

[a]relative to stoichometry of perester

Table 7. Investigation of different bases

Effect of temperature and rate of addition:

We then want to look at the effect of temperature and the rate of addition. Not surprisingly, the TBAF-promoted decomposition of monoperester **1b** was observed (TLC) to proceed significantly faster at higher temperatures; however, the yield of trapped $^1O_2$ was improved at lower temperatures (Table 8, entries 1-4). The base-promoted decomposition of the 1,1-dihydroperoxide monoesters is rapid; for example, rapid (1-2 sec) injection of 1*M* THF solution of TBAF into a rapidly stirring solution of monoester **1a** (1M in THF) results in immediate effervescence. However, a slow rate of addition was associated with a significant increase in the yield of trapped $^1O_2$ (entries 5 and 6).

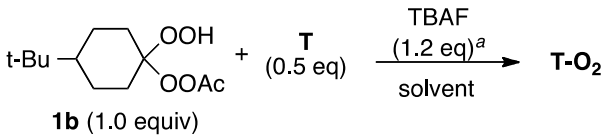

Entry	T (℃)	Solvent	Reaction time (h)	Mixing time (h)	yield T-O_2 [c]
1	rt	THF	0.25	10^{-3}	10%
2	0	THF	0.25	10^{-3}	13%
3	- 40	THF	0.25	10^{-3}	19%
4	- 78	THF	0.25	10^{-3}	24%
5	rt	CH_3CN	0.25	3×10^{-4}	24%
6	rt	CH_3CN	0.25	0.25	42%

[a] nominally 1M in THF. [b]Single injection or timed delivery from syringe pump. [c]Yield **T-O_2** relative to perester

Table 8. Influence of temperature and rate of addition

Attempted gas-phase transfer

The inverted relationship between the yield of oxygen transfer and the rate of substrate decomposition (Table 8, entries 5 and 6) led me to investigate whether $^1O_2$ could be escaping into the gas phase. A septum-covered flask was charged with an acetonitrile solution of perester **1b** and the head space was exhausted via a short Teflon tube into an acetonitrile solution of terpinene (Figure 19). Rapid (≤ 10 sec) addition of TBAF/THF into the solution of monoester **1b** led to vigorous effervescence and net efflux of a high volume of gas through the receiving solution. However, no significant amount of ascaridole (**T-O_2**) was detected.

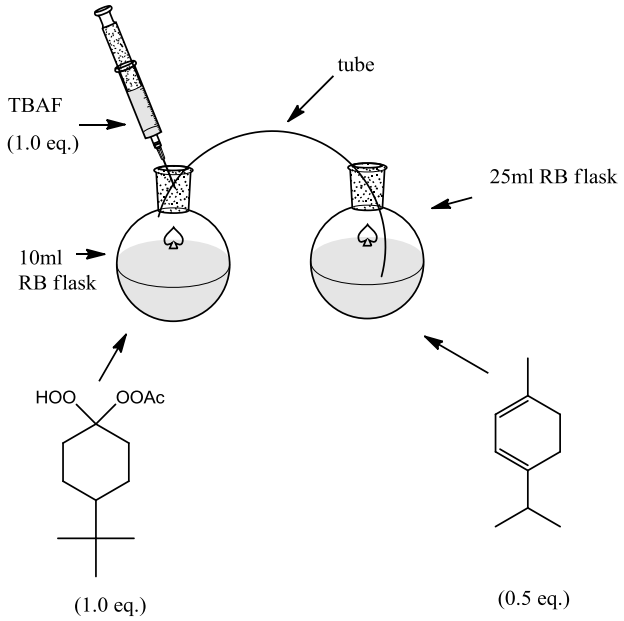

Figure 19. Gas-phase transfer attempt of singlet oxygen generation

Generation of the peroxyanion via nucleophilic desilylation

I investigated an alternative route to the presumed peroxyanion intermediate through nucleophilic desilylation. Monotrialkylsilylated substrates were readily available via silylation of the monoesters (Scheme 4). Curiously, the signal corresponding to the perester carbonyl remained invisible by ^{13}C NMR despite use of pulse delays ($\geq$ 5 sec) or the addition of $Ni(acac)_2$ as a relaxation agent.[85] The peracyl carbon could be observed as a single sharp signal at 167.8 ppm for spectra acquired at $\leq$ 40 °C (**9a**, **9b**, **11**). However, this phenomenon was not encountered with either the monoperesters (e.g. **1b**) or a bisperester (**16**).

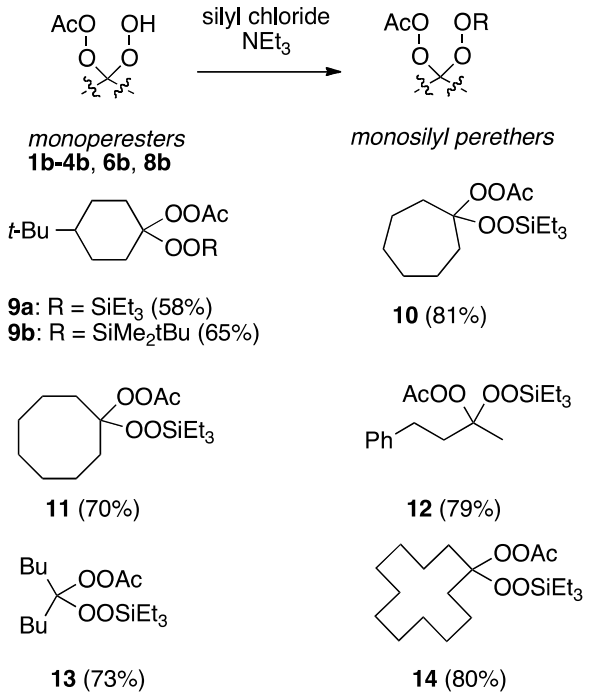

Scheme 4. Synthesis of silylated peresters

Reaction of the silylated monoesters with TBAF in the presence of a trapping agent resulted in yields of transferred $^1O_2$ equal to or exceeding those observed through deprotonation of the dihydroperoxide monoesters (Table 9).

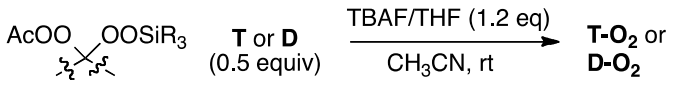

Subs	SiR_3	t (min)	Trap	Yield[a]
9a	$SiEt_3$	5	**D**	33%
9b	TBS	5	**D**	29%
9b	TBS	5	**T**	25%
9b	TBS	10	**D**	25%
10	$SiEt_3$	30	**D**	34%

11	$SiEt_3$	20	**D**	37%
12	$SiEt_3$	10	**D**	41%
13	$SiEt_3$	16	**D**	38%
14	$SiEt_3$	5	**D**	28%

[a]Yield of **T-O_2** or **D-O_2** relative to peroxide starting material.

Table 9. Frgamentation of silylated dihydroperoxide monoesters

Reactivity of bissilyl and bisacyl derivatives of a 1,1-dihydroperoxide

Preparation of bissilyl and bisacyl derivatives of dihydroperoxide **1a** are illustrated in Scheme 5. The bistriethylsilyl derivative (**15**) was an oily compound that decomposed at ~ 140 ℃. The bisacyl derivative (**16**) was a solid that melted without decomposition at 54-56 ℃. Saponification of **16** with cesium hydroxide in CH_3CN resulted in reformation of the parent ketone and generation of $^1O_2$. 1,1-Dihydroperoxide **1a** was unreactive towards base; the derived bissilyl ether (**15**) was decomposed by nBu_4NF without apparent transfer of oxygen.

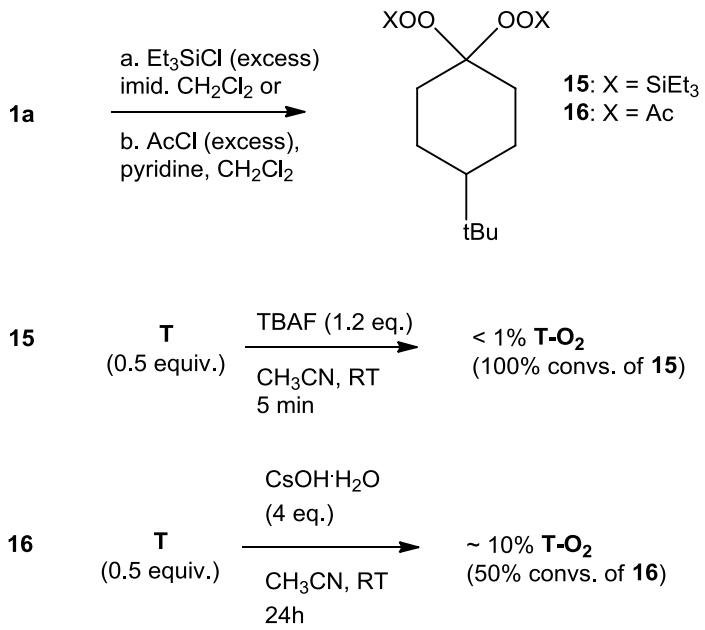

Scheme 5. Reactivity of bissilyl and bisacyl derivatives of 1,1-dihydroperoxides

Tandem activation and fragmentation

Intrigued by the possibility of generating and decomposing the monoactivated bisperoxide intermediate *in situ*, I inverstigated the reactivity of dihydroperoxide **1a** with four classes of reagents anticipated to form an activated derivative: an electron-poor nitrile, a heteroaromatic known to undergo S_NAr reaction with tertiary hydroperoxides, a sulfonyl chloride, and an acid anhydride. The initial assay qualitatively monitored the formation of ketone upon addition of base to solutions containing both the 1,1-dihydroperoxide **1a** and the additive (Table 10). In each case, the addition of stoichometric electrophile and excess KOtBu resulted in rapid conversion of the 1,1-dihydroperoxide to 4-*tert*-butylcyclohexanone without any evidence of intermediates. Although these reactions should in theory require only two equivalents of base, I found

that four equivalents were invariably required to achieve complete consumption of the dihydroperoxide.

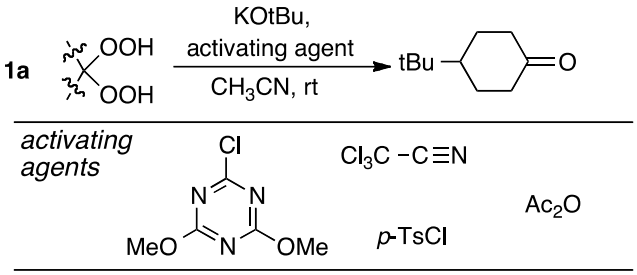

Activator	KOtBu (eq)	t (h)	Convs[a]
CCl_3CN	2.0	0.75	incomplete
CCl_3CN	4.0	≤ 0.1	complete
triazene	2.0	>12	incomplete
triazene	4.0	≤ 0.1	complete
p-TsCl	2.0	0.3	incomplete
p-TsCl	4.0	≤ 0.1	complete
Ac_2O	2.0	0.5	incomplete
Ac_2O	4.0	0.25	complete

[a]Consumption of **1a** (TLC, NMR)

Table 10. Investigation of electrophiles for activation/fragmentation

Then I reinvestigated the most promising conditions in the presence of a trapping agent. The yields of oxygen transfer were similar regardless of activating agent and proved to be as good or better as those obtained with the dihydroperoxide monoesters (Table 11).

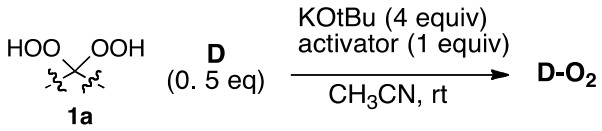

Activator	t (min)	Yield D-O_2 [a]
CCl_3CN	5	36%
triazene	5	39.5%
p-TsCl	5	39%
Ac_2O	5	31%

[a] relative to dihydroperoxide **1a**

Table 11. Oxygen transfer via in-situ activation

Preparative Reactions

I investigated the amount of reagent necessary to completely consume a trapping reagent using either the fragmentation of a preformed perester (**1b**, **8b**) or the tandem activation/fragmentation of dihydroperoxide **1a**. As illustrated in **Table 12**, complete consumption of terpinene could generally be achieved with as little as 5 equiv of reagent.

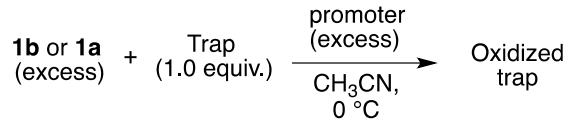

Subs (eq)	Trap	Reagents (eq)	t (min)	Product (yield[a])
1b (5)	**T**	TBAF (5)	10	**T-O$_2$** (83%)
1b (6)	**T**	TBAF (6)	10	**T-O$_2$** (100%)
1b (2.5)	**D**	TBAF (2.5)	5	**D-O$_2$** (100%)
1a (5)	**T**	triazine (5), KOtBu (20)	15	**T-O$_2$** (69%)
1a (7)	**T**	triazine (7), KOtBu (28)	15	**T-O$_2$** (100%)
8b (6)	**T**	TBAF (6)	10	**T-O$_2$** (100%)

[a] yield of **T-O$_2$** or **D-O$_2$**

Table 12. Investigation of preparative conditions

Reaction order and apparent rate constant

To gain information about the reaction rate and order, I followed the base-promoted decomposition of monoperbenzoate **1c** at 272 nm (Figure 20). In the first experiment, rapidly stirred THF solutions (0.5 mM) of dihydroperoxide monoester **1c** in a cuvette were mixed with a series of THF solutions of TBAF ranging in concentration from 0.5 to 2.00 mM. The reaction solutions were then placed in the UV spectrophotometer, and the absorbance at 272 nm monitored for 1.0 minute. Plotting the log of the initial concentration of TBAF against the negative log of the change in absorbance revealed an apparent reaction order of 0.94 in TBAF and a calculated rate constant of 10^2 L/mol-sec. Repeating the experiment with a constant concentration of TBAF and varying concentrations of **1c** indicated an order of 1.2 in peroxide and a calculated rate constant of 10^2 L/mol-sec. Overall, the results support a mechanism that is first-order in both peroxide and base.

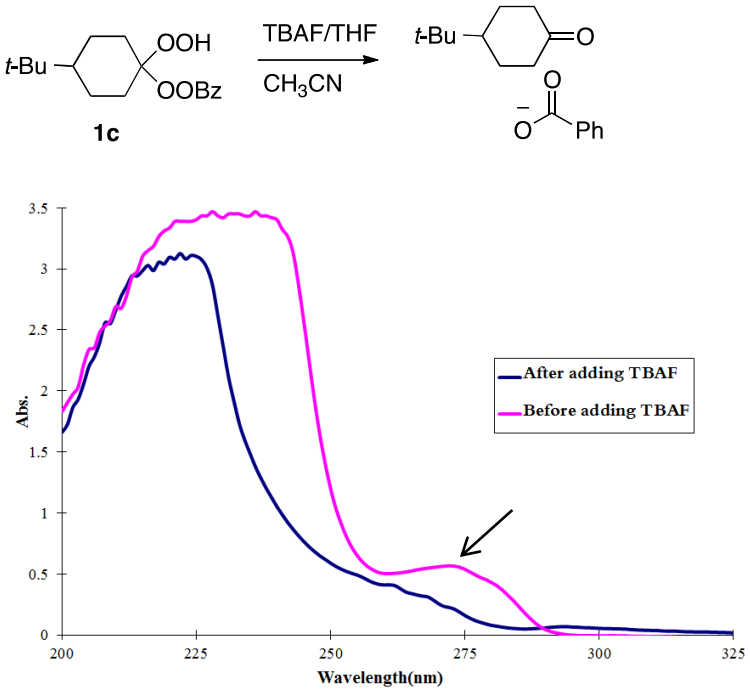

Figure 20. Monitoring rate of decompositions

Theoritical investigations

Collaborators Dr. Kuwata and his group in Macalester College finished the theoretical study of this new fragmentation.

The base-promoted fragmentation of the monoactivated 1,1-dihydroperoxides could conceivably involve a concerted Grob-like fragmentation. B3LYP/6-31+G(d,p) calculations suggest a concerted fragmentation to offer the lowest energy pathway for generation of $^1O_2$ and a carbonyl. The alternative pathway is disfavored both by the strain in the trioxetane intermediate, presumably reflecting electron pair repulsions, as well as by the high barrier for loss of $^1O_2$ (Figure 21). The detailed results were reported in *J. Org. Chem*, **2012**, 77, 1233.

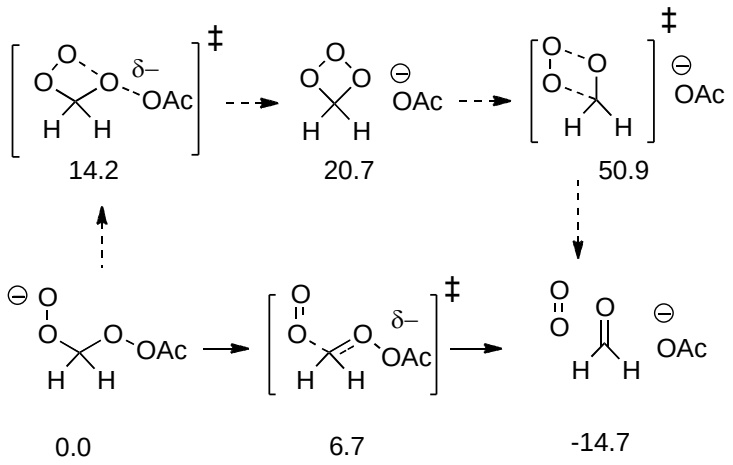

Figure 21. Theoretical study of fragmentation of the monoactivated 1,1-dihydroperoxides

Discussions

This reaction constitutes a new class of fragmentation involving a peroxyanion geminally linked to an electrophilically activated peroxide (Figure 22). The peroxyanion intermediate can be generated by deprotection, nucleophilic desilylation, or deacylation, but it must be highly dissociated. The data from competition reactions suggests that deprotonation may be rate limiting.

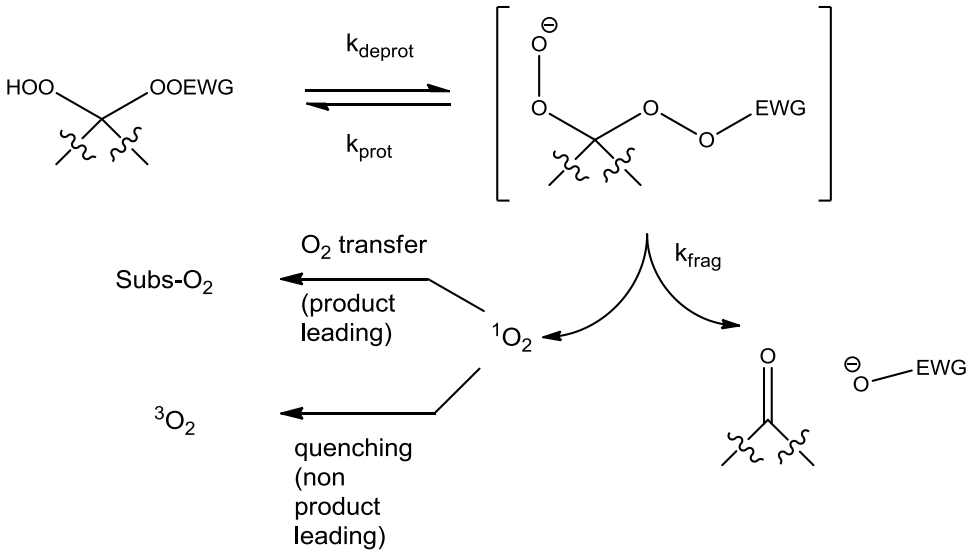

Figure 22. Mechanistic overview

The ability to achieve tandem activation and fragmentation of readily available 1,1-dihydroperoxides is noteworthy. Hydroperoxyimidates, while not isolable, have been postulated as short-lived intemediates in epoxidations.[86] Peroxytriazenes, which have been prepared from SN_{Ar} reactions of tertiary hydroperoxides, have mainly been of interest as radical sources.[87]

The observation of more efficient oxygen transfer in deuterated or halogenated solvents is not surprising given the enhanced lifetime $^1O_2$ in solvent lacking C-H, O-H, or N-H bonds. The failure of the results to scale linearly to $^1O_2$ lifetime results from the fact that the trapping substrate is by definition a potent quenching agent. However, the observation of an inverted relationship between the rate of fragmentation and the yield of trapped $^1O_2$ remains perplexing. The lifetime of $^1O_2$ in organic solvent varies little with temperature.[88] The reaction of $^1O_2$ with electron-rich alkenes has a near-zero enthalpy of activation and a strongly negative entropy of activation;[89] photosensitized oxygenations are often quite rapid even at low temperature. The observations of lower trapping yields at higher reaction rates suggest quenching or loss of $^1O_2$. However, there is no evidence of either $^1O_2$ escape into the gas phase nor any luminescence or other evidence of dimol quenching.[90]

3.3 Experimental Section

Standard procedure for preparation of 1,1-dihydroperoxide (illustrated for 1a)

To a stirred room temperature solution of 4-tert-Butylcyclohexanone (0.50 mmol) and Re_2O_7 (0.025 mmol, 5 mol%) in CH_3CN (typically 3 mL, but up to 8 mL in the case of 1h) was added 50% aqueous H_2O_2 (112 μL, 2.0 mmol). Following consumption of ketone (TLC), the reaction mixture was passed through a plug of silica, which was washed with EtOAc. Following partial concentration in vacuo, the residue was purified by flash column chromatography to give a white solid **1a**.

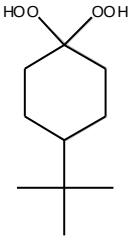

1,1-Dihydroperoxy-4-*tert*-butylcyclohexane (**1a**): 84%, white solid, mp 81-83 ℃, R_f = 0.33 (30% EA/Hex), other physical data were identical to literature reports.[41]

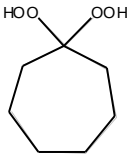

1,1-Dihydroperoxycycloheptane (**2a**): 83%, white solid, mp 59-61 ℃, R_f = 0.33 (30% EA/Hex), other physical data were identical to literature reports. [41]

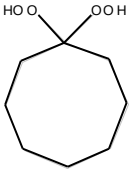

1,1-Dihydroperoxycyclooctane (**3a**): 58%, colorless oil, R_f = 0.33 (30% EA/Hex), other physical data were identical to literature reports. [41]

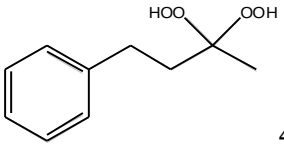

4-Phenyl-2,2-dihydroperoxybutane (**4a**): 72%, white solid, mp 61-63 ℃, R_f = 0.36 (40% EA/Hex), other physical data were identical to literature reports.[41]

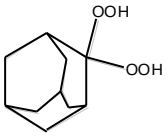

1,1-Dihydroperoxyadamantane (**5a**): 88%, white solid, mp 148-150 ℃, R_f = 0.30 (30% EA/Hex), other physical data were identical to literature reports.[41]

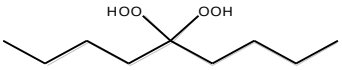

5,5-Dihydroperoxynonane (**6a**): 75%, colorless oil. R_f = 0.25 (20% EA/Hex), other physical data were identical to literature reports.[41]

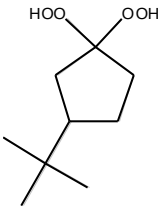

1,1-Dihydroperoxy-3-*tert*-butylcyclopentane (**7a**): 84%, colorless oil. R_f = 0.30 (30% EA/Hex), IR: 3420, 2956, 2870, 1365, 1104, 963 cm^{-1}; ^1H NMR δ 9.83 (s, 2H), 2.05 (m, 2H), 1.9 (m, 2H), 1.7 (m, 2H), 1.47 (m, 1H), 0.85 (s, 9H); ^{13}C NMR δ 121.7, 49.2, 34.5, 32.6, 31.5, 27.4, 25.6; HRMS (ESI, MeOH/H_2O, NaOAc), calc. for $C_9H_{18}NaO_4$ $(M+Na)^+$: 213.1103; found 213.1110

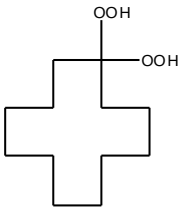

1,1-Dihydroperoxycyclododecane (**8a**): 93%, colorless oil, R_f = 0.33 (30% EA/Hex), other physical data were identical to literature reports.[41]

Standard procedure for preparation of 1,1-dihydroperoxide monoacetate (illustrated for 1b):

To a solution of 4-*tert*-butylcyclohexyl-1,1-dihydroperoxide **1a** (1.48 g, 7.2 mmol) in CH_2Cl_2 (15 mL), was added DMAP (0.09 g, 0.75 mmol), and pyridine (0.57 g, 7.2 mmol). The reaction mixture was cooled to 0 ^oC and a solution of Ac_2O (0.74 g, 7.2 mmol) in CH_2Cl_2 (10 mL) was added dropwisely over 10 min. Upon completion of addition, the reaction was stirred for 30 min at 0 ℃, and then diluted with CH_2Cl_2 (100 mL). The solution was washed with saturated $NaHCO_3$ (20 mL), water (20 mL), brine (20 mL), and then dried over anhydrous Na_2SO_4. The residue obtained upon removal of the solvent *in vacuo* was purified by silica flash chromatography (5% EA/Hex) to give a white solid (1.47 g, 84% yield).

The acid anhydride could be replaced by acid chloride (peresters) or ethoxycarbonyl chloride (percarbonates) without any other change.

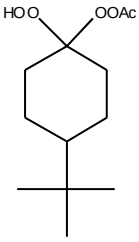

1-Acetyldioxy-1-hydroperoxy-4-*tert*-butylcyclohexane (**1b**): 84%, white solid, mp 35-37 ℃. R_f = 0.33 (10% EA/Hex); other physical data were identical to literature reports.[40]

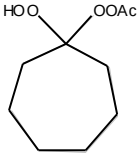

1-Acetyldioxy-1-hydroperoxycycloheptane (**2b**): 76%, colorless oil. R_f = 0.33 (10% EA/Hex); IR: 3345, 2930, 2859, 1756, 1425, 1171, 1006, 899 cm^{-1}; ^1H NMR δ 10.13 (s, 1H), 2.09 (2, 3H), 1.92 (m, 4H), 1.54 (br, 8H); ^{13}C NMR δ 171.7, 117.4, 32.5, 29.6, 22.6, 17.5; HRMS (ESI, MeOH/H_2O, NaOAc), calc. for $C_9H_{16}NaO_5$ $(M+Na)^+$: 227.0895; found 227.0898

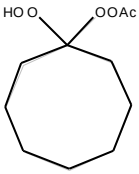

1-Acetyldioxy-1-hydroperoxycyclooctane (**3b**): 73%, colorless oil. R_f = 0.33 (10% EA/Hex); IR: 3340, 2924, 1756, 1409, 1200, 1078, 898 cm^{-1} ; ^1H NMR δ 10.13 (s, 1H), 2.15 (s, 3H), 2.00 (m, 2H), 1.89 (m, 2H), 1.63 (br, 4H), 1.57 (br, 6H); ^{13}C NMR δ 171.7, 116.8, 27.8, 27.4, 24.9, 21.8, 17.6; HRMS (ESI, MeOH/H_2O, NaOAc), calc. for $C_{10}H_{18}NaO_5$ $(M+Na)^+$: 241.1052; found 241.1046

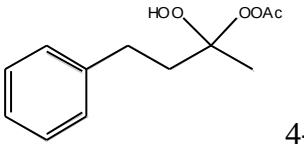

4-Phenyl-1-acetyldioxy-1-hydroperoxybutane (**4b**): 86%, colorless oil. R_f = 0.33 (10% EA/Hex); IR: 3340, 2988, 2900, 1758, 1378, 1066, 899, 748, 698 cm^{-1}; ^1H NMR δ 10.39 (s,1H), 7.35 (m, 2H), 7.28 (m, 3H), 2.86 (m, 2H), 2.24 (dd, J = 5.46, 12.9 Hz, 1H), 2.20 (s, 3H), 2.09 (dd, J = 5.46, 12,2 Hz, 1H), 1.61 (s, 3H); ^{13}C NMR δ 171.7, 141.0, 128.6, 128.4, 126.3, 113.7, 34.9, 30.2, 18.1, 17.6; HRMS (ESI, MeOH/H_2O, NaOAc), calc. for $C_{12}H_{16}NaO_5$ $(M+Na)^+$: 263.0895; found 263.0899

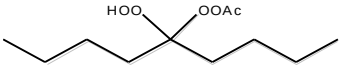

5-Acetyldioxy-5-hydroperoxynonane (**6b**): 76%, colorless oil. R_f = 0.33 (10% EA/Hex); IR: 3350, 2960, 2873, 1760, 1198, 1056, 899 cm^{-1}; ^1H NMR δ 10.13 (s, 1H), 2.12 (s, 3H), 1.73 (m, 2H), 1.56 (m, 2H), 1.34 (m, 8H), 0.90 (t, J = 7.15 Hz, 3H); ^{13}C NMR δ 171.6, 116.0, 28.9, 25.6, 22.7, 17.4, 13.8; HRMS (ESI, MeOH/H_2O, NaOAc), calc. for $C_{11}H_{22}NaO_5$ $(M+Na)^+$: 257.1365; found 257.1361

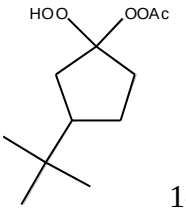

1-Acetyldioxy-1-hydroperoxy-3-*tert*-butylcyclopentane (**7b**): 84%, colorless oil. R_f = 0.33 (10% EA/Hex); IR: 2959, 2869, 1758, 1365, 1184, 1070, 962; ^1H NMR δ 10.516/10.501 (two s, totaling 1H), 2.17 (s, 3H), 2.0 (m, 4H), 1.75 (m, 2H), 1.54 (m, 1H), 0.88 (s, 9H); ^{13}C NMR δ 171.6, 122.9, 122.8, 49.3, 49.2, 34.6, 34.5, 32.7, 32.6, 31.6, 27.38, 27.36, 25.6, 17.6; HRMS (ESI, MeOH/H_2O, NaOAc), calc. for $C_{11}H_{20}NaO_5$ $(M+Na)^+$: 255.1208; found 255.1199

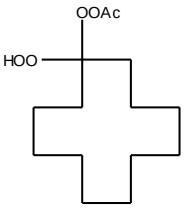

1-Acetyldioxy-1-hydroperoxycyclododecane (**8b**): 81% colorless oil. R_f = 0.33 (10% EA/Hex);. IR: 3307, 2946, 2851, 1748, 1426, 1190, 997, 850 cm^{-1}; ^1H NMR δ 10.22 (s, 1H), 2.17 (s, 3H), 1.76 (m, 2H), 1.59(m, 6H), 1.39 (br, 14H); ^{13}C NMR δ 171.7, 116.8, 26.1, 25.9, 25.8, 22.1, 21.8, 19.3, 17.7; HRMS (ESI, MeOH/H_2O, NaOAc), calc. for $C_{14}H_{26}NaO_5$ $(M+Na)^+$: 297.1678; found 297.1679

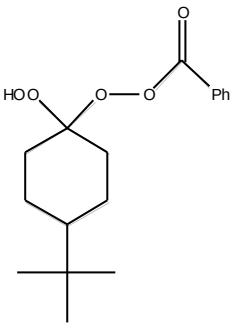

1-Benzoyldioxy-1-hydroperoxy-4-*tert*-butylcyclohexane (**1c**), 37%, white solid, mp 76-78 ℃, R_f = 0.43 (10% EA/hex), other physical data were identical to literature reports.[40]

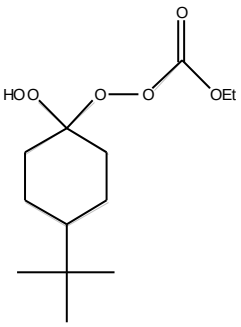

4-*tert*-Butyl-1-hydroperoxycyclohexyl ethyl carbonoperoxoate (**1d**), 76%, colorless oil, R_f = 0.22 (10% EA/Hex), other physical data were identical to literature reports.[40]

Standard procedure for preparation of monosilylated peresters (illustrated for 8a)

To a solution of monoacetate **1b** (2.46 g, 10 mmol) in CH_2Cl_2 (150 mL), was added DMAP (0.24 g, 2.0 mmol), and Et_3N (2.7 ml, 20 mmol), The reaction mixture was cooled to 0 ^oC and a solution of TESCl (1.5 g, 10 mmol) in CH_2Cl_2 (50 mL) was added dropwise over 10 min. The

reaction was stirred for 30 min at 0 ℃, and then the solvent was removed in vacuo. The residue obtained was purified by silica flash chromatography (5% EA/Hex) to give a colorless oily product (2.09 g, 58% yield).

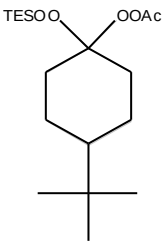

1-Acetyldioxy-1-triethylsilyldioxy-4-*tert*-butylcyclohexane (**9a**): 58%, colorless oil, R_f = 0.65 (20% EA/Hex); IR 2954, 1777, 1366, 1180, 865 cm^{-1}; ^1H NMR δ 2.33 (d, J = 14.48Hz, 2H), 2.15 (s, 3H), 1.70 (d, J = 13.2Hz, 2H), 1.46 (dt, J = 3.78,

13.8Hz, 2H), 1.30 (m, 2H), 1.05 (m, 1H), 0.98 (t, J = 7.69Hz, 9H), 0.87 (s, 9H), 0.69 (dd, J = 7.55, 16.27Hz, 6H) ; ^{13}C NMR (233K) δ 167.9, 110.6, 47.2, 32.5, 30.4, 27.7, 23.2, 18.3, 7.0, 3.4; HRMS (ESI, MeOH/H_2O, NaOAc), calc. for $C_{18}H_{36}NaO_5Si$ $(M+Na)^+$: 383.2230; found 383.2224

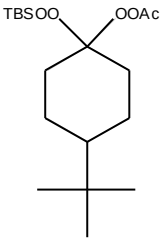

1-Acetyldioxy-1-*tert*-butyldimethylsilyldioxy-4-*tert*-butylcyclohexane (**9b**): TESCl was replaced by TBSCl without any other change, 65%, colorless oil. R_f = 0.65 (20% EA/Hex); IR: 2954, 2859, 1777, 1365, 1178, 873, 830, 784 cm^{-1} ; ^{1}H NMR δ 2.33 (m, 2H), 2.14 (s, 3H), 1.68 (m, 2H), 1.46 (dt, J = 3.85, 13.63Hz, 2H), 1.29 (m, 2H), 1.05 (m, 1H), 0.93 (s, 9H), 0.87 (s, 9H), 0.14 (s, 6H); ^{13}C NMR (233K) δ 167.9, 110.7, 47.2, 32.5, 30.4, 27.7, 26.3, 23.2, 18.6, 18.3 ; HRMS (ESI, MeOH/H_2O, NaOAc), calc. for $C_{18}H_{36}NaO_5Si$ $(M+Na)^+$: 383.2230; found 383.2235

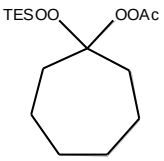

1-Acetyldioxy-1-triethylsilyldioxycycloheptane (**10**): 81%, colorless oil. R_f = 0.65 (20% EA/Hex); IR: 2969, 1776, 1409, 1170, 1056, 796 cm^{-1} ; ^{1}H NMR δ 2.08 (s, 3H), 1.95 (m, 4H), 1.55 (br, 8H), 0.97 (t, J = 7.86 Hz, 9H), 0.68 (q, 6H); ^{13}C NMR δ

115.9, 33.0, 30.2, 22.8, 17.8, 6.6, 3.7; HRMS (ESI, MeOH/H_2O, NaOAc), calc. for $C_{15}H_{30}NaO_5Si$ $(M+Na)^+$: 341.1760; found 341.1759

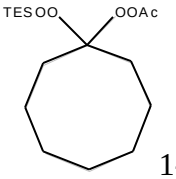

1-Acetyldioxy-1-triethylsilyldioxycyclooctane (**11**): 70%, colorless oil. R_f = 0.65 (20% EA/Hex); IR: 2956, 1776, 1363, 1184, 1066, 833, 729 cm^{-1}; ^1H NMR δ 2.10 (s, 3H), 1.97 (m, 4H), 1.56 (br, 10H), 0.97 (t, J = 7.63 Hz, 9H), 0.68 (q, 6H); ^{13}C NMR (233K) δ 168.1, 115.0, 27.8, 27.2, 24.7, 22.0, 18.2, 7.0, 3.7; HRMS (ESI, MeOH/H_2O, NaOAc), calc. for $C_{16}H_{32}NaO_5Si$ $(M+Na)^+$: 355.1917; found 355.1906

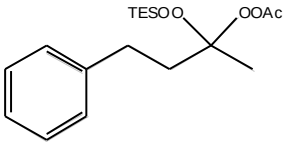

4-Phenyl-1-acetyldioxy-1-triethylsilyldioxybutane (**12**): 79%, colorless oil. R_f = 0.65 (20% EA/Hex); IR: 2957, 1780, 1182, 1103, 825, 698 cm^{-1} ; ^1H NMR δ 7.31 (m, 2H), 7.23 (m, 2H), 2.78 (t, J = 8.95 Hz, 2H), 2.15 (m, 5H), 1.57 (s, 3H), 1.04 (t, J = 7.95 Hz, 9H), 0.75 (q, 6H); ^{13}C NMR δ 141.3, 128.5, 128.3, 126.1, 111.9, 35.5, 30.4, 18.5, 17.8, 6.7, 3.7; HRMS (ESI, MeOH/H_2O, NaOAc), calc. for $C_{18}H_{30}NaO_5Si$ $(M+Na)^+$: 377.1760; found 377.1756

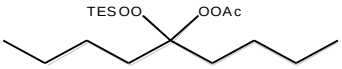

1-Acetyldioxy-1-triethylsilyldioxynonane (**13**): 73%, colorless oil. R_f = 0.65 (20% EA/Hex); IR: 2959, 1781, 1409, 1184, 1066, 802, 729 cm^{-1} ; ^1H NMR δ 2.04 (s, 2H), 1.69 (m, 2H), 1.30 (br, 8H), 0.93 (t, J = 7.85 Hz, 9H), 0.85 (t, J = 6.35Hz, 6H), 0.63 (q, 6H); ^{13}C NMR δ 114.1, 29.6, 25.5, 22.7, 17.7, 13.7, 6.5, 3.6; HRMS (ESI, MeOH/H_2O, NaOAc), calc. for $C_{18}H_{30}NaO_5Si$ $(M+Na)^+$: 377.1760; found 377.1768

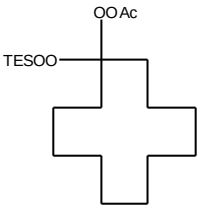

1-Acetyldioxy-1-triethylsilyldioxycyclododecane (**14**): 80%, colorless oil. R_f = 0.65 (20% EA/Hex); IR: 2929, 1779, 1470, 1186, 1003, 851, 728 cm^{-1}; ^1H NMR δ 2.08 (s, 3H), 1.73 (m, 4H), 1.37 (br, 18H), 0.96(t, J = 7.96 Hz, 9H), 0.66 (q, 6H); ^{13}C NMR δ 114.9, 26.7, 26.1, 26.0, 22.3, 21.9, 19.4, 6.7, 3.7; HRMS (ESI, MeOH/H_2O, NaOAc), calc. for $C_{20}H_{40}NaO_5Si$ $(M+Na)^+$: 411.2543; found 411.2536

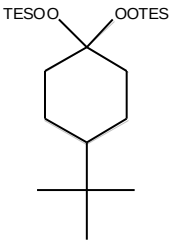

1,1-Triethylsilyldioxy-4-*tert*-butylcyclohexane (**15**)

To a solution of 4-*tert*-butylcyclohexyl-1,1-dihydroperoxide **1a** (0.50 g, 2.5 mmol) in DMF (30 mL), was added Et_3N (0.76 ml, 5.4 mmol), The reaction mixture was cooled to -40 ^oC and TESCl (0.91 ml , 5.4 mmol) was added. The reaction was stirred for 1 hour at -40 ℃. Upon completion of addition, the reaction was added with brine (100 mL). The

solution was washed extracted with hexane (50 ml) three times and then combined organic layer was dried over anhydrous Na_2SO_4. The residue obtained upon removal of the solvent *in vacuo* was purified by silica flash chromatography (5% EA/Hex) to give colorless oil. (0.57g, 53%), R_f = 0.80 (20% EA/Hex), other physical data were identical to literature reports.[91]

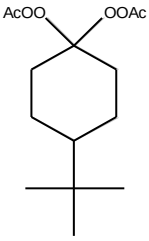

1,1-Diacetyldioxy-4-*tert*-butylcyclohexane (**16**)

To a solution of 4-*tert*-butylcyclohexyl-1,1-dihydroperoxide **1a** (1.48 g, 7.2 mmol) in CH_2Cl_2 (15 mL), was added DMAP (0.09 g, 0.75 mmol), and pyridine (0.57 g, 7.2 mmol). The reaction mixture was cooled to 0 ^oC and a solution of Ac_2O (1.48 g, 14.4 mmol) in CH_2Cl_2 (10 mL) was added dropwise over 10 min. Upon completion of addition, the reaction was stirred for 30 min at 0 ℃, and then diluted with CH_2Cl_2 (100 mL). The solution was washed with saturated $NaHCO_3$ (20 mL), water (20 mL), brine (20 mL), and then dried over anhydrous Na_2SO_4. The residue obtained upon removal of the solvent *in vacuo* was purified by silica flash chromatography (10% EA/Hex) to give a white solid (1.55 g, 75% yield). mp 54-56 ℃; R_f = 0.30 (20% EA/Hex); IR: 2960, 2869, 1785, 1361, 1187, 1057, 896 cm^{-1}; ^1H NMR δ 2.34 (d, J = 12.81 Hz, 2H), 2.08 (s, 3H), 2.07 (s, 3H), 1.75 (d, J = 14.12 Hz, 2H), 1.62 (m, 2H), 1.31 (m, 2H), 1.09 (m, 1H), 0.86 (s, 9H); ^{13}C NMR δ 167.5, 167.4, 111.5, 47.1, 32.2, 30.1, 27.5, 23.2, 17.5, 17.4; HRMS (ESI, MeOH/H_2O, NaOAc), calc. for $C_{14}H_{24}NaO_6$ $(M+Na)^+$: 311.1471; found 311.1467

Standard procedure for fluoride-mediated decomposition of silylated monoesters:

To a solution of **9a** (77 mg, 0.2 mmol) and 1,3-diphenylisobenzofuran (DPBF, **D**, 27 mg, 0.1 mmol) in CH_3CN (2 ml), was injected TBAF (1M in THF, 0.24 ml, 0.24 mmol) within 5 seconds, and the reaction mixture stirred at room temperature for 5 minutes. Then solvent was removed by vacuum, and the residue was purified by column chromatography on silica gel to give the pure product **D-O_2** (19 mg, 66%)

NMR method for quantification of oxygen transfer (illustrated for dioxygenation of terpenine)

To a solution of **1b** (50 mg, 0.2 mmol) and α-terpinene (**T**, 90%, 15 mg, 0.1 mmol) in CH_3CN (2 ml), TBAF (1M in THF, 0.24 ml, 0.24 mmol) was injected within 5 seconds, and the reaction mixture stirred at room temperature for 5 minutes. Then solvent was removed by vacuum. Internal standard 1,2- dichloroethane was added and **T-O_2** was measured by NMR.

The alkene peak at 6.3 ppm (dd, J = 8.56, 25.93Hz) of T-O_2 will be used for calculation via following equations:

$\text{Actual Mole}_{\text{T-O2}} = \text{Mole}_{\text{standard}} * 2 * \text{Area}_{\text{T-O2}} / \text{Area}_{\text{standard}}$

$\text{Therefore, the calculated \%yield} = 100 * \text{Actual Mole}_{\text{T-O2}} / \text{Theoretical Mole}_{\text{T-O2}}$

Alternatively, quantification of **T-O_2** can be conducted by GC/MS using a reported procedure [5]

GC/MS quantification of relative reactivity of dihydroperoxide monoesters (Illustrated for 1b and 4b)

Prepare a standard solution of 4-*tert*-butylcyclohexanone (1 mmol) and benzylacetone (1 mmol) in CH_3CN (2 ml) . The standard ratio α = $Area_{4\text{-}tert\text{-butylcyclohexanone standard}}/Area_{benzylacetone\ standard}$. The mole ratio of the ketone products from the competitive reaction is $Area_{4\text{-}tert\text{-butylcyclohexanone actual}}/(\alpha * Area_{benzylacetone\ actual})$

Standard procedure for tandem activation and decomposition of 1,1-dihydroperoxides (Illustrated for CCl_3CN activator)

To a solution of **1a** (41 mg, 0.2 mmol), CCl_3CN (29 mg, 0.2 mmol) and 1,3-diphenylisobenzofuran (DPBF, **D**, 27 mg, 0.1 mmol) in CH_3CN (2 ml), was added KO*t*Bu (90 mg, 0.8 mmol). The reaction was monitored by TLC and stirred at room temperature for 5 minutes. Then solvent was removed by vacuum, and the residue was purified by column chromatography on silica gel to give the pure product **D-O_2** (21 mg, 72% yield based upon **D** or 36% based upon consumed 1,1-dihydroperoxide).

Investigations of Reaction Order and Reaction Kinetics

Part I. Fixed monoperester concentration unchanged, variable [TBAF].

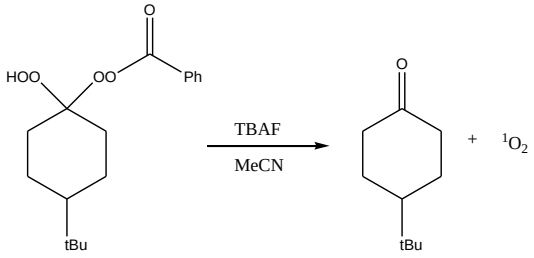

Conditions: 0.5mM monoperester 3mL, TBAF 15μL: Rapidly stirred THF solutions (0.5 mM) of dihydroperoxide monoester **1c** in a cuvette were individually treated with a series of THF solutions of TBAF ranging in concentration from 0.5 to 2.00 mM. The reaction

solutions were mixed and the cuvettes then placed in the UV spectrophotometer, with the absorbence at 272 nm monitored for 1.0 minute.

$$V_0 = k \times [\text{Monoperester}]_0^m \times [\text{TBAF}]_0^n$$

$$-\frac{d[\text{Monoperester}]_0}{dt} = k \times [\text{Monoperester}]_0^m \times [\text{TBAF}]_0^n$$

$$\text{Abs} = e \times b \times [\text{Monoperester}]$$

$$-\frac{d(\text{Abs})_0}{dt} = k \times [\text{Monoperester}]_0^m \times e \times b \times [\text{TBAF}]_0^n$$

$$K_1 = k \times [\text{Monoperester}]_0^m \times e \times b$$

$$-\frac{d(\text{Abs})_0}{dt} = K_1 \times [\text{TBAF}]_0^n$$

$$\text{Lg}\left(-\frac{d(\text{Abs})_0}{dt}\right) = n \times \text{Lg}\left([\text{TBAF}]_0\right) + \text{Lg}\left(K_1\right)$$

At the initial point, V_0 is the initial rate, $(Abs)_0$ is the initial absorbance, $[Monoperester]_0$ and $[TBAF]_0$ are the initial concentration

$[TBAF]_0$/mM	$-d(Abs)_0/dt$	$Lg([TBAF]_0)$	$Lg(-d(Abs)_0/dt)$
0.50	0.0302	-0.301	-1.520
0.75	0.0339	-0.125	-1.470
1.00	0.0524	0.000	-1.281
1.25	0.0647	0.097	-1.189
1.50	0.0789	0.176	-1.103
1.75	0.0845	0.243	-1.073
2.00	0.1055	0.301	-0.977

Then plot $Lg(-d(Abs)_0/dt)$ vs $Lg([TBAF]_0)$

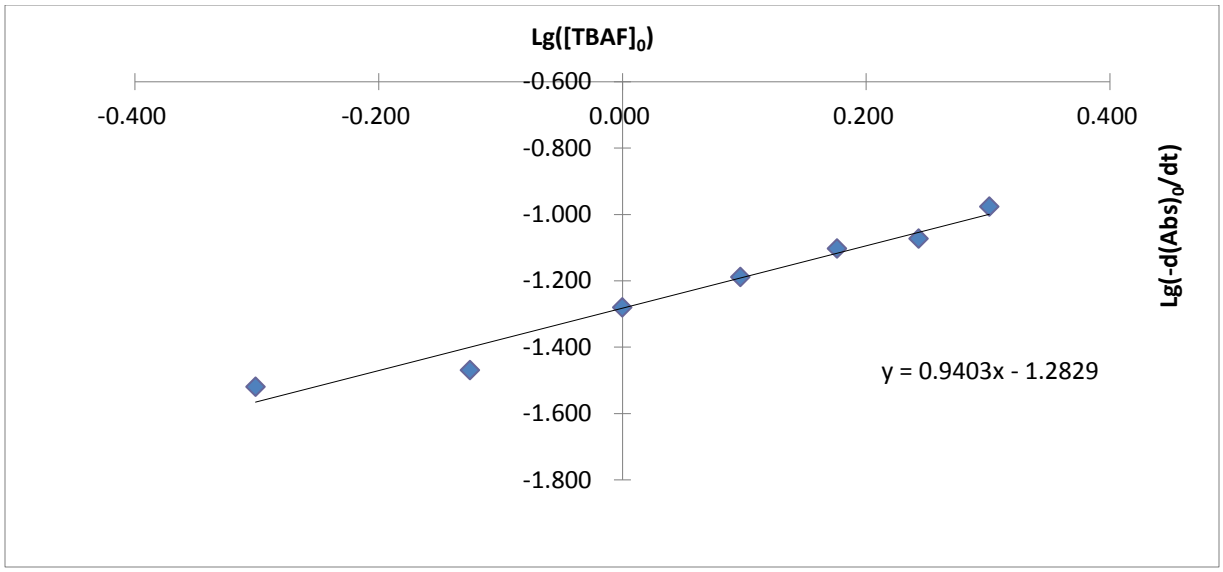

n = 0.9403. This indicates the reaction is a first order reaction to TBAF reactant

K_1 = 0.05213 L ↗$mmol^{-1}$ ↗s^{-1}

Part II. Fixed TBAF concentration unchanged, variable [Monoperester]

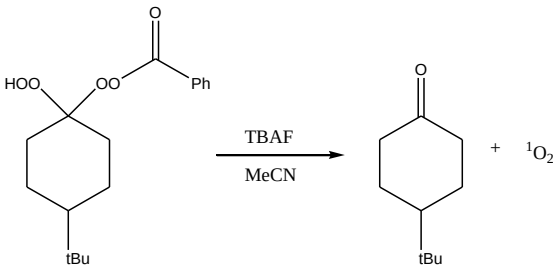

Conditions: Monoperester 3mL, TBAF 0.3M 15µL: The experiment described above was repeated except that the concentration of TBAF was held constant while the concentration of **1c** was varied.

$$V_0 = k \times [\text{Monoperester}]_0^m \times [\text{TBAF}]_0^n$$

$$-\frac{d[\text{Monoperester}]_0}{dt} = k \times [\text{Monoperester}]_0^m \times [\text{TBAF}]_0^n$$

$$\text{Abs} = e \times b \times [\text{Monoperester}]$$

$$-\frac{d(\text{Abs})_0}{dt} = k \times [\text{Monoperester}]_0^m \times e \times b \times [\text{TBAF}]_0^n$$

$$K_2 = k \times [\text{TBAF}]_0^n \times e \times b$$

$$-\frac{d(\text{Abs})_0}{dt} = K_2 \times [\text{Monoperester}]_0^m$$

$$\text{Lg}\left(-\frac{d(\text{Abs})_0}{dt}\right) = m \times \text{Lg}\left([\text{Monoperester}]_0\right) + \text{Lg}\left(K_2\right)$$

At the initial point, V_0 is the initial rate, $(Abs)_0$ is the initial absorbance, $[Monoperester]_0$ and $[TBAF]_0$ are the initial concentration

$[Monoperester]_0$/mM	**$-d(Abs)_0/dt$**	**$Lg([Monoperester]_0)$**	**$Lg(-d(Abs)_0/dt)$**
0.3	0.0352	-0.523	-1.453
0.4	0.0551	-0.398	-1.259
0.5	0.0695	-0.301	-1.158
0.6	0.0824	-0.222	-1.084
0.7	0.111	-0.155	-0.955
0.8	0.113	-0.097	-0.947
0.9	0.133	-0.046	-0.876

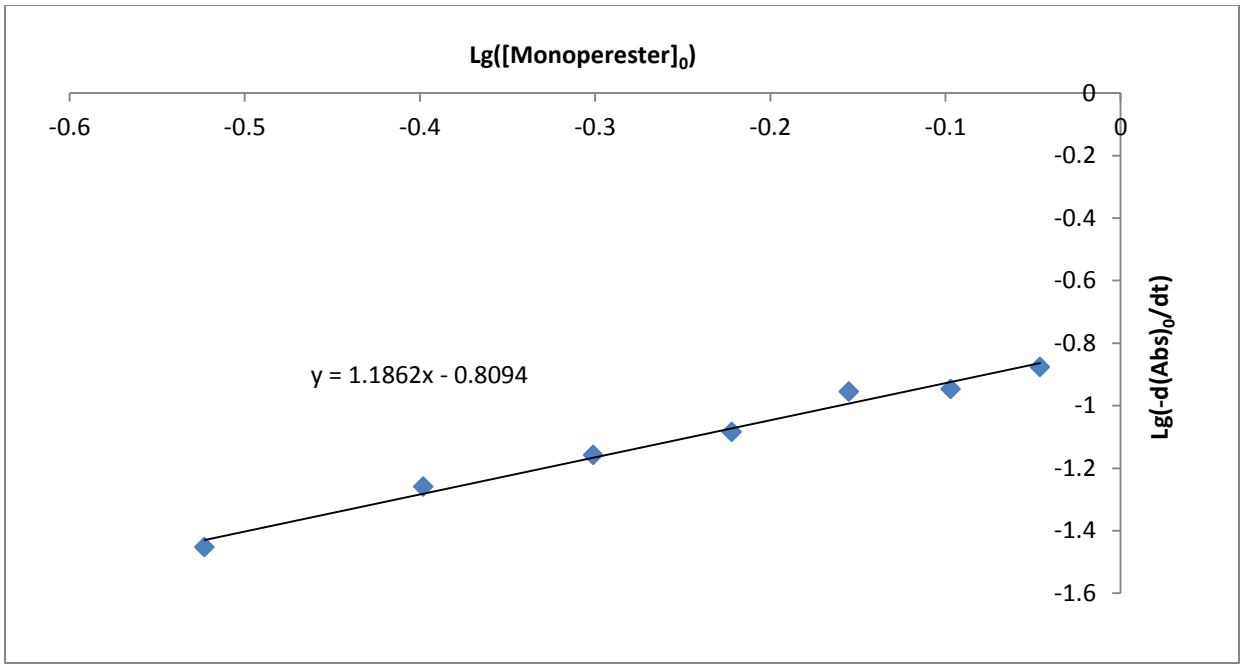

m = 1.1862. This indicates the reaction is a first order reaction to Peroxide reactant

K_2 = 0.1551 L ↗mmol-1 ↗s-1

Part III. Calculation of apparent rate constant.

Abs = e×b ×[Monoperester]

[Monoperester]/mM	**Abs**
0.3	0.323
0.4	0.405
0.5	0.511
0.6	0.612
0.7	0.732
0.8	0.827
0.9	0.927

1.0 1.036

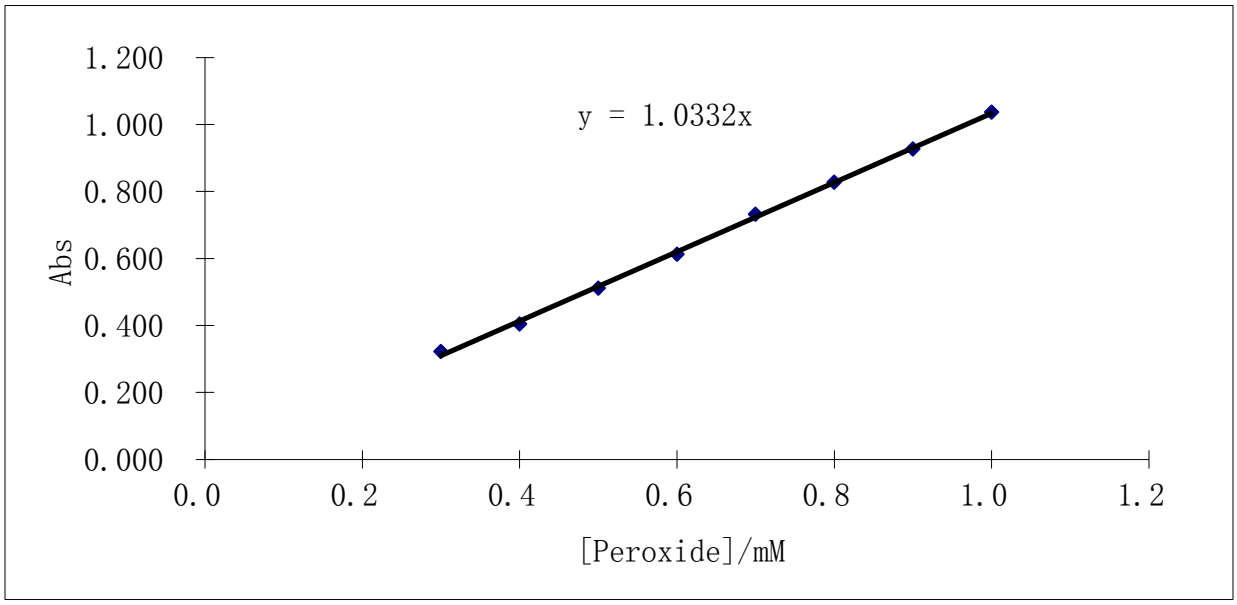

εb =1.0332 L mmol^{-1}

With Part I result:

K_1 = 0.05213 L mmol^{-1} s^{-1}, [Monoperester]$_0$ = 0.5 mmol L^{-1}

$K_1 = k \times [\text{Monoperester}]_0 \times \varepsilon b$

k = 0.101 L mmol^{-1} s^{-1}

With Part II result

K_2 = 0.1551 L mmol^{-1} s^{-1}, [TBAF]$_0$ = 1.5 mmol L^{-1}

$K_2 = k \times [\text{TBAF}]_0 \times \varepsilon b$

k = 0.100 L mmol^{-1} s^{-1}

Therefore the reaction constant k is 0.101 L mmol^{-1} s^{-1}

Chapter 4

Synthesis of a tetramic acid as a standard for identification of an intermediate in HSAF biosynthesis

(Portions of the material in this chapter have been published: Lili Lou, Guoliang Qian, Yunxuan Xie, Jiliang Hang, Haotong Chen, Kathia Zaleta-Rivera, Yaoyao Li, Yuemao Shen, Patrick H. Dussault, Fengquan Liu, Liangcheng Du, Biosynthesis of HSAF, a Tetramic Acid-Containing Macrolactam from Lysobacter enzymogenes, *J. Am. Chem. Soc*., **2011**, 133, 643-645)

4.1 Introduction

Heat stable antifungal factor (HSAF) is a kind of polyketide compound produced by the bacterium *Lysobacter enzymogenes* strain C3, which is used as a biological control agent for fungal disease of plants.[92] The strain C3 has been demonstrated to be able to control many fungal diseases, including *Bipolaris sorokiniana*,[93] *Fusarium graminearum*,[94] *Rhizoctonia solani*,[95] and *Uromyces appendiculatus*.[3] This novel polyketide compound HSAF, which usually affects formin-mediated microfilament assembly at hyphal tips, can also disrupt the formation of stable polarity axes, and thus exhibits a very high potential antifungal activity.[96]

Structurally, HSAF is a type of macrolactam, containing a tetramic acid (2,4-pyrrolidinedione) skeleton within a macrocycle fused onto a 5,5,6-tricyclic ring system. The tetramic acid skeleton is found widely in natural products, including Alteramide A,[97]

and Aburatubolactam A,[98] and has been reported to be a key structural feature in terms of biological activity. (Figure 1).[99]

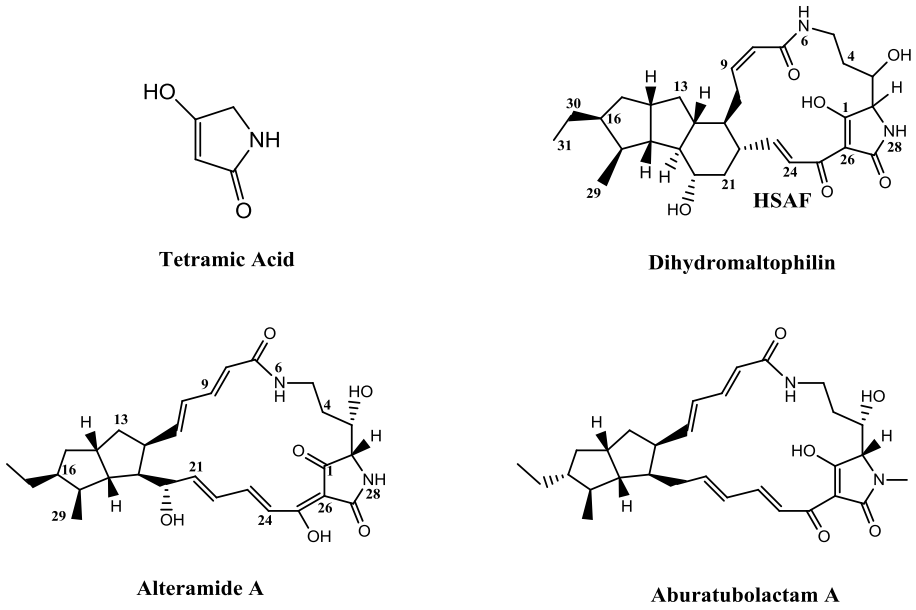

Figure 1. Structures of tetramic acid, HSAF and related tetramic acid-containing macrolactams.

Dr. Liangcheng Du and coworkers (UNL Department of Chemistry) reported four HSAF biosynthetic genes, including a hybrid polyketide synthase/nonribosomal peptide synthetase (PKS/NRPS). Once they had the complete sequence of the gene cluster based on the genome sequences, they expressed the NRPS module and demonstrated in vitro that it can specifically convert two acyl thioesters and *L*-ornithine thioester to a tetramate product (Figure 2). However, in order to confirm the structure of the biosynthetic product, the Du group required an authentic sample for comparison. Our collaboration focused on the synthesis of this tetramic acid.

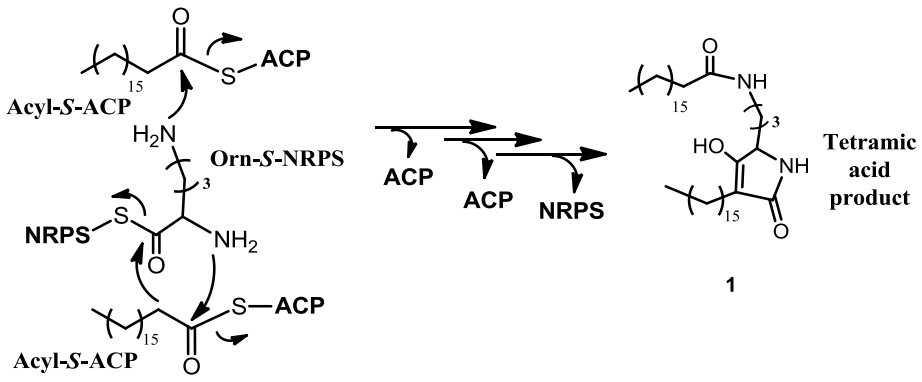

Figure 2. Proposed mechanism for biosynthesis of tetramic acid-containing product

4.2 Results and discussion

The tetramic acid skeleton is generally synthesized using a Dieckmann intramolecular condensation as the key step.[100] The Dieckmann condensation involves the attack of an ester enolate or similar nucleophile on an ester or related acyl group to generate β-ketoesters.[101] Several results had been reported to prepare tetramic acid derivatives via Dieckmann condensation (Figure 3).[102, 103]

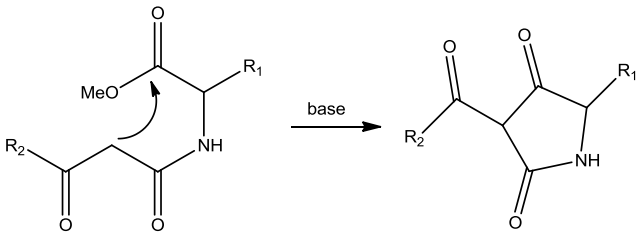

Figure 3. Tetramic acid preparation via Dieckmann condensation.

An alternative method for the preparation of the tetramic acid skeleton involves treatment of a *N*-protected amino acid with Meldrum's acid in the presence of N,N-dimethylaminopyridine and isopropenyl chloroformate to afford an intermediate, which rearranges to a tetramic acid upon heating (Figure 4). .[104]

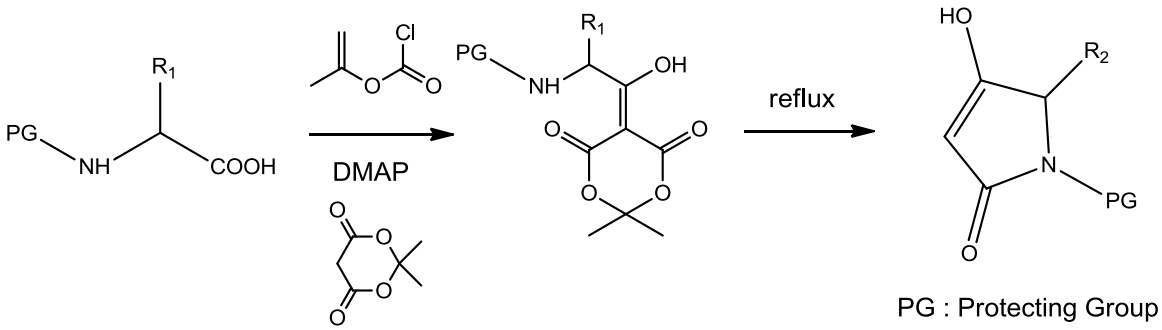

Figure 4. Alternative synthesis of tetramic acid

Recently, another method for synthesis of tetramic acid derivatives has been reported (Figure 5). [105] The reaction of carbonyldiimidazole and α-diimines led to the N-alkyl-4-alkylamino-5-methylenepyrrol-2-ones intermediates, which could be converted to tetramic acid derivatives in two steps.

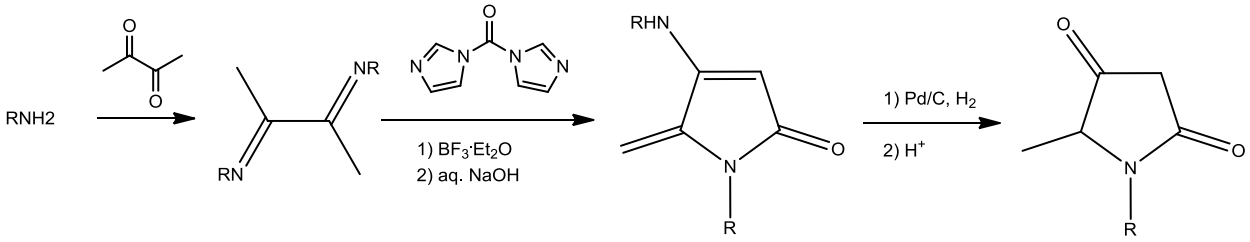

Figure 5. Synthesis of tetramic acid derivatives.

A retrosynthetic summary of our planned approaches to the target molecule is illustrated in Figure 6. Three synthetic routes were investigated in our efforts to prepare the target tetramic acid. All employ Dieckmann condensation as the key step to construct the tetramic acid ring skeleton.

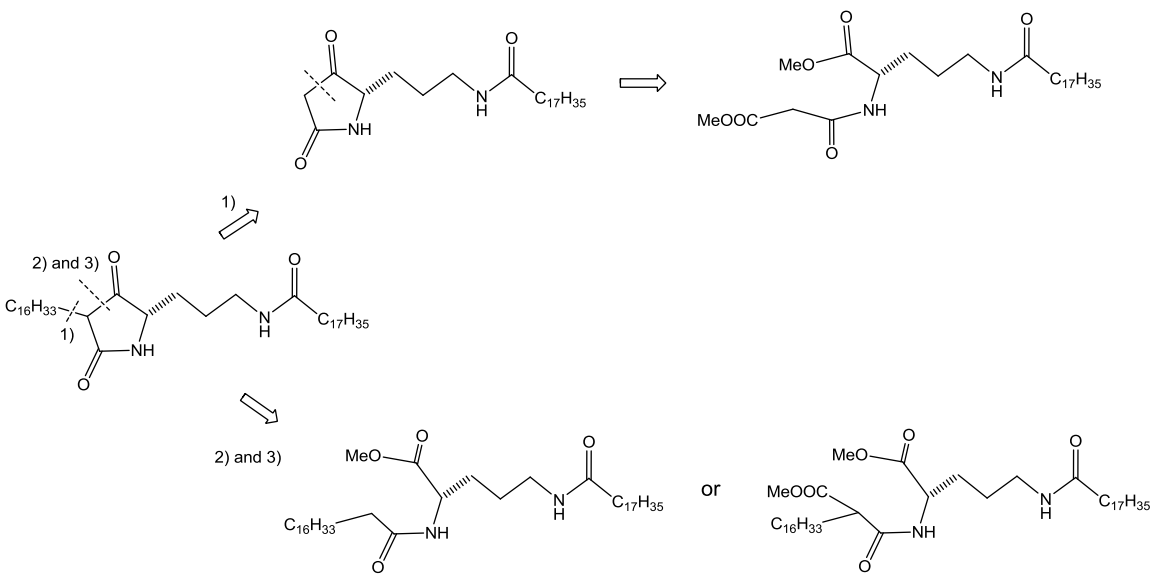

Figure 6. Retrosynthetic analysis

The first route, illustrated in Scheme 1, begins with bisacylation of *L*-ornithine methyl ester (**2)** with stearoyl chloride to furnish diamide (**3**). However, the planned Dieckmann condensation failed to furnish the desired target tetramic acid under a variety of standard conditions, including the use of KOtBu, LDA, LiHMDS, or nBuLi as bases.[106]

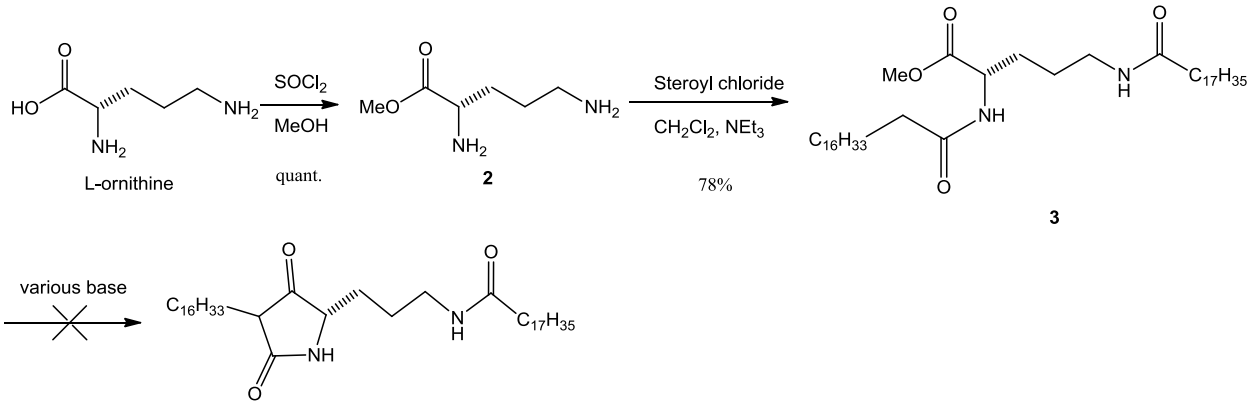

Scheme 1. Attempt of target synthesis

Scheme 2 illustrates an alternative route to the tetramic acid based upon Dieckmann condensation using the stabilized enolate derived from a 1,3-dicarbonyl as a nucleophile. The approach began with the N5 monocarbamate of L-ornithine methyl ester, which was acylated at N2 with the acid chloride of a malonic acid monoester. This intermediate underwent successful Dieckmann condensation with in the presence of soidum methoxide to furnish intermediate **6**, a carboxyethyl derivative of a tetramic acid**.** Then decarboxylation of **6** in CH_3NO_2/H_2O led to intermediate **7**. Unfortunately, attempted introduction of the hexadecyl side chain introduction to C_3 position of the 3,5-dioxopyrrolidine failed in the typical condition of NaH/THF. This reaction instead furnished the enol ether derived from *O*-alkylation as the only product. A similar result has been previously reported during attempted alkylation of tetramic acid ring systems with a long-chain electrophile, [107] suggesting that we needed to identify a route that would introduce the hexadecyl sidechain prior to tetramic acid formation.

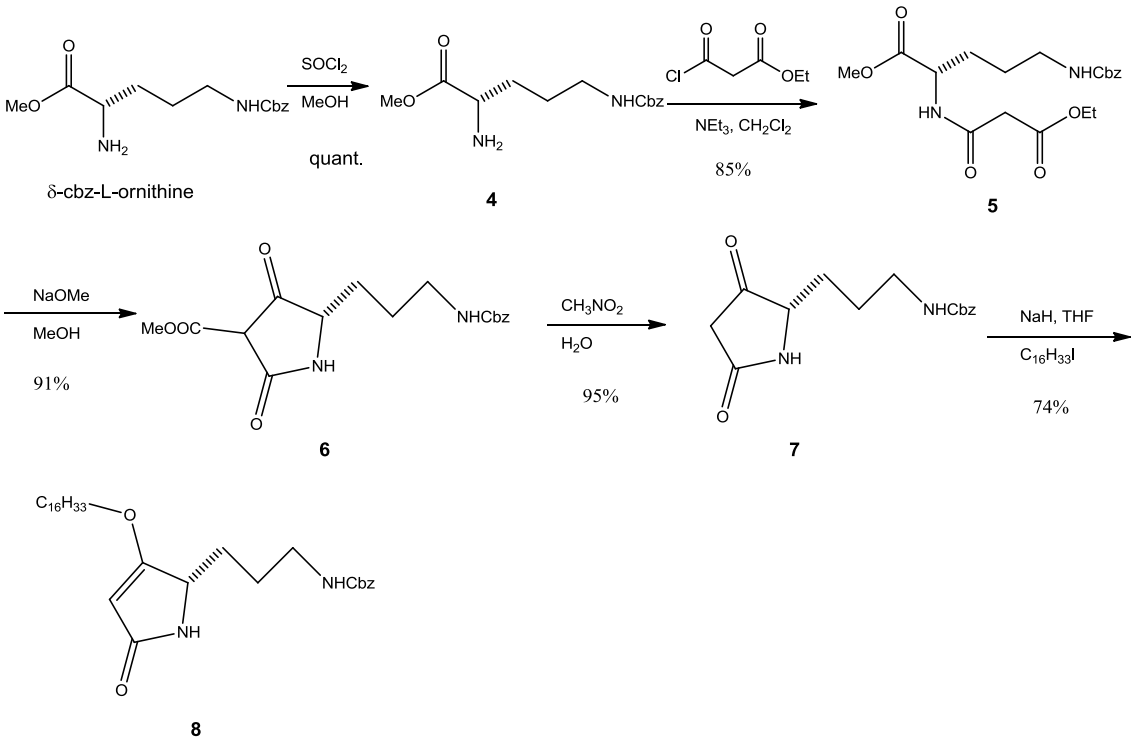

Scheme 2. Attempt of target synthesis

The successful approach to the target (Scheme 3) took advantage of the lessons gained in the previous route by incorporating the hexadecyl sidechain in the malonic ester deriative used to acylate the N2 of ornithine. The synthesis began with the boroxazolidinone adduct of L-ornithine, which was selectively acylated at the terminal amino group with octadecanoyl chloride to furnish a monoamide.[108] Deprotection of the boroxazolidinone with ethylenediamine, followed by reaction with thionyl chloride in methanol, furnished methyl ester **11**. Conversion of the amino acid ester to the tetramic acid was accomplished through a modification of a published approach.[109] Condensation of the amino ester with 2-benzyloxycarbonyloctadecanoic acid **13**, which was prepared in two steps from dibenzyl malonate, furnished the α,δ-bisamide **14** as inseparable mixture of diastereomers (1:1). Reaction of **14** with excess sodium hydride resulted in tandem Dieckmann condensation and deacylation to furnish tetramic acid **15** as a 1:1 mixture of epimer at C_3 of the 3,5-dioxopyrrolidine. The carboxylbenzyl group is generally removed by catalytic hydrogenation. However, there is no evidence that sodium hydride could remove carboxylbenzyl group directly. A possible mechanism might be nucleophilic attack of the liberated sodium methoxide on the carbonyl of the benzyl ester. The tetrahedral intermediate can either return to an ester or else lose a dialkyl carbonate to generate a highly stabilized enolate. This mechanism is probably related to the removal of ethoxycarbonyl group from **6** to**7** in Scheme 2

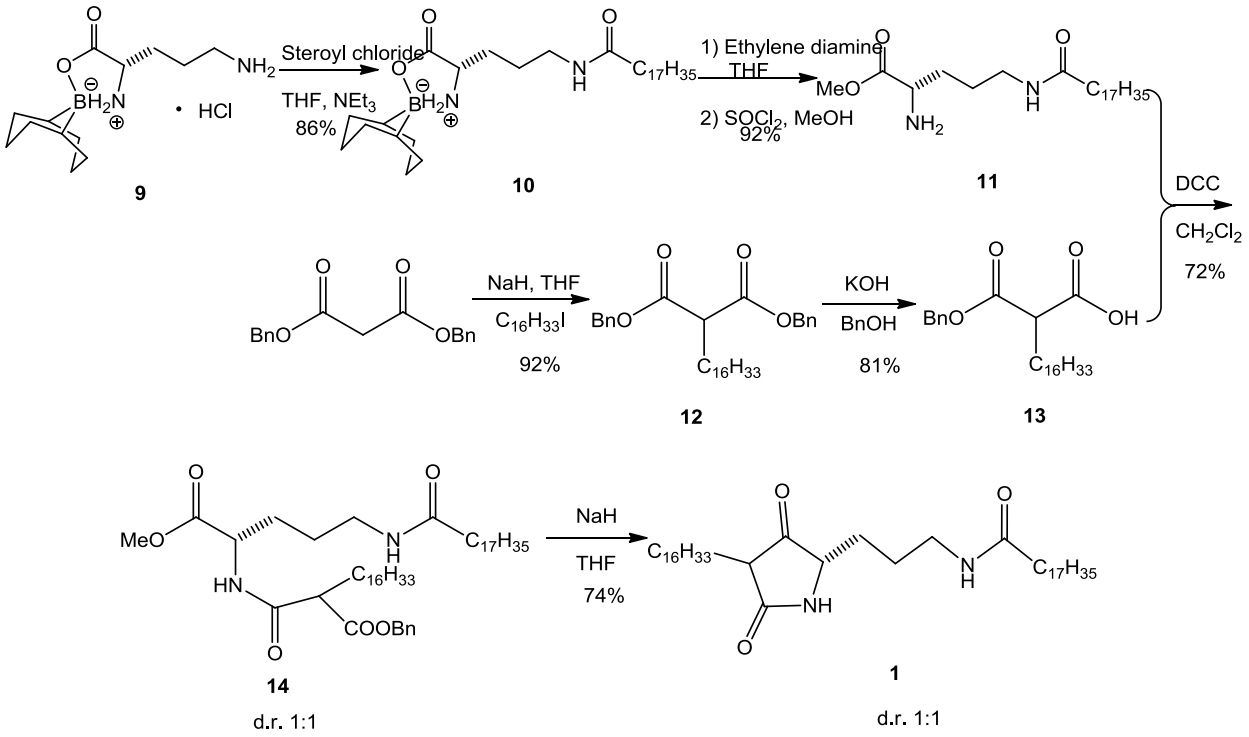

Scheme 3. Synthesis of target molecule

The synthetic tetramic acid was compared with the enzymatically synthesized material by LC/MS and found to have the same retention time and to generate the same mass spectra.

4.3 Experimental Section

***L*-ornithine monohydrochloride, 9-borabicyclononane complex (9)**

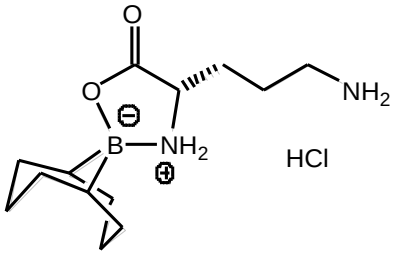

9

Compound **9** was prepared by the procedure of Fields from *L*-ornithine monohydrochloride.[4] The product, which retained solvent, was carried on into the next procedure without purification.

N_5-octadecanoyl-*L*-ornithine, 9-borabicyclononane complex (10)

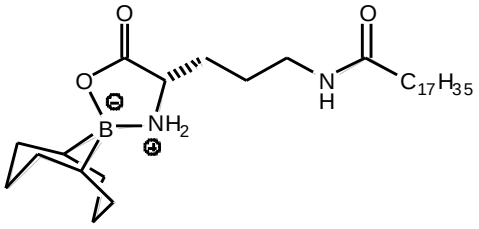

10

To a solution of compound **9 (**3.06 g, 10 mmol) in THF 100 ml was added Et_3N (6.0 ml, 40 mmol) and stearoyl chloride (4.30 g, 12 mmol). The reaction mixture was stirred at rt for 6 h and then concentrated *in vacuo*. The residue was dissolved in 200 ml water, and the aqueous layer was extracted with CH_2Cl_2 (100 ml × 3). The combined organic layers were dried over anhydrous Na_2SO_4 and filtered. The residue obtained upon concentration was purified by chromatography (CH_2Cl_2/MeOH, 95:5) to afford the octadecanoic amide as a white solid **10** (4.40 g, 86%), R_f 0.6 (CH_2Cl_2/MeOH 90/10), Mp 69-70 °C. $[\alpha]_D$ = -13.8 ($CHCl_3$, c = 1.0). IR 3344, 3128, 3110, 2920, 2850, 1692, 1681, 1544, 1376, 1273, 963, 878, 722 cm^{-1}; ^1H NMR: δ 6.60 (t, J= 6.4 Hz, 1H), 5.92 (t, J= 8.8 Hz, 1H), 5.01 (t, J= 9.6 Hz, 1H), 3.78 (t, J= 6.3 Hz, 1H), 3.28 (m, 1H), 3.20 (m, 1H), 2.16 (t, J= 7.1 Hz, 2H), 2.05 (m, 1H), 1.94-1.12 (45H), 0.88 (t, J= 6.9 Hz, 3H), 0.57 (d, J= 10.8 Hz, 2H); ^{13}C NMR: 175.0, 174.3, 55.1, 38.7, 36.7, 31.9, 31.7, 31.4, 31.3, 31.2, 29.73, 29.67, 29.58,

29.44, 29.41, 29.36, 28.1, 26.4, 25.9, 24.5, 24.0, 22.7, 14.1; HRMS (m/z) calcd for $C_{31}H_{59}BN_2NaO_3$ $[M+Na]^+$: 541.4516; found: 541.4471

***L*-ornithine, N_5-octadecanoylamide, methyl ester (11)**

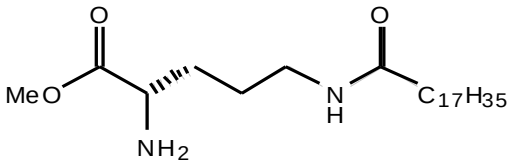

11

Ethylene diamine (1.7 ml, 25 mmol) was added to a solution of N_5-octadecanoyl-L-ornithine, 9-borabicyclononane complex (2.80 g, 5.5 mmol) in THF (15 ml).[4] The solution was heated to just below boiling for 1 min, and then cooled and filtered. The precipitate was washed with THF (25 ml × 3), and dried in vacuo to give a white solid, which was suspended in MeOH (100 ml). $SOCl_2$ (1.9 ml, 25 mmol) was added dropwise, and the reaction mixture was refluxed for 2 h. After removal of solvent in vacuo, the residue was dissolved in water 100 ml. The solution was adjusted to pH 10 with sat. aq. K_2CO_3, and then extracted with CH_2Cl_2 (50 ml × 3). The combined organic layers were dried over anhydrous Na_2SO_4, and the filtrate concentrated in vacuo to afford **11** as a white solid (2.26 g, 92%), which was used without further purification. R_f 0.3 (CH_2Cl_2/MeOH/NEt_3 90/10/1), Mp 59-61 °C; $[\alpha]_D$ = -7.1 ($CHCl_3$, c = 1.0). IR 3318, 2916, 2848, 1741, 1646, 1553, 1232, 718 cm^{-1}; ^1H NMR: 6.01 (t, J= 5.4 Hz, 1H), 3.70 (s, 3H), 3.44 (t, J= 6.9 Hz, 1H), 3.24 (m, 2H), 2.13 (t, J = 7.2 Hz, 2H), 1.60 (m, 4H), 1.30-1.21 (32H), 0.86 (t, J = 6.9 Hz, 3H); ^{13}C NMR: 176.2, 173.2, 54.0, 52.1, 39.0, 26.8, 32.1,

31.9, 29.67, 29.63, 29.5, 29.37, 29.33, 25.9, 25.8, 22.7, 14.1; HRMS (m/z) calcd for $C_{24}H_{48}N_2NaO_3$ $[M+Na]^+$: 435.3563; found: 435.3562. Small impurities could be seen in ^1H NMR at 3.65 ppm and 2.28 ppm

2-(Benzyloxycarbonyl)octadecanoic acid, benzyl ester (12)

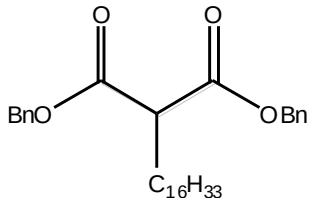

12

Dibenzylmalonate (2.84 g, 10 mmol) was added to a stirred solution of NaH (0.24 g, 10 mmol) in dry THF (10 ml) and dry DMF (10 ml) and the mixture was stirred at rt for 1 h. 1-Iodohexadecane (3.52 g, 10 mmol) was then added and the reaction mixture was refluxed for 3 h. The cooled reaction mixture was concentrated in vacuo and the residue added to sat. aq. NH_4Cl (100 ml), and the aqueous layer was extracted by Et_2O (100 ml × 3). The combined organic layers were dried over anhydrous Na_2SO_4 and the filtrate was concentrated in vacuo. Flash chromatography (Hexane/EtOAc, 95:5) afforded the diester as a low-melting white solid **12** (4.67 g, 92%). R_f 0.3 (Hexane/EtOAc 95/5). Mp 41-42 ° C; IR 2914, 2848, 1752, 1728, 1463, 1455, 1184,1143, 724, 669 cm^{-1}; ^1H NMR: δ 7.34 (m, 10H), 5.19 (s, 4H), 3.48 (t, J= 7.5 Hz, 1H), 1.97 (dd, J= 7.1 Hz, 13.8 Hz, 2H), 1.38-1.21 (28H), 0.93 (t, J= 7.0 Hz, 3H); ^{13}C NMR: δ 169.3, 135.5, 128.6, 128.3, 128.2, 67.0,

52.1, 32.0, 29.73, 29.69, 29.64, 29.5, 29.4, 29.3, 29.2, 28.8, 27.2, 22.7, 14.2 ; HRMS (m/z) calcd for $C_{33}H_{48}NaO_4$ $[M+Na]^+$: 531.3450; found: 531.3411

2-(Benzyloxycarbonyl)octadecanoic acid (13) was prepared by a modification of a procedure reported for malonic acid monobenzyl ester

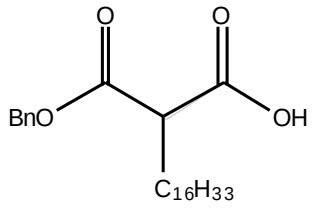

13

To a suspension of KOH (0.28 g, 5 mmol) in benzyl alcohol (5.0 ml) was added gradually to a solution of the diester (2.62 g, 5 mmol) in benzyl alcohol (25 ml). The reaction mixture was stirred at rt for 24 h, and the solvent was then removed in vacuo. The residue was dissolved in water (100 ml) and the solution acidified to pH 2 with 3 M HCl. The aqueous layer was extracted with CH_2Cl_2 (100 ml × 3) and then combined organic layers were dried over anhydrous Na_2SO_4. The filtrate was concentrated in vacuo to afford a solid which was recrystallized from heptane to afford the monoester as a white solid **13** (1.69 g, 81%): R_f 0.6 (Hexane/EtOAc/AcOH 20/20/1). Mp 46-48 ℃; IR 2916, 2848, 1745, 1696, 1470, 1259, 1231, 936, 730, 718 cm^{-1}; ^1H NMR: δ 10.08 (br, 1H), 7.40 (m, 5H), 5.23 (s, 2H), 3.47 (t, J= 7.4 Hz, 1H), 1.97 (m, 2H), 1.40-1.24 (28H), 0.92 (t, J= 6.7 Hz, 3H); ^{13}C NMR: 175.2, 169.3, 135,3, 128.6, 128.4, 128.2, 67.3, 51.7, 32.0,

29.73, 29.69, 29.63, 29.5, 29.39, 29.31, 29.2, 28.9, 27.2, 22.7, 14.1; HRMS (m/z) calcd for $C_{26}H_{42}NaO_4$ $[M+Na]^+$: 441.2981; found: 441.2993.

***L*-ornithine,N_5-octadecanoylamide-N_2-(2-benzyloxycarbonyl)octadecanoylamide (14)**

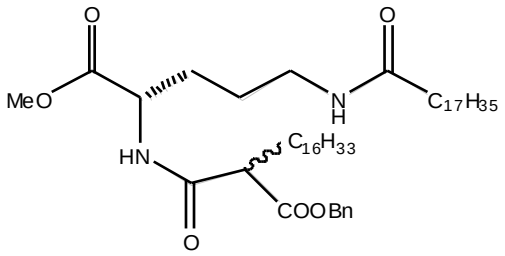

14

To a solution of compound **11** (0.20 g, 0.48 mmol) in CH_2Cl_2 (20 ml) was sequentially added *N,N'*-dicyclohexylcarbodiimide (0.12 g, 0.58 mmol) and monoester **13 (**0.20 g, 0.48 mmol). The reaction mixture was refluxed for 4 h, cooled to rt, and then filtered. The filtrate was dried over anhydrous Na_2SO_4, and then refiltered before being concentrated in vacuo. Flash chromatography (Hexane/EtOAc, 60:40) afforded **14** as a white solid (0.28 g, 72%), R_f 0.4 (Hexane/EtOAc 50/50). Mp 100-101 ℃; IR 3304, 2916, 2849, 1736, 1639, 1545, 1272, 1236, 720, 695 cm^{-1}; ^1H NMR: δ 7.37 (m, 5H), 7.17 (d, J= 7.5 Hz, 0.5H), 7.13 (d, J= 7.8 Hz, 0.5H, isomer), 5.72 (t, J= 6.3 Hz, 1H), 5.20 (m, 2H), 4.58 (m, 1H), 3.75 (s, 1.5H), 3.74(s, 1.5H, isomer), 3.31 (dd, J= 7.1, 14.3 Hz, 1H), 3.24 (m, 2H), 2.15 (m, 2H), 1.86 (m, 4H), 1.65-1.25 (60H), 0.89 (t, J= 6.9 Hz, 6H); ^{13}C NMR 173.38, 173.31(isomer), 172.3, 172.2(isomer), 171.7, 171.4(isomer), 168.4, 168.3(isomer), 135.32, 135.29(isomer), 128.6, 128.5, 128.4, 67.2, 52.95, 52.86(isomer), 52.51, 52.48(isomer), 51.93, 51.91(isomer), 38.6, 26.8, 31.9, 30.9, 30.5, 29.71, 29.66,

29.5, 29.40, 29.37, 29.22, 29.17, 27.25, 27.21, 25.8, 25.4, 22.7, 14.1 ; HRMS (m/z calcd for $C_{50}H_{88}N_2NaO_6$) $[M+Na]^+$: 835.6540; found: 835.6465.

3-Hexadecyl-5-(3-aminopropyl)-pyrrolidine-2,4-one, octadecanoyl amide (1) was prepared using a modification of a procedure reported for other tetramic acids.

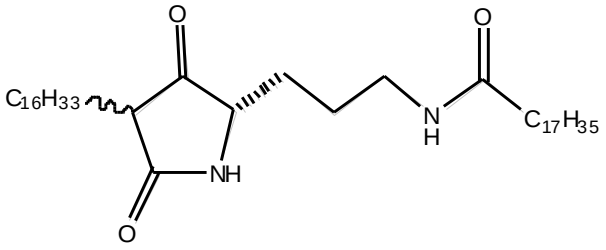

1

NaH (60% dispersion in mineral oil, 13 mg, 0.37 mmol) was washed with pentane 20 ml three times in a 100ml RB flask, then compound **14** (81 mg, 0.10 mmol) was added in THF (10 ml). The reaction mixture was refluxed for 6 h and then cooled to rt. After removal of solvent in vacuo, the residue was suspended in water (15 ml) and the solution acidified to pH 2 with 3 M HCl. The combined CH_2Cl_2 extracts (10 ml × 3) were dried over anhydrous Na_2SO_4 and the filtrate concentrated in vacuo. Flash chromatography (CH_2Cl_2/MeOH, 95:5) afforded **1** as a white solid (48 mg, 74%). R_f 0.5 (CH_2Cl_2/MeOH 90/10). Mp 108-109 ℃. IR 2916, 2848, 1686, 1639, 1467, 720 cm^{-1}; ^1H NMR: δ 6.94 (d, J= 3.9 Hz, 0.5H), 6.88 (d, J= 8.4 Hz, 0.5H, isomer), 5.60 (t, J= 5.4 Hz, 1H), 4.01 (t, J= 6.7 Hz, 0.5H), 3.92 (t, J= 5.4 Hz, 0.5H, isomer), 3.29 (m, 2H), 2.83 (t, J= 5.8 Hz, 0.5H), 2.76 (t, J= 5.8 Hz, 0.5H, isomer), 2.17 (t, J= 7.6 Hz, 2H),1.91-1.56(8H), 1.47-1.20 (56H), 0.90 (t, J= 6.6 Hz, 3H); ^{13}C NMR (150 MHz): 211.1, 210.7 (isomer), 174.2, 173.9 (isomer), 173.6, 62.3, 61.9(isomer), 49.7, 49.1(isomer), 38.5, 36.8, 31.9, 29.71, 29.67,

29.58, 29.52, 29.37, 29.34, 29.31, 28.7, 27.2, 26.6, 26.5, 26.20, 25.9, 25.8, 25.5, 22.7, 14.1; HRMS (m/z) calcd for $C_{41}H_{78}N_2NaO_3^+$ $[M+Na]^+$: 669.5910; found: 669.5889

LC/MS analysis

Tetramic acid **1** was subjected to LC/MS under the following conditions:

LC/MS column Alltima C18LL (5u, 1.0mm * 250 mm); solvent A H_2O containing 5 mM ammonium acetate; solvent B MeOH containing 5 mM ammonium acetate. Flow rate was 50 µl/min, with a gradient system (0-5 min, 30% B; 5-20 min, 30% B to 100% B gradient; 20-30 min, 100% B; 30-40 min, 100% B to 30% B gradient; 40-45 min, 30% B). One of the main signals observed, at 25.8 minutes, coincided exactly with the signal observed for material derived from the biosynthetic pathway described in the introduction. For both the synthetic material and the material derived from the biosynthetic pathway, the peak at 25.8 minutes gave a mass spectrum the major peak at 647.6080.

References

[1] Akhisa T., Kokke, W., (1991). In G. W. Patterson, W. D. Nes. Physiology and Biochemistry of Sterols. Champaign, IL: American Oil Chemists' Society. pp. 172–228.

[2] Moreau R.A., Whitaker B.D., Hicks K.B., *Prog. Lipid Res.*, **2002**, 41, 457.

[3] Moghadasian M.H., *Life Sci.*, **2000**, 67, 605.

[4] Moreau R.A., Whitaker B.D., Hicks K.B., *Prog. Lipid. Res.*, **2002**, 41, 457.

[5] Ling W.H., Jones P.J.H., *Life Sci*., **1995**, 57, 195.

[6] Bao L., Li Y., Deng S.X., Landry D., Tabas I., *J. Biol. Chem.*, **2006**, 281, 33635.

[7] Xu W.L., Huang Y.B., Qian J.H., Sha O., Wang Y.Q., *Sep. Purif. Technol*., **2005**, 41, 173.

[8] Kircher H.W., Rosenstein F., *Lipids*, **1973**, 8, 97.

[9] McCarthyl F., Chopra J., Hogan S.A., Kerry J.P., O'Brien N.M., Ryan E., Maquire A.R., *Org. Biomol. Chem.*, **2005**, 3, 3059.

[10] Raney M., U.S. Patent 1,628,190, May 10, **1927**.

[11] Kiros Y., Majari M., Nissinen T.A., *J. Alloys Compd.*, **2003**, 360, 279.

[12] Fouilloux P., *Appl. Catal.*, **1983**, 8, 1.

[13] Mozingo R., *Org. Synth.*, **1955**, Coll. Vol. 3, 181.

[14] Rieke R.D., *Science*, **1989**, 246, 1260.

[15] Rieke R.D., *Acc. Chem. Res.*, **1977**, 10, 301.

[16] Rieke R.D., Wu T.C., Rieke L.I., *Org. Synth.*, **1995**, 72, 147.

[17] Alonso F., Osante I., Yus M., *Tetrahedron*, **2007**, 63, 93.

[18] Voorhees V., *J. Am. Chem. Soc.*, **1922**, 44, 1397.

[19] Deng K., Chalker J., Yang A., Cohen T., *Org. Lett.*, **2005**, 7, 3637.

[20] Koskenniska L.A., US Patent 4,298,539, Nov. 3, **1981**.

[21] McMurry J.E., Fleming M.P., *J. Am. Chem. Soc.*, **1974**, 96, 4708.

[22] Baqi Y., Giroux S., Corey E.J., *Org. Lett.*, **2009**, 11, 959.

[23] Wong H.N., Fok C.M., Wong T., *Heterocycles*, **1987**, 26, 1345.

[24] Sarmah P., Barua N.C., *Tetrahedron Lett*., **1988**, 29, 5815.

[25] Petterson H., Norlin M., Anderson U., Pikuleva I., Bjorkhem I., Misharin A.Y., Wikvall K., *Biochim. Biophys. Acta*., **2008**, 1781, 383.

[26] Misharin A.Y., Ivanov V.S., Mehtiev A.R., Morozevich G.E., Tkachev Y.V., Timofeev V.P., *Steroids*, **2007**, 72, 305.

[27] Tietze L.F., Raith C., Brazel C.C., Holsken S., Magull J., *Synthesis*, **2008**, 2, 229.

[28] Blakemore P.R., *J. Chem. Soc. Perkin Trans.*, **2002**, 1, 2563.

[29] Khripach V.A., Zhabinskii V.N., Konstantinova O.V., Khripach N.B., Antonchick A.V., Antonchick A.P., Schneider B., *Steroids*, **2005**, 70, 551.

[30] Wang S.M., Zhang Y.B., Liu H.M., Yu G.B., Wang K.R., *Steroids*, **2007**, 72, 26.

[31] Promprom W., Kupittayanant P., Indrapichate K., Wray S., Kupittayanant S., *Reprod. Sci.*, **2010**, 17, 288.

[32] Bao L., Li Y., Deng S.X., Landry D., Tabas I., *J. Biol. Chem.*, **2006**, 281, 33653.

[33] Banwell M.G., McRae K.J., *J. Org. Chem*., **2001**, 66, 6768.

[34] Kung H., Hoyert D.L., Xu J., Murphy S.L., *Natl. Vital. Stat. Rep*., **2008**, 56, 1

[35] Highlander P., Shaw G.P., *Ther. Adv. Cardiovasc Dis*., **2010**, 4, 43

[36] Begemann F., Bandomer G., Herget H.J., *Scand. J. Gastroenterol*., **1978**, 13, 57

[37] Garrett R.H., Grisham C.M., Biochemistry, 2nd Ed., 1995, Saunders College Publishing.

[38] Jesch E.D., Carr T.P., *Nutr. Res*., **2006**, 26, 579

[39] Miettinen T.A., Vuoristo M., Nissinen M., Jarvinen H.J., Gylling H., *Am. J. Clin. Nutr*., **2000**, 71, 1095

[40] Armstrong M.J., Carey M.C., *J. Lipid. Res*., **1987**, 28, 1144

[41] Chen Q., Sternby B., Nilsson A., *Biochem. Biophys. Acta*., **1989**, 1004, 372

[42] Heidrich J.E., Contos L.M., Hunsaker L.A., Deck L.M., Vander Jagt D.L., *BMC Pharmacology*, **2004**, 4, 5

[43] Choudhary M.I, Devkota K.P., Nawaz S.A., Ranjit R., Rahman A., *Steroids*, **2005**, 70, 295

[44] Ngatha B.T., Luu-The V., Labrie F., Poirier D., *J. Med. Chem*., **2005**, 48, 5257

[45] Wang B., Du H., Zhang J., *Steroids*, **2011**, 76, 204

[46] Kircher H.W., Rosensterin F.U., *Lipids*, **1973**, 8, 101

[47] Kukis A., Beveridge J.M.R., *J. Org. Chem*., **1960**, 25, 1209.

[48] Degn H., Balslev I., Brook R., *Meas. Oxygen, Proc. Interdiscip. Symp*., **1976**, 248.

[49] Bruchet P., Huchet T., Inizan M., *Industre Ceramique & Verriere*, **1997**, 923, 116.

[50] Arnold S.J., Kubo M., Ogryzlo E.A., *Adv. Chem. Ser*., **1968**, 77, 133.

[51] Merkel P.B., Kearns D.R., *J. Am. Chem. Soc*., **1972**, 94, 1029.

[52] Wasserman H.H., Murray R.W., Singlet Oxygen, **1979**, Academic Press, New York.

[53] Calvert J.G., Pitts Jr. J.N., *Photochemistry*, **1966**, John Wiley and Sons, New York.

[54] Wilkinson F., Helman W.P., Ross A.B., *J. Phys. Chem. Ref. Data*., **1993**, 22, 113.

[55] Foote, C.S., Clennan E.L., In Active Oxygen in Chemistry; Foote C.S., Valentine J.S., Greenberg A., Liebman J.E., Eds.; Blackie Academic and Professional: London, **1995**, p 105.

[56] Thompson Q.E., *J. Am. Chem. Soc*., **1961**, 83, 845.

[57] Adam W., Kazakov D.V., Kazakov V.P., *Chem. Rev*., **2005**, 105, 3371.

[58] Catir M., Kilic H., Nardello-Rataj V., Aubry J. M., Kazaz C., *J. Org. Chem*., **2009**, 74, 4560.

[59] Corey E.J., Mehrotra M.M., Khan A.U., *J. Am. Chem. Soc*., **1986**, 108, 2472.

[60] Pierlot M.C., Gonzalez-Lopez M., Urbano A., *Angew. Chem. Int. Ed*., **2006**, 45, 2737.

[61] Pierlot C., Nardello V., Schrive J., Mabille C., Barbillat J., Sombret B., Aubry J.M., *J. Org. Chem*., **2002**, 67, 2418.

[62] Aubry J. M., Pierlot C., Rigaudy J., Schmidt R., *Acc. Chem. Res*., **2003**, 36, 668.

[63] Thompson Q.E., *J. Am. Chem. Soc*., **1961**, 83, 845.

[64] Corey E.J., Mehrotra M.M., Khan A.U., *J. Am. Chem. Soc*., **1986**, 108, 2472.

[65] Deslongchamps P., Atlani P., Frehel D., Malaval A., Moreau C., *Can. J. Chem*., **1974**, 52, 3651.

[66] Niu Q., Mendenhall G.D., *J. Am. Chem. Soc*., **1990**, 112, 1656.

[67] Dewar M. J.S., Thiel W., *J. Am. Chem. Soc*., **1977**, 99, 2338.

[68] Bloodworth A.J., Eggelte H.J., Endoperoxides in Singlet O_2, Vol II, CRC press, Boca Raton, FL, pp93-203

[69] Held C., Frohlich R., Metz P., *Angew. Chem. Int. Ed*., **2001**, 40, 1058.

[70] Schenk G.O., *Naturwissenschaften*., **1948**, 35, 28.

[71] Song Z., Beak P., *J. Am. Chem. Soc*., **1990**, 112, 8126.

[72] Lerdal D., Foote C.S., *Tetrahedron Lett.*, **1978**, 19, 3227.

[73] Frimer A.A., *Chem. Rev.*, **1979**, 79, 359.

[74] Kearns D.R., Fenical W., Radlick P., Ann N.Y., *Acad. Sci.*, **1970**, 171, 32.

[75] Krasnovsky A.A., Jr. *Biofizika*, **1976**, 21, 748.

[76] Kanofsky J.R., *Chem.-Biol. Interaction*, **1988**, 70, 1.

[77] Gorman A.A., Rodgers M.A.J., Singelt oxygen, in CRC handbook of Organic Photochemistry, Vol II, CRC press, Boca Raton, FL, pps 229-247.

[78] Oliveira M. S., Severino D., Prado F.M., Angeli J.P.F., Motta F.D., Baptista M.S., Medeiros M.H.G., DiMascio P., *Photochem. Photobiol. Sci.*, **2011**, 10, 1546.

[79] Moan J., Peng Q., *Anticancer Res*., **2003**, 23, 3591.

[80] Clennan E., Pace A., *Tetrahedron*, **2005**, 61, 6665.

[81] Schwartz, C., Raible, J., Mott, K., Dussautl P.H., *Org. Lett*., **2006**, 8, 3199.

[82] Ghorai, P., Dussault, P.H., *Org. Lett*., **2009**, 11, 4572.

[83] Ghorai, P., Dussault, P.H., *Org. Lett*., **2008**, 10, 4577.

[84] Salokhiddinov K.I., Byteva I.M., Gurinovich G.P., *J. Appl. Spectrosc*., **1981**, 34, 561.

[85] Miller J., Abernathy S., Sharp R. *J. Phys. Chem. A*., **2000**, 104, 4839.

[86] Payne, G.B., *Tetrahedron*, **1962**, 18, 763.

[87] Davies, A.G., Sutcliffe, R.J., *J. Chem. Soc. Perkins Trans*., **1981**, 2, 1512.

[88] Long, C.A., Kearns D.R., *J. Am. Chem. Soc.*, **1975**, 97, 2018.

[89] Frimer A.A., *Chem. Rev*. **1979**, 79, 359.

[90] Matheson I.B.C., Lee J., Yamanashi B.S., Wolbarsht M.L., *Chem. Phys. Lett*., **1974**, 27, 355.

[91] Ramirez A., Woerpel K.A., *Org. Lett*., **2005**, 7, 4617.

[92] Yu F., Zaleta-Rivera K., Zhu X., Huffman J., Millet J.C., Harris S.D., Yuen G., Li X.C., Du L., *Antimicrob. Agents Chemother.*, **2007**, 51, 64.

[93] Zhang Z., Yuen G.Y., *Phytopathology*, **1999**, 89, 817.

[94] Yuen G.Y., Jochum C.C., Osborne L.E., Jin Y., *Crop Protect*., **2003**, 20, 395.

[95] Glesler L.J., Yuen G.Y., *Crop Protect*., **1998**, 17, 509.

[96] Li S., Du L., Yuen G., Harris S.D., *Mol. Biol. Cell*, **2006**, 17, 1218.

[97] Shigemori H., Bae M.A., Yazawa K., Sasaki T., Kobayashi J., *J. Org. Chem*., **1992**, 57, 4317.

[98] Bae M.A., Yamada K., Ijuin Y., Tsuji T., Yazawea K., Tomono Y., Uemura D.. *Heterocycl. Commun*. **1996**, 2, 315.

[99] Schobert R., Schlenk A., *Bioorg. Med. Chem*., **2008**, 16, 4203.

[100] Poncet J., Jouin P., Castro B., *J. Chem., Soc., Perkin Trans. I*, **1990**, 611.

[101] Dieckmann, W. *Ber.* **1894**, 27, 102.

[102] DeShong P., Cipollina J.A., Lowmaster N.K., *J. Org. Chem.*, **1988**, 53, 1356.

[103] Spatz J.H., Welsch S.J., Duhaut D.E., Jager N., Boursier T., Fredrich M., Allmendinger L., Ross G., Kolb J., Burdack C., Umkehrer M., *Tetrahedron Lett*., **2009**, 50, 1705.

[104] Jouin P., Castro B., *J. Chem. Soc. Perkin Trans. I*, **1987**, 1177.

[105] Fustero S., Torre M.G., Sanz-Cervera J.F., Arellano C.R., Piera J., Simon A., *Org. Lett*., **2002**, 4, 3651.

[106] Mallinger A., Le Gall T., Mioskowski C., *Synlett*., **2008**, 386.

[107] Albrecht D., Basler B., Bach T., *J. Org. Chem*., **2008**, 73, 2345.

[108] Dent W.H., Erickson W.R., Fields S.C., Parker M.H., Tromiczak E.G., *Org. Lett*., **2002**, 4, 1249.

[109] Page P.C.B., Hamzah A.S., Leach D.C., Allin S.M., Andrews D.M., Rassias G.A., *Org. Lett*., **2002**, 5, 353.